T.C.
BOLU ABANT İZZET BAYSAL ÜNİVERSİTESİ
INSTITUTE OF GRADUATE STUDIES
DEPARTMENT OF CHEMISTRY

SYNTHESIS OF 1,(3S)-BIS[N-*p*-ARYL)-CARBAMOYLOXY]BUTANE AS NEW LOW MOLECULAR WEIGHT ORGANOGELATORS

MASTER OF SCIENCE, CHEMISTRY

BÜŞRA İREM ŞİMŞEK TOPÇU

THESIS SUPERVISOR
Prof. Dr. Öznur DEMİR ORDU

BOLU, 12/30/2024

ACCEPTANCE AND APPROVAL PAGE

The thesis entitled "**SYNTHESIS OF 1,(3S)-BIS[N-*p*-ARYLCARBAMOYLOXY]BUTANE AS NEW LOW MOLECULAR WEIGHT ORGANOGELATORS**" prepared and submitted by **Büşra İrem ŞİMŞEK TOPÇU** in partial fulfillment of the requirements for the degree of **Master of Science** in Department of **CHEMISTRY** with unanimity vote is hereby approved. 12/30/2024

Jury Members	**Signature**
Supervisor Prof. Dr. Öznur DEMİR ORDU BAİBU	.....
Member Prof. Dr. Erol AKPINAR BAİBU	.....
Member Assist. Prof. Dr. Şule EROL GÜNAL Istanbul Cerrahpasa University	.....

Institute of Graduate Studies Approval

Prof. Dr. İbrahim KÜRTÜL

Director of Institute of Graduate Studies

ETHICAL DECLARATION

In this thesis study, which I have prepared in accordance with Bolu Abant İzzet Baysal University, Institute of Graduate Studies' Thesis Writing Guide and Template;

- I have obtained the data, information and documents presented in the thesis within the framework of academic and ethical rules,
- I have presented all information, documents, evaluations, and results in accordance with the rules of scientific ethics and morality,
- I have cited and referenced all the works I have benefited from in the thesis study,
- I have not made any changes to the data used,
- I declare that the work I have presented in this thesis is original, and in any other case, I declare that I accept all loss of rights that may arise against me.

According to the similarity report obtained by applying the filters determined by the directorate of the institute in the Turnitin program related to the thesis, the similarity index of the thesis does not exceed 30%.

.....

BÜŞRA İREM ŞİMŞEK TOPÇU

ABSTRACT

SYNTHESIS OF 1,(3S)-BIS[N-*p*-ARYL)-CARBAMOYLOXY]BUTANE AS NEW LOW MOLECULAR WEIGHT ORGANOGELATORS

MSC THESIS
BÜŞRA İREM ŞİMŞEK TOPÇU
BOLU ABANT IZZET BAYSAL ÜNİVERSİTESİ
INSTITUTE OF GRADUATE STUDIES
DEPARTMENT OF CHEMISTRY
(SUPERVISOR: PROF. DR. ÖZNUR DEMİR ORDU)

BOLU, 30 DECEMBER 2024
XV + 94

Low molecular weight organic compounds (LMWOs) have the potential to form gels at low concentrations (below 5 wt%) in organic solvents. These compounds form supramolecular networks with weak, non-covalent bonds such as hydrogen bonds, van der Waals forces and π-π interactions. These networks lead to the components forming fibrous, tubular or helical structures and the entrapment of solvent molecules. Structural groups such as aromaticity, hydrogen bonds and aliphatic chains play an important role in gel formation. Moreover, self-assembly processes are influenced by the spatial arrangement of the functional groups of compounds, which creates differences in the gelation abilities of chiral compounds. By influencing molecular stacking, chiral centers can determine whether a compound will function as an organogelator or not. In this project, chiral *p*-alkyl and *p*-alkoxy substituted 1,(3S)-Bis-[N-(p-aryl)-carbamoyloxy]butane derivatives were synthesized by reacting *p*-aryl isocyanates with (S)-(+)-1,3-Butanediol or by the reaction of *p*-substituted benzoic acid with diphenylphosphoryl azide. After purification and characterization of the compounds, their organogelization abilities in achiral solvents were investigated by test tube inversion method.

KEYWORDS: Low molecular weight organogelator, chiral recognition, N-aryl carbamate, organogel, 1,(3S)-Bis[N-(*p*-aryl)-carbamoyloxy]butane

ÖZET

1,(3S)-BİS[N-*p*-ARİL)-KARBAMOİLOKSİ]BÜTAN BİLEŞİKLERİNİN YENİ DÜŞÜK MOLEKÜL KÜTLELİ ORGANOJELLEŞTİRİCİLER OLARAK SENTEZLENMESİ

YÜKSEK LİSANS TEZİ
BÜŞRA İREM ŞİMŞEK TOPÇU
BOLU ABANT IZZET BAYSAL ÜNİVERSİTESİ
LİSANSÜSTÜ EĞİTİM ENSTİTÜSÜ
KİMYA ANA BİLİM DALI
(TEZ DANIŞMANI: PROF. DR. ÖZNUR DEMİR ORDU)

BOLU, 30 ARALIK 2024
XV + 94

Düşük molekül ağırlıklı organik bileşikler (LMWOs), organik çözücülerde düşük konsantrasyonlarda (ağırlıkça %5'in altında) jel oluşturma potansiyeline sahiptir. Bu bileşikler, hidrojen bağları, van der Waals kuvveti ve zayıf π-π etkileşimleri gibi, kovalent olmayan bağlarla supramoleküler ağlar oluşturur. Bu ağlar, bileşenlerin lifli, tüp ya da helikal yapılar oluşturmasına ve çözücü moleküllerinin hapsolmasına yol açar. Jel oluşumunda aromatiklik, hidrojen bağları ve alifatik zincirler gibi yapısal gruplar önemli rol oynar. Ayrıca, öz-toparlama süreçleri, bileşiklerin fonksiyonel gruplarının uzaysal düzenlenmesinden etkilenir, bu da kiral bileşiklerin jelleşme yeteneklerinde farklılıklar yaratır. Kiral merkezler, moleküler istiflenmeyi etkileyerek, bir bileşiğin organojelleştirici olarak işlev görüp görmeyeceğini belirleyebilir. Bu projede, önce kiral *p*-alkil ve *p*-alkoksi sübstitüye 1,(3S)-Bis-[N-(*p*-aril)-karbamoiloksi]bütan türevleri, (S)-(+)-1,3-bütandiolün *p*-aril izosiyanatlar ya da *p*-aril benzoik asit ve difenilfosforil azid ile tepkimesinden elde edilmiş ve bunların akiral çözücüler içindeki organojelleşme yetenekleri, test tüp ters çevirme yöntemi ile incelenmiştir.

ANAHTAR KELİMELER: Düşük molekül ağırlıklı jelleştiriciler, kiral tanıma, N-aril karbamat, organojel, 1,(3S)-Bis[N-(*p*-aril)-karbamoiloksi]bütan

TABLE OF CONTENTS

Page

LIST OF FIGURES

Page

LIST OF TABLES

Page

LIST OF SCHEMES

Page

LIST OF ABBREVIATIONS AND SYMBOLS

3D : Three Dimensional

ACN : Acetonitrile

^{13}C NMR : Carbon-13 Nuclear Magnetic Resonance

CAB : 3-β-cholesteryl-4-(2-anthryloxy)butanoate

°C : Degree Celsius

$CDCl_3$: Deuterated Chloroform

cm^{-1} : Wavenumber

d : Doublet

DNA : Deoxyribonucleic acid

DPPA : Diphenylphosphoryl Azide

DSC : Differential Sanning Calorimetry

EL : Ethyl Laurate

equiv : Equivalence

FTIR : Fourier Transform Infrared Spectroscopy

g : Gram

^{1}H NMR : Proton Nuclear Magnetic Resonance

HRMS : High Resolution Mass Spectrometry

IPM : Isopropyl Myristate

IPP : Isopropyl Palmitate

LMOGs : Low Molecular-Mass Organic Gelators

m : Multiplet

MGC : Minimum Gelation Concentration

MHz : Megahertz

mL : Mililiter

mmol : Milimole

Na : Sodium

NaN_3 : Sodium Azide

NEt_3 : Triethylamine

NBP : n-Butyl Palmitate

NMR : Nuclear Magnetic Resonance

p : Para

PG **:** Partial Gel

ppm **:** Parts per million (NMR)

ppt **:** Precipitate

q **:** Quartet

RT **:** Room Temperature

s **:** Singlet

SEM **:** Scanning Electron Microscope

SOL **:** Solution

TEM **:** Transmission Electron Microscopy

δ **:** Chemical Shift (NMR)

ACKNOWLEDGEMENT

I would like to express my heartfelt gratitude to my esteemed advisor, Prof. Dr. Öznur DEMİR ORDU, for her invaluable guidance throughout this study. Her insightful ideas and unwavering dedication at every stage of the research were instrumental in shaping this work. Whenever I encountered challenges, she was there to encourage and steer me in the right direction, ensuring the successful completion of this project. Her continuous support has strengthened me both academically and personally. I am deeply thankful for her extensive knowledge, constructive suggestions, and patience, all of which were crucial to the success of this thesis. I consider myself extremely lucky to have had the opportunity to work with such an exceptional mentor, whose faith in me and constant support have been crucial throughout this journey.

I wish to thank my roommate Ece Nur ÇETKİN for supporting me under all circumstances.

I wish to thank colleagues Yunus KESGÜN for his help.

I am also deeply grateful to my husband, Samet TOPÇU, for his unwavering support and encouragement during all the emotional highs and lows of this journey.

I want to thank my family very much for their endless support of me.

.

1. INTRODUCTION

1.1 Low Molecular Weight Organogels: Synthesis and Applications

Compounds with a molecular mass of 3000 g/mol or less are known to gel organic solvents at concentrations below 5 wt%. These substances are termed low molecular weight organogelators.

One of the first studies in this field was carried out by Lin and coworkers in 1987. Photochemical investigations on 3-β-cholesteryl-4-(2-anthryloxy) butanoyl (Scheme 1.1) led to the serendipitous discovery of its gelling ability in many organic solvents at low concentrations (below 2%).

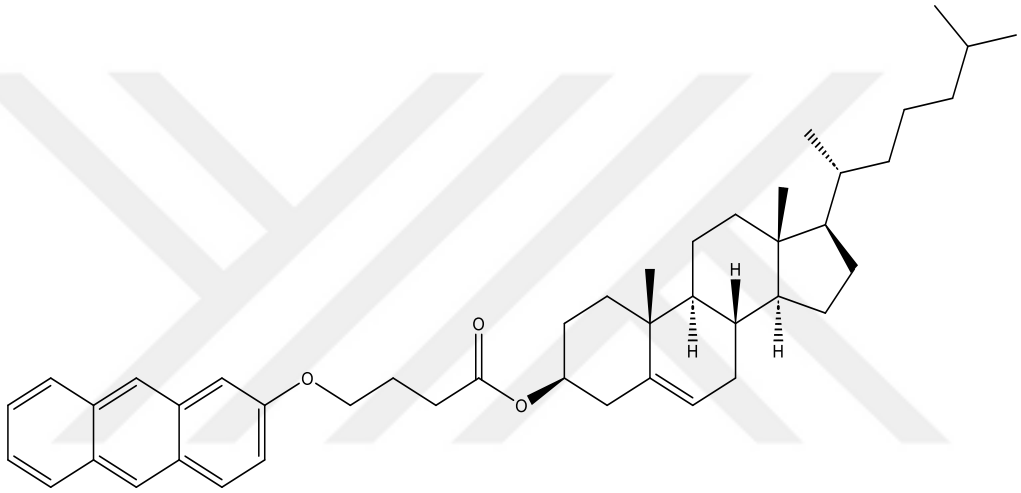

CAB (ALS)

Scheme 1.1. The CAB molecular structure

The research conducted by P. Terech and colleagues in 1997 examined how low molecular weight gel-forming agents (LMOGs) with fatty acids, anthryl groups, and steroid groups form organogel structure. Their findings revealed that the molecular arrangements of gel filaments and gelators in their pure crystalline forms differ. Additionally, it was found that many gelators display polymorphism even in their solid state. This reveals that the structural properties and behavior of gelators are more complex. Such studies provide important insights into the application areas and formulations of gels.

Esch and his coworkers (1999) investigated the gelling properties of cyclic bis-urea derivatives in organic solvents and to reveal the gel structures they used

infrared spectroscopy (IR), differential scanning calorimetry (DSC) and electron microscopy (SEM).

Murdan and his team successfully gelled sorbitone monostearate (Scheme 1.2) using a range of solvents, including long-chain hydrocarbons, fatty acid esters, and vegetable oils. The gel formed exhibited characteristics like a translucent, semi-viscous texture and the capacity to undergo thermal transitions. They carried out various experiments to assess its use in antigen delivery systems (Murdan et al., 1999).

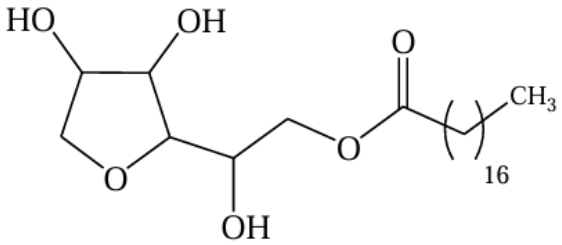

Scheme 1.2. The sorbitan monostearite molecular structure

Hanabusa and his collaborators (1999) synthesized 2-amino-2-phenylethanol based gelling agents in 1999. The effects of hydrogen bond forming chiral groups in the molecules on the gel structure were studied.

Tomioka and his collaborators synthesized didodecanoyl amides of α,ω-alkylidinedionamines and examined their gelation properties (2001).Their study demonstrated that the size of the alkylidene segment linking the amide groups plays an important role in gelation.

Maitra and his coworkers developed 1-pyrene-based organogelators in 2001. In this work, they explained how the helical structure resulting from the chiral molecule (Scheme 1.3) is formed in the gel.

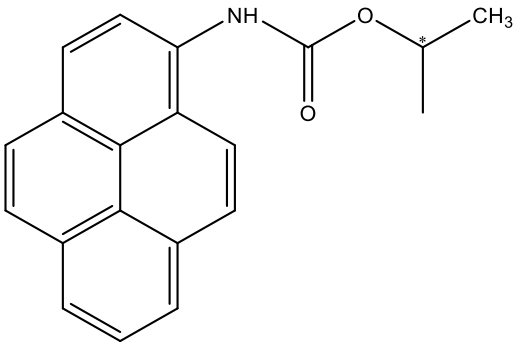

Scheme 1.3. The molecular structure of the chiral organogelators derived from 1-pyrene

Laan and his collaborators (2002) synthesized azobenzene bis-urea compounds and observed their gelation in many organic solvents. They reported that in some derivatives, gelation concentrations can be reduced down to 0.2 mM.

Suzuki and colleagues (2003) synthesized oxalyl amide derivatives as organogelators (Scheme 1.4) using a straightforward and cost-effective approach. They found that these molecules demonstrate outstanding gel-forming ability, with the resulting gels showing impressive resistance to thermal breakdown. The hydrogen bonding within the gel structures was analyzed using NMR and FT-IR spectroscopy.

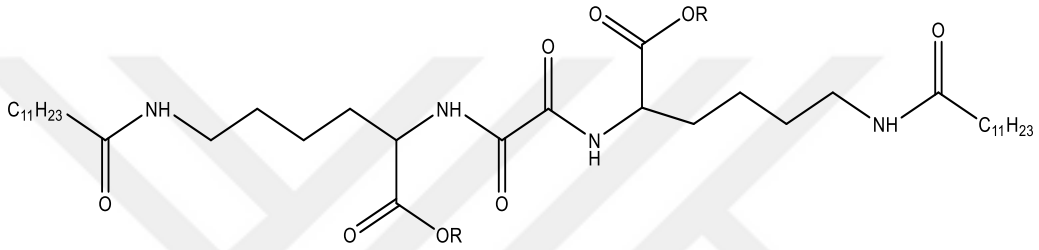

R: H, C_2H_5, C_6H_{13}, $C_{10}H_{21}$, $C_{12}H_{21}$

Scheme 1.4. Molecular structures of different oxalyl amide forms

Nigawara and his collaborators produced L-lysine based esters and investigated the gelation properties and thermal stability of these gels (2003). They used NMR and IR methods to understand the gelation mechanism.

Hirst and Smith (2004) prepared two-component dendritic gels containing diamidododecane and L-lysine-based peptides (Scheme 1.5.) and investigated the thermal stability of the resulting structures and the solvent effect on gelation.

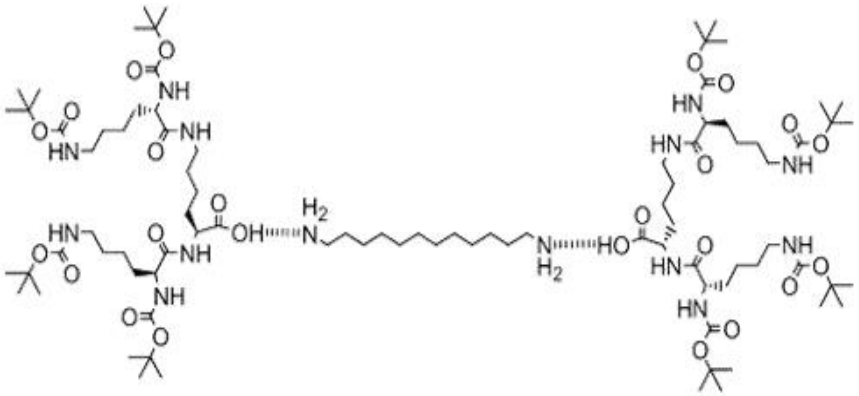

Scheme 1.5. Two-component dendric structure

Mohenmeyer and Schmidt (2005) synthesized urea and amide derivatives from *p*-phenylenediamine and investigated their gel-forming properties in polar solvents like valeronitrile and γ-butyrolactone. They also assessed the thermal stability of these gels at various concentrations and used scanning electron microscopy (SEM) to examine their morphology.

Tan and his collaborators (2006) synthesized new organogelators agents based on benzoic acid hydrazine. They investigated the interactions that facilitate gel formation. To elucidate the gel structure, they used UV-Visible and IR analytical methods. They also imaged the three-dimensional gel structure using SEM analysis.

Zhu and his coworkes (2006) investigated the solvent effect on the gelation properties of trehalose diesters (Scheme 1.6). They found that both the solvent's polarity and its interaction with the organic molecule play a key role in gelation. They highlighted that for successful gel formation, the organic molecule should interact with the solvent, but the interaction needs to be controlled or limited to control the solubility.

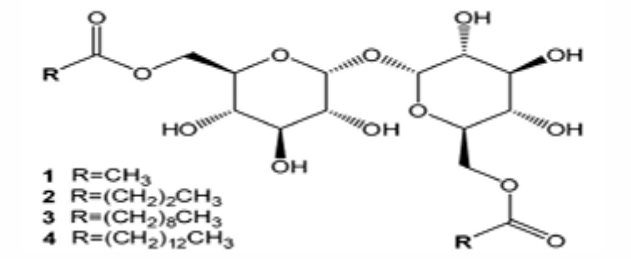

Scheme 1.6. General structure of trehalose-based organogelators

Lebel and coworkers (2006) investigated the gelation of sodium salts of diaminotriazine carboxylic acids in dimethyl sulfoxide. They used dynamic NMR (DNMR) for gelation mechanism studies, and SEM, atomic force microscopy (AFM) for morphology studies. They employed DSC methods to assess the thermal stability of the gels and emphasized the significant roles of long alkyl chains, sodium ions, and DMSO in the gelation mechanism.

Hardy and coworkers (2007) synthesized new low molecular mass organogelator agents derived from amides, carbamates, and ureas. They investigated the gelation capabilities of these molecules in organic solvents such as toluene and cyclohexane. They imaged the fibrous structures of the gels using SEM (Figure 1.1). Additionally, they examined the gelation of these molecules in oils

commonly used in the industry, including olive oil, sunflower oil, ethyl laurate, isopropyl myristate, and isopropyl palmitate. They indicated that the gels they prepared could be used in controlled drug release systems.

Figure 1.1. SEM image of the gel formed by the 2-amide molecule in toluene.

Wang and his coworkers (2007) investigated the gelation properties of urea-containing anthracene derivatives in solvents like cyclohexane, n-hexane and used the NMR spectra of the solution prepared at different concentrations to explain the gelation mechanism.

Mohenmeyer and his team (2007) synthesized a series of amphiphilic molecules containing urea-amide and bis-amide groups to investigate the relationship between structure and gelation properties. They explored how these compounds gelled in polar solvents, including valeronitrile, γ-butyrolactone, and toluene. They tested the gel properties against concentration both in toluene and in polar solvents and utilized SEM and TEM methods for morphology and IR methods for mechanism.

Li and his coworkers (2007) prepared L-glutamic acid based dendric compounds and investigated the effect of ultrasound on their gelation in toluene, hexane and water. In their study, they proved by FTIR method that ultrasound causes gelation by breaking some hydrogen bonds. They also used SEM, TEM for gel network structure.

D'Aleo and his team (2007) investigated how the number of methylene groups in the chain influenced gelation in long-chain benzyl and tert-butyl carbamate derivatives (D'Aleo et al., 2007).

Suzuki and his coworkers (2008) synthesized molecules based on N^{α},N^{ε}-diacyl-L-lysine. They investigated their gelation ability by attaching long alkyl chains to these molecules. They proved the existence of hydrogen bonds in the

structure of organogel by IR and NMR and explained the mechanism of organogel formation (Scheme 1.7) (Suzuki et al., 2008).

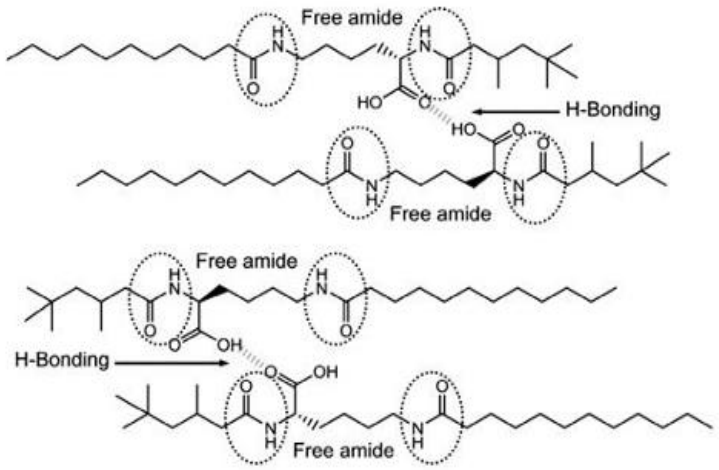

Scheme 1.7. The mechanism of organogel formation (Hydrogen Bond is observed between O-H----O=C)

Lim and his coworkers (2008) gelled terpenes, a type of organogel, in propylene glycol and dibutyrylglutamide. They used these structures in drug delivery systems and investigated their physicochemical parameters. They visualized the moment of gelation as shown in Figure 1.2.

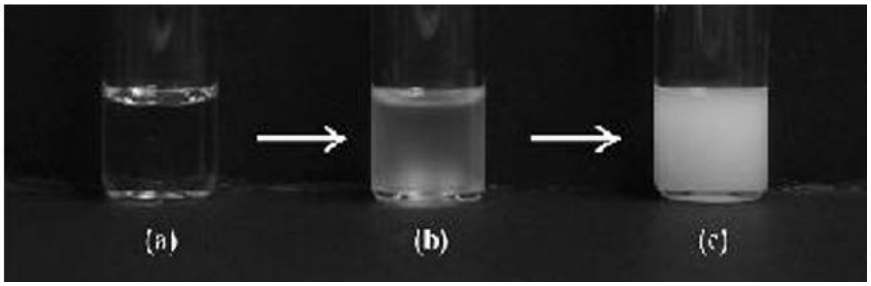

Figure 1.2. Gelation process: (a) a clear solution after heating; (b) a uniform, opaque suspension formed upon cooling and resting; (c) a white gel that develops after extended standing.

Vintiloiu and Leroux (2008) published research on the potential application of several organogelator molecules (listed in Table 1.1) within drug delivery systems.

Table 1.1. Drug delivery systems using organogels.

Organogelators	**Application Locations**	**Administered Drugs**
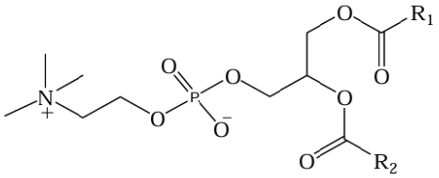 R_1 and $R_{2=}$ Fatty acids [Linoleic acid (55%) and Palmitic acid (13%) Lesitin	Application to the body through the skin	Diclofenac Piroxicam Tetrabenzamidine Scopolamine and boxaterol Propranolol Nicardipine Aceclofenac İndomethanic and diclofenac
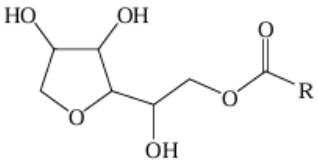 R = $(CH_2)_{16}CH_3$ veya $(CH_2)_{10}CH_3$ Sorbitan monostearate and molaureate	Nose Mouth Subcutaneous Kasichi	Propranolol Cyclosporin A

Table 1.1. (continued). Drug delivery systems using organogels.

Organogelators	Application Locations	Administered Drugs
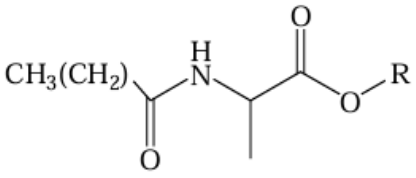 R = CH_3 veya CH_2CH_3 N-steroyl-1-alanine methyl or ethyl ester	Subcutaneous	Rivastigmine Leuprolide
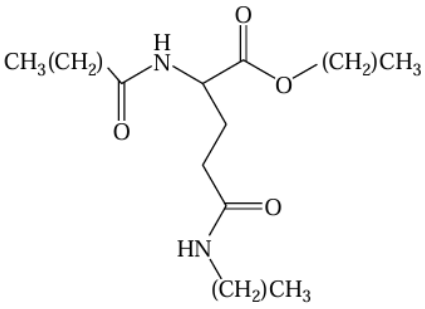 N-lauryl-1-glutamic acid di-n-butylamide	Application to the body through the skin	Haloperidol

Luo and his coworkers (2009) synthesized succinic acid derivatives shown in Scheme 1.8**.** They gelled these molecules in solvents such as benzene, toluene, o-xylene, CCI_4 and isopropyl alcohol. They visualized the structures of the gels formed in toluene and CCI_4 by SEM and proved the hydrogen bonds formed in the gel by FT-IR. They drew the hydrogen bonds formed within the organogel structure in Scheme 1.8.

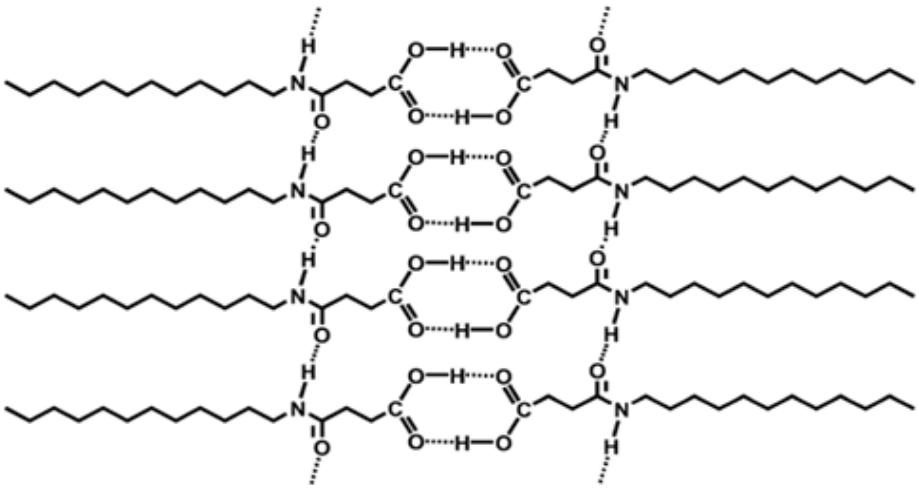

Scheme 1.8. Molecular structure of gel

Li and his coworkers (2009) synthesized ethydiamine-based derivatives as organogelators. They found that these structures formed strong gel structures in polar and apolar solvents. They investigated the fibrous structures within the gel samples using optical microscopy and scanning electron microscopy (SEM). To further explore the organogel's composition, they employed FT-IR and XRD techniques.

Zweep and his coworkers (2009) investigated the gelling ability of cyclohexane-based bisamide and bisurea compounds in polar and apolar solvents. In their research, they concluded that gelation occurred through hydrogen bonding in nonpolar solvents, while van der Waals interactions were dominant in polar solvents.

He and his coworkers (2010) synthesized 1,3,5-triphenylbenzene-based organogels. They observed that the solvent-to-gel transition of organogels (structures 3 and 4), depicted in Scheme 1.9, was reversible from a thermodynamic perspective when toluene was used as the organogelating solvent. On the other hand, the solvent-to-gel transition of organogels 2 and 5 in dioxane was primarily influenced by kinetic factors. The fibrous structures of the gels formed by molecule 2 (Scheme 1.9) in THF and dioxane were visualized by SEM (Scheme 1.10).

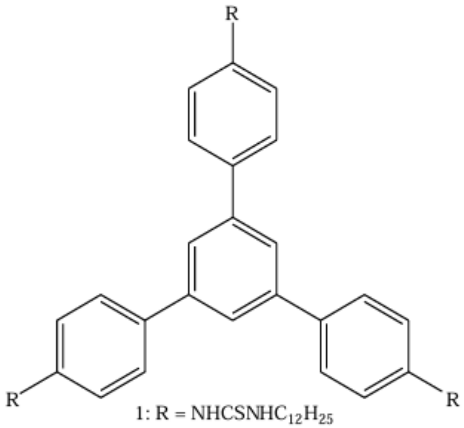

Scheme 1.9. General structure of synthesized molecules

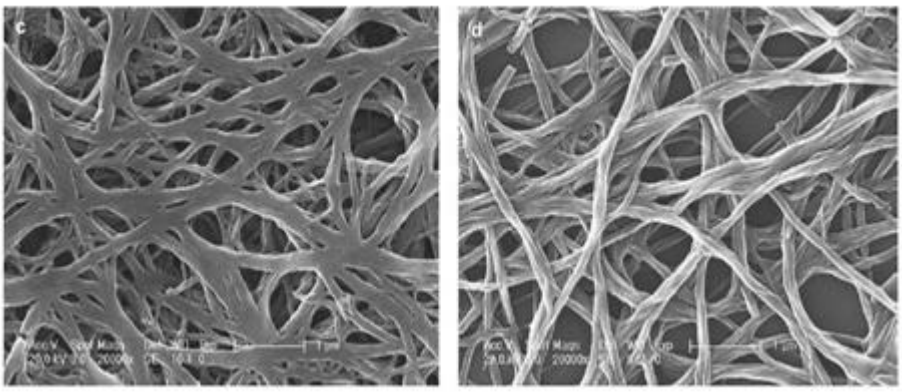

Scheme 1.10. SEM images of gels formed in THF and dioxane

Allix and his coworkers (2010) effectively employed IR and temperature-dependent NMR techniques to demonstrate the role of hydrogen bonding and π-π stacking in the gelation process of amino acid-based low molecular weight organogelators.

Cui and his team (2010) investigated how the size of *p*-alkoxy chains influences the gelation properties of compounds containing biphenyl and sugar structures. Their results showed that these groups impact gelation by altering solubility or through hydrophobic interactions.

Dutta and his coworkers (2010) studied tripeptide-based organogelators and emphasized the importance of **π-π** interaction in the gelation mechanism. They stated that the **π-π** interaction (Scheme 1.11), which occurs in addition to hydrogen bonding, causes the formation of layers and as a result of these layers coming together, solvents are trapped (Dutta et al., 2010).

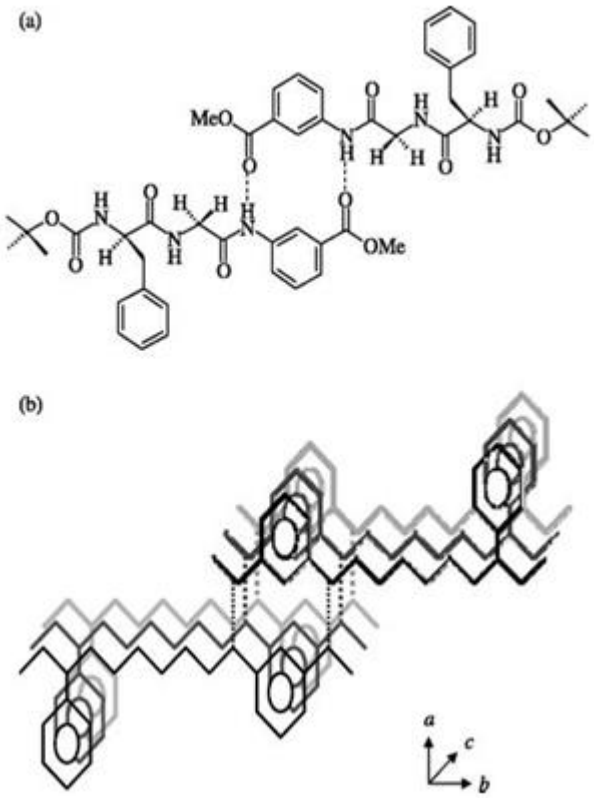

Scheme 1.11. Modeling (a) hydrogen bond formation, (b) **π-π** interaction for peptide-based organogelizing molecules

Bastiat and his coworkers (2010) synthesized gels using tyrosine-based organogelators in safflower oil and investigated their potential as delivery systems for rivastigmine, a drug used to inhibit acetylcholinesterase in the management of Alzheimer's disease.

Khan and Sundararajan (2010) synthesized bis-carbamate-based organogelator molecules and found that the gels formed by these compounds in benzonitrile formed tubular fibers. They also examined the inclusion of silver nanoparticles, phthalocyanine compounds, and perylene-based dyes within these structures (Figure 1.3).

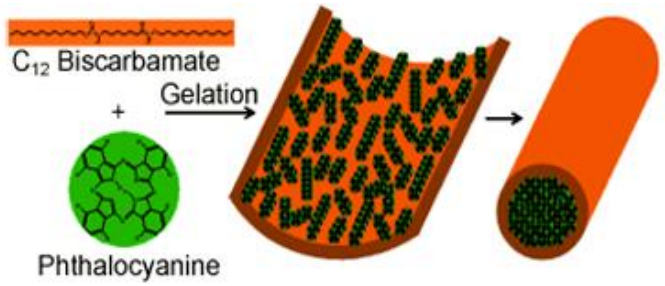

Figure 1.3. Modeling for phthalocyanine entrapped in bicarbamate gels.

Pal and his team (2011) investigated how the length of the alkyl chain influenced the gelation process of alanine-based organogelators. They discovered that structures like urea promoted gel formation.

Adhikari and his coworkers (2011) synthesized peptide-based molecules containing pyrine structure and investigated the gelation of these compounds especially in aromatic solvents. They found that the gels they prepared have fluorescent properties and stated that more solid gels can be obtained by adding graphene to the gels obtained in *o*-dichlorobenzene.

Rajaganesh and his coworkers (2012) reported that N-glycosylazobenzene structures selectively gel aromatic solvents and the gels obtained were photosensitive due to cis-trans isomerization. They reported that the gels obtained can be used in the purification of water from toxic aromatic solvents.

Tsai and his collaborators (2013) explored the gelation behavior of biscalix[4]arene compounds in alcoholic solvents and reported that the resulting gels have potential applications in cleaning diesel-contaminated seawater (see Figure 1.4).

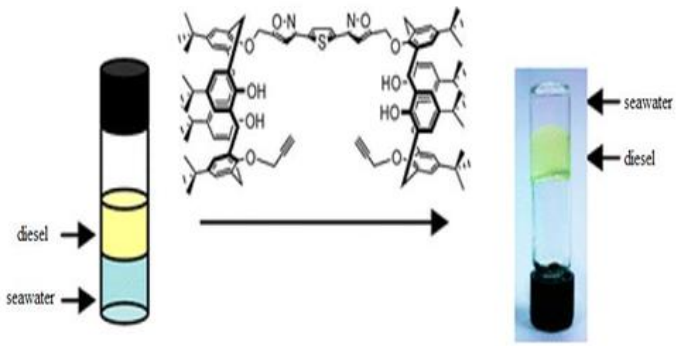

Figure 1.4. Phase selective gel formation of biscalix[4]arene compound.

Aneesh and his collaborators (2014) reported that oxadiazole-based stilbine molecules (OXD1,4,6,6,8,8,10,12, Scheme 1.12) behave as super gelators in apolar solvents and the gels they form high thermal and mechanical stability-gels. They have shown that gel structure is formed exclusively by π-π aromatic interactions without hydrogen bonding.

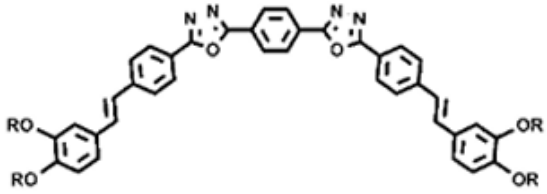

OXD1: R = CH_3 OXD4: R = C_4H_9

OXD6: R = C_6H_{13} OXD8: R = C_8H_{17}

OXD10: R = $C_{10}H_{21}$ OXD12: R = $C_{12}H_{25}$

Scheme 1.12. The molecular structure of stilbene derivatives bearing oxadiazole rings

Pang and his coworkers (2015) reported that naphthalimide-based gelling molecules form fluorescent gel after ultrasound application at room temperature. They analyzed their gelling abilities in n-propanol using several techniques, including UV-Vis spectroscopy, fluorescence measurements, infrared analysis, and SEM imaging (Figure 1.5).

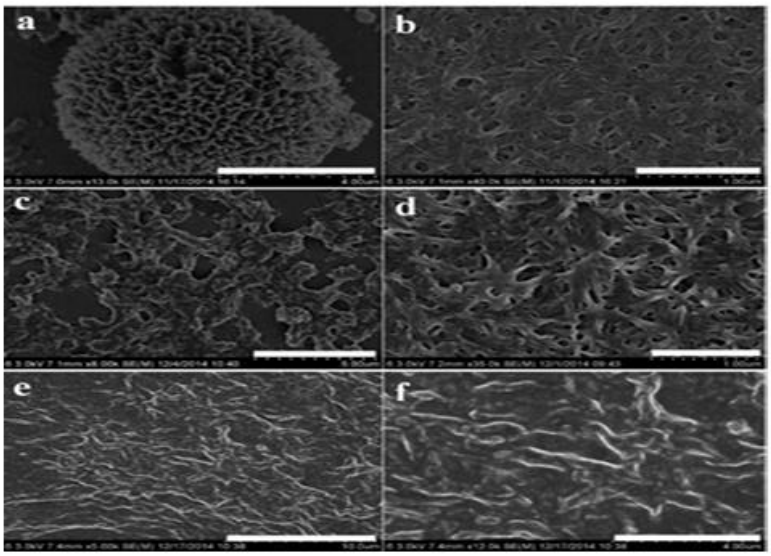

Figure 1.5. SEM images of naphthaline based xerogels

Xu and his collaborators (2015) synthesized low molecular weight gelling agents based on phenylboronic acid, incorporating hydrocarbon chains of varying lengths (Figure 1.6), and examined their gelation properties. They found that the gels formed nanofiber and spherical structures, with gelation efficiency improving as the length of the alkyl chains increased. The interactions necessary for gel formation were studied through FT-IR and ^{1}H NMR analysis.

,

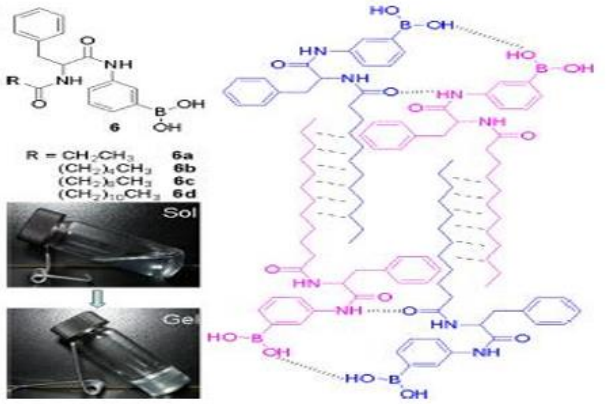

Figure 1.6. The molecular design of gelators, the interactions occurring between their molecules, and the transition from sol to gel in organogels.

Demir-Ordu (2015) synthesized molecules containing bis-carbamate functional groups and investigated their gelling properties in organic solvents (Scheme 1.13). In this study, it was observed that solvent selection, molecular structure, concentration and especially temperature effects for some substances were very important in gelation phenomena. The best gels were obtained with an "n" number of three, and groups in the para position were also found to affect gelation. *p*-Alkoxy derivatives can gel better than *para*-alkyl derivatives and gel structures form nanofibers (Figure 1.7). Fiber thickness of 60-180 nm was proved by SEM. In the *p*-alkyl series, cryogels were obtained at -18 ^{0}C with increasing chain length. In the scanning electron microscopy images of the dry gels, it was observed which the gel morphology was nanoporous only for the *p*-hexyl (n:3) derivative, although the gel morphology was nanofiber for most gels. It was observed that the gels formed at -18 ^{0}C were more transparent and their structures formed finer fibers or pores. The minimum gelation concentration of the *p*-hexyloxy (n:5) derivative in n-butyl palmitate gel is below 0.2% (by mass), which classifies it as a "super gelling agent". In this project, the gelation mechanism was

also elucidated by NMR and IR studies, and hydrogen bonding between C=O...N-H, **π-π** interactions between aromatic sctructures and van der Waals forces of *p*-alkyl groups were investigated.

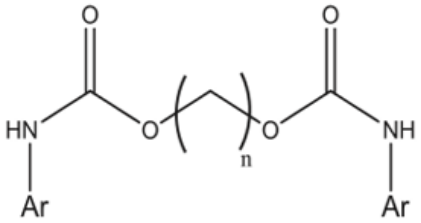

Ar = **α**-naphthyl, *p*-tolyl, *p*-methoxyphenyl, *p*-ethylphenyl, *p*-ethoxyphenyl, *p*-propyphenyl, *p*-butylphenyl, *p*-butoxyphenyl, *p*-hexylphenyl, *p*-hexyloxyphenyl (n= 3, 4, 5, 6)

Scheme 1.13. Structural formulas of the bis-carbamates

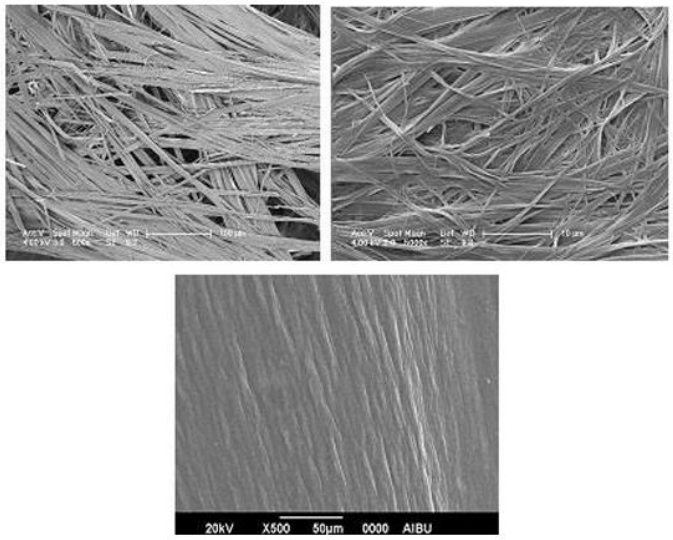

Figure 1.7. (a) SEM image of 3-OBu (n=3, *p*-butoxy) toluene dry gel (b) SEM image of 5-OHex (n=5, *p*-hexyloxy) toluene dry gel (c) SEM image of 3-Pr (n=3, *p*-propyl) toluene dry gel

Wang and his coworkers (2017) synthesized carbamate molecules with different alkyl chains as supramolecular organogelators (Figure 1.21). They noted that the self-assembly of these molecules is driven by hydrogen bonding, π-π stacking, and van der Waals forces. They also found that the gels formed by these

structures have phase selective properties in oil-based substances, unrefined petroleum, diesel fuel, petrol, cyclohexane compound, mixtures of hexane and water.

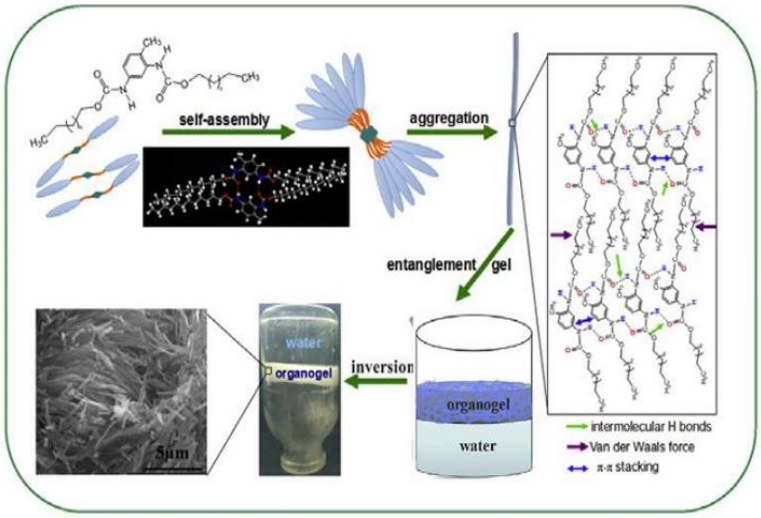

Figure 1.8. Diagram illustrating the self-assembly process in the gel

Ongaratto and his coworkers (2019) reported that new long alkyl chain N-acylamino hydrazides with N-acetylamino hydrazides have low molecular mass gelling properties in apolar and polar organic solvents and their use as molds for the preparation of gold nanoparticles. Without using a reducing agent, it was reported that organogelators reduce $HAuCl_4$ and cause nanoparticle formation. They used SEM for structure determination of gel morphologies and found that short-chain molecules formed more compact and more regular structures.

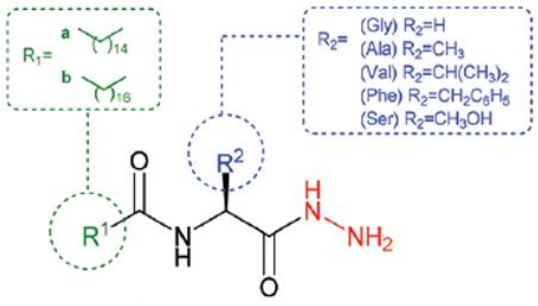

Figure 1.9. Structure of organogelizing molecules

Podder and his coworkers (2019) synthesized and characterized new tripeptide-based low molecular mass super-organogelator molecules. They also tested the gelation properties of the derivatives in hydrocarbons, crude oil and aromatic solvents. They reported that peptide derivatives with electron-rich phenyl system interacted with cationic dyes and therefore could be used in wastewater treatment. In addition, they also investigated the phase selective properties of these gels in water-oil mixtures. They also gave some examples for the application of these gels in removing oil from contaminated water.

Kodama and his team (2022) investigated the development of low molecular mass gelators derived from carboxylic acids that are derived from chiral cyclic β-amino acids, as well as the properties of the supramolecular structures formed by these gelators. In the study, stereochemical effects on the gelation processes are discussed in detail and techniques such as infrared spectroscopy, X-ray diffraction, scanning electron microscopy are used to analyze the intermolecular interactions in xerogels. Additionally, the impact of alkyl chain length on gelation performance was assessed by considering the crystallographic properties of the corresponding model compounds. Another important finding of the study is the effects of amine groups on chiral recognition. In interactions with amines, gelation occurred successfully only when a diastereomeric salt was formed, whereas other interactions resulted in the formation of precipitates. Chiral recognition was investigated within a gel matrix, and the chirality of the gels, formed by adding different enantiomers, could be visually identified due to the changes in their appearance (Figure 1.10).

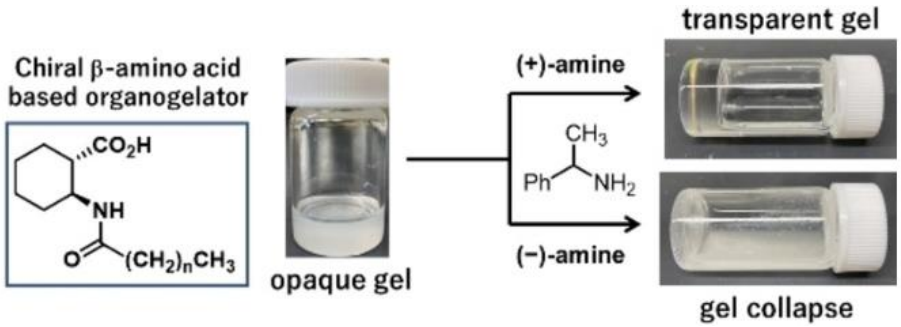

Figure 1.10. Visual identification of the enantiomers of amines by preparing chiral gels

Komba (2024) synthesized D-glucono-1,4-lactones by esterifying all hydroxyl groups with linear saturated fatty acids to create a novel low molecular weight organogelator, and investigated its gelation properties. The study showed that the addition of a fatty acid led to the conversion of the six-membered ring D-glucono-1,5-lactone into the five-membered ring D-glucono-1,4-lactone, regardless of the fatty acid chain length (Figure 1.10). However, the gelation strength was found to depend on the fatty acid length, with compounds esterified with palmitic acid (16 carbons) and stearic acid (18 carbons) exhibiting more robust gel formation. Analysis using electron microscopy revealed that the structure of the xerogels varied based on the fatty acid length, with some samples forming fibrous structures, while others displayed porous or plate-like crystalline forms. In addition, the emulsification properties and crystal polymorphism of these compounds were confirmed, and a detailed analysis of the polymorphic crystals was carried out using FT-IR to examine the intermolecular packing arrangement.

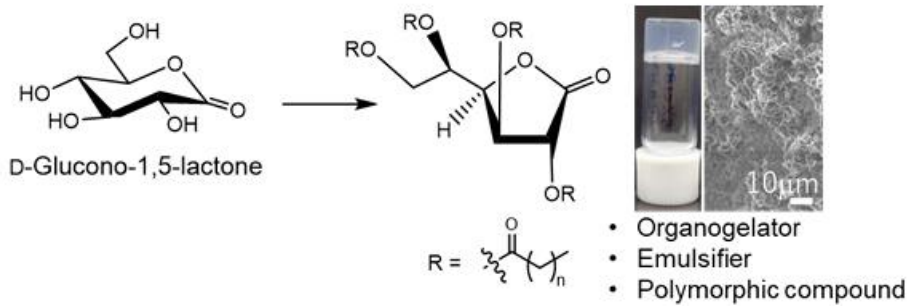

Figure 1.11. The six-membered ring is transformed into a five-membered ring.

1.2 Theory

1.2.1 The Explanation and Categorization of Gel Types

Lloyd's statement from 1926 remains relevant: "Recognizing a gel is simpler than defining it" (Lloyd, 1926).

Flory's definition provides the most comprehensive framework. He stated that for a substance to be classified as a gel, it must meet the following conditions: It must possess a continuous structure with macroscopic dimensions that remain stable throughout the course of an analytical experiment, and its rheological

properties should mimic those of a solid. Given these expansive criteria, it becomes evident that a wide variety of systems can be categorized as gels (Lloyd, 1926).

An alternative perspective derives from Gelbart and Ben-Shaul, who suggest using the term "Complex Liquids" to describe the different forms of solutions, emulsions, suspensions, and gels (Lloyd, 1926).

Most gels can be described as having a solid-like phase, which consists of a small component that forms a three-dimensional network within a liquid or gas. In solid-liquid gels, this network typically stops the solvent from flowing at a larger scale, while the liquid phase helps keep the structure intact, preventing it from collapsing (Lucas, 2001).

Gels are commonly categorized according to their chemical or physical characteristics. In chemical gels, the network is established entirely by covalent bonds, which makes the gelation process irreversible. On the other hand, physical gels are typically composed of smaller molecular units connected through non-covalent interactions. Thanks to these non-covalent bonds, physical gels can undergo reversible transitions between the gel and solution phases at moderate temperatures. This category includes a variety of gels such as mineral clays, polymers, and proteins. A specific subset of physical gels is low molecular weight organogels, which are capable of self-assembling into fibrous structures and forming gels through interactions like hydrogen bonding, π-π stacking, electrostatic forces, and van der Waals interactions. Furthermore, solvophobic interactions and entropy-driven effects significantly contribute to the gelation process (Lucas, 2001).

Gels are commonly divided into two major types based on the solvents involved in their gelation: hydrogels and organogels (Sri et al., 2012).

1.2.1.1 Hydrogels

A hydrogel is a network system that forms in a hydrated environment. Sometimes they can exist in the form of a colloidal gel, which acts as a dispersion medium for water. Hydrogels consist of polymer networks cross-linked either chemically or physically, allowing them to absorb significant amounts of water. Hydrogels containing hydrophobic groups expand more slowly than those with hydrophilic groups. This is because hydrophobic groups tend to aggregate when exposed to water, reducing their interaction with water molecules (Sri et al., 2012).

Hydrogels can be analyzed in three different classes according to their structure (Sri, et al., 2012):

- Amorphous hydrogels
- Semi-crystalline hydrogels
- Hydrogen bonded hydrogels

1.2.1.2 Organogels

An organogels are gel-like materials, characterized by its flexible, solid-like nature, in which a non-polar external phase is trapped within its network. The non-polar phase is immobilized in the voids of the three-dimensional network structure resulting from physical interactions between the structures formed by the gelling compounds themselves. Organogels are naturally and thermodynamically stable and have been studied for their potential to deliver bioactive substances in a controlled manner. The article published in 2011 explores the properties of organogels, different categories of organogelators, and their use in controlled release systems. (Sahoo et al., 2011).

Organogels are composed of two interconnected systems: gelling molecules and molecules of organic solvents (Esch et al., 2015). Gelator compounds can spontaneously organize into fibrous structures through physical or chemical interactions. These fibers intertwine to form a complex, multidimensional network. This network structure restricts the movement of the organic solvent, which is contained within the self-assembled framework of the gelator.

Organogels are classified into two categories according to the molecular weight of the gelling compound: low molecular weight organogelators (LMOGs) and polymer-based organogelators (Vintiloiu and Leroux, 2008).

1.2.1.2.1 Low Molecular Weight Organogelators (LMOGs)

A group of organic compounds with low molecular weight (less than 3000) has been found to act as organogelators, forming gels at very low concentrations (around 5 wt%) in a variety of organic solvents (Demir-Ordu et al., 2015). Non-covalent interactions, such as hydrogen bonding, π-π stacking, and other forces like hydrophobic attraction, play a crucial role in the creation of gel networks (Lucas, 2001). These forces lead to the formation of fibrous, nanoscale networks in which

the solvent is encapsulated within a three-dimensional structure. In materials, in their gelled state, even extremely small quantities of organic gelators, sometimes as low as 0.1 wt%, can effectively trap the solvent and form a stable, self-sustaining structure (Smith, 2007). The ability of a low molecular weight compound to create a gel is governed by its minimum concentration for gel formation (MGC), which indicates the smallest amount of gelator required to form a stable gel (Lin and Weiss, 1987).

The primary factors influencing the formation of low molecular weight organogels are outlined by Hoare and Kohane (2008):

- Fiber formation by control of an anisotropic growth process
- Intertwining of the aggregates in a 3D network
- Prevention of crystallization

1.2.1.2.2 Polymeric Organogelators

Polymeric gelators cause the solidification of organic liquids by forming either physical or chemical bonds. These gels can take on various structures, including linear, branched, or star-like polymer arrangements (Vintiloiu and Leroux, 2008).

1.3 Factors Necessary for Gel Formation

For gelation to take place, three key conditions must be met:

1. The molecule should exhibit some degree of solubility in the solvent. This allows it to dissolve upon heating and to form a gel when the temperature is lowered.
2. The molecule must have partial solubility in the solvent. If the solubility is insufficient, complete dissolution does not occur upon heating, and gelation fails to take place.
3. The molecule should demonstrate the ability to self-organize through non-covalent forces, such as hydrogen bonding, π-π interactions, and hydrophobic effects. Among these, hydrogen bonding plays a crucial role in the formation of the gel structure (Smith, 2007).

1.4 Types of Intermolecular Interactions

The interactions between gelator molecules can arise from several forces, such as van der Waals forces, dipole-dipole interactions, ionic forces, hydrogen bonds, London dispersion, and π-π stacking. It has been noted that there is a direct connection between the gelator's molecular structure, these intermolecular forces, and its gelation behavior. Even a minor modification in the chemical structure of the gelator can lead to a significant change in its ability to form a gel (Vintiloiu and Leroux, 2008).

1.4.1 Hydrogen Bonding

In simple valence bond theory, it is generally understood that a hydrogen atom can form only a single bond. However, in many instances, hydrogen is treated as capable of forming an additional bond, which is known as a hydrogen bond. There are two types of hydrogen bonds (Kollman and Allen, 1971):

1. Hydrogen bonds that connect atoms whose electronegativity is higher than that of the hydrogen atom.
2. Hydrogen bonds linking atoms with lower electronegativity than the hydrogen atom.

A hydrogen bond is formed between a proton donor group, A-H, and a proton acceptor group, M, where A is an electronegative atom such as O, N, N, S, P, P, Se, X (such as F, Br, I, Cl). The acceptor group can be only the electron pair of an electronegative atom or the π electron orbitals of a poly bond (unsaturated) system. In the M-H···H-A system (M = a metal such as Ir or Re, A = O, N, etc.), the H···H distance is around 1.75-1.90 Å (Alkorta, et al., 1998). In general, a hydrogen bond can be defined as a proton shared by two lone electron pairs. Strengthening the dipole moment of the donor and the electron pair in the acceptor atom increases the strength of the hydrogen bond (Lucas, 2001).

Examples of spontaneously formed hydrogen bond sequences include base pairs between cytosine and guanine, adenine and thymine, and complementary hydrogen bonds in double-stranded spiral structure of DNA (Scheme 1.14) (Lucas, 2001).

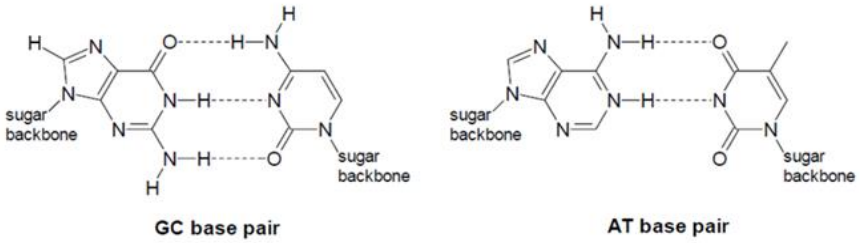

Scheme 1.14. Hydrogen bonding in DNA

1.4.2 π – π Interaction

π-π interactions refer to stabilizing non-covalent forces between parallel aromatic rings. These interactions are common in various contexts, influencing processes like molecule self-assembly, DNA binding, guest-host interactions, and protein side-chain behavior. It has been observed that when groups that pull electron density away from the phenyl rings are introduced, the strength of these interactions increases. This increase is due to the shift of electron density away from the center of the ring, which reduces repulsive forces between the rings.

1.4.3 van der Waals Interactions

Substances' properties like melting point, boiling point, solubility, electrical and thermal conductivity, structure, and hardness are influenced by forces between molecules. These forces are based on the attraction between opposite charges. For molecules that don't have any charge, these attractions can generally be grouped in the following ways (Ebbing and Gammon, 2009).

A) Dipole- dipole interactions

B) London forces

A) Dipole-Dipole Interactions

Polar molecules interact with each other due to the attraction between their oppositely charged regions. These molecules tend to align so that the positively charged part of one molecule is positioned near the negatively charged part of another. A molecule is classified as polar when its structure leads to a separation of charge (Ebbing and Gammon, 2009).

B) London Forces

London forces, or dispersion forces, are weak interactions between molecules that arise from temporary fluctuations in electron distribution, leading to momentary charge imbalances. These forces become stronger as the molecule's size increases, due to an enhanced ability to be polarized and a larger exposed area (Ebbing and Gammon, 2009).

1.5 Gelation Process

Organogelators with low molecular weight are capable of forming gels in organic solvents at concentrations under 2% (Demir-Ordu et al., 2015).

The process of molecules coming together is influenced by different types of forces depending on the solvent involved. In organic liquids that don't form hydrogen bonds, the main force driving the gelation process is typically the attraction between hydrogen atoms. However, other factors such as the interactions between ring structures, coordination of metals, and charges between particles can also play important roles. In water, and to a lesser extent in certain other liquids, the importance of hydrogen bonds and charge-based forces is reduced, depending on how well the liquid can engage in these types of attractions. In these cases, the primary factors driving the arrangement of molecules are the repulsion between water and the molecules, as well as other weak forces and interactions between the rings. Regardless of the type of liquid used, for the molecules to form a gel, a careful balance between their attraction to water and their tendency to repel it must be maintained. If the molecules dissolve too easily, they won't come together as expected. On the other hand, if they strongly avoid the liquid, they may cause the solution to separate or form solid structures (i.e. precipitation) instead (Lucas, 2001).

Typically, the process of gel formation occurs in the following stages (Figure 1.12). At high temperatures, gelling molecules are necessary to eliminate the strong intermolecular interactions responsible for self-assembly. As the solution cools, these interactions become stronger and gelation occurs (Lucas, 2001):

1. Because these interactions are directionally dependent, the self-assembly process happens in just one direction, resulting in the creation of narrow threads. These threads can either grow or intertwine with one another, eventually forming groups of multiple fine threads that reduce the overall surface energy of the individual threads.
2. With increasing entanglement, a 3D network structure develops over time.
3. This process is considered a gel formation at the macroscopic level.

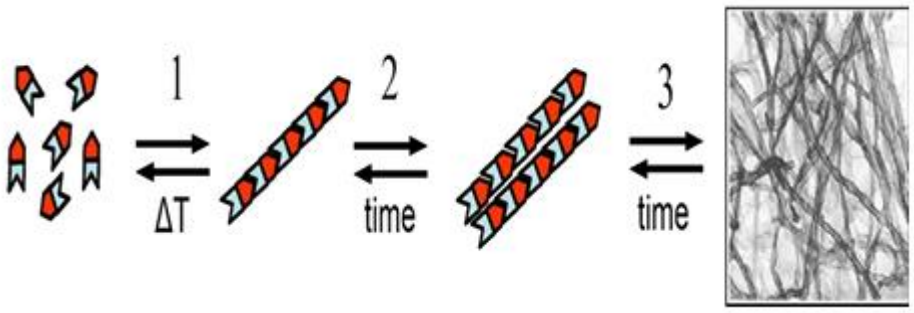

Figure 1.12. Diagram illustrating the creation of a three-dimensional network beginning with gelator molecules in solution (Lucas, 2001)

As shown in Figure 1.13, when the heated solution cools, the molecules begin to cluster, resulting in the formation of three distinct phases:

- A somewhat orderly grouping of molecules that forms crystals,
- An irregular grouping that results in an amorphous solid,
- A transition between these two processes that leads to the gel form (Maity, 2007).

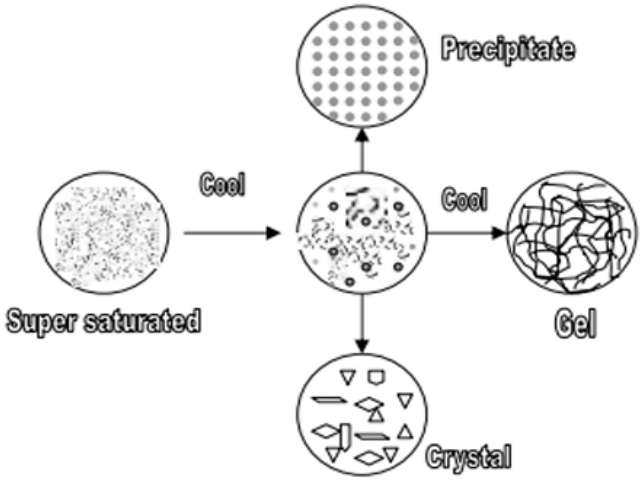

Figure 1.13. Diagram illustrating the different modes of aggregation (Maity, 2007)

1.6. Aim and Scope of the Work

Many low molecular mass organic compounds (molecular mass≤3000 g/mol) gel organic solvents at concentrations below 5 wt% thanks to the network structure they form, forming supramolecular gels, one of the physical gel types. Compounds with this property are called "low molecular mass organogelators". The gels formed by organogelators are nanoscale and network structured and are classified as soft materials. During gelation, organogelating molecules come together with physical forces like hydrogen bonding, van der Waals or π-π interactions to form a nano-fiber structure (5-100 nm in diameter) and then a supramolecular network structure with non-covalent cross-links formed between the fibers. Organic solvent is trapped in this network structure and in this way, the flow of solvent is stopped and gel formation is achieved. The gelation process is thermoreversible and solution-gel transition can be achieved repeatedly by heating-cooling. In recent years, these molecules, which are capable of gelling organic solvents, have attracted significant attention due to the distinctive structures of the gels they form and their diverse applications. Due to their nanostructures, low molecular mass organogels, like their polymeric derivatives, are also used in drug delivery systems (Bastiata and Leroux, 2009), separation processes (Bhattacharya et al., 2001; Debnath et al., 2008; John et al., 2010; Chen et al., 2011; Rajaganesh et al., 2012; Feng et al., 2014) and as liquid crystal materials (Xin et al., 2008; Hou et al., 2009; Huang et al., 2014).

Gelation is a phenomenon between solution and precipitate and depends on many factors. Therefore, although it is not possible to predict gelation in advance, it has been possible to design gelable molecules by knowing these factors. The most important factor is the compound structure. Structures such as long aliphatic chains, hydrogen bonding groups, aromatic rings are very important in the gelation mechanism. In general, low molecular mass organogelators with double hydrogen bonding groups, such as bis-urea (Figure 1.14) (van Esch et al., 1997; van der Laan et al., 2002; Zweep et al., 2009; Kim et al, 2011) and bis-amides (Figure 1.15) (Suzuki et al., 2008; Zweep et al., 2009; Huang et al., 2014; Mohenmeyer and

Schmidt, 2007; Kocasoy et al., 2018)) form the network structure by intermolecular hydrogen bonding with two neighboring molecules.

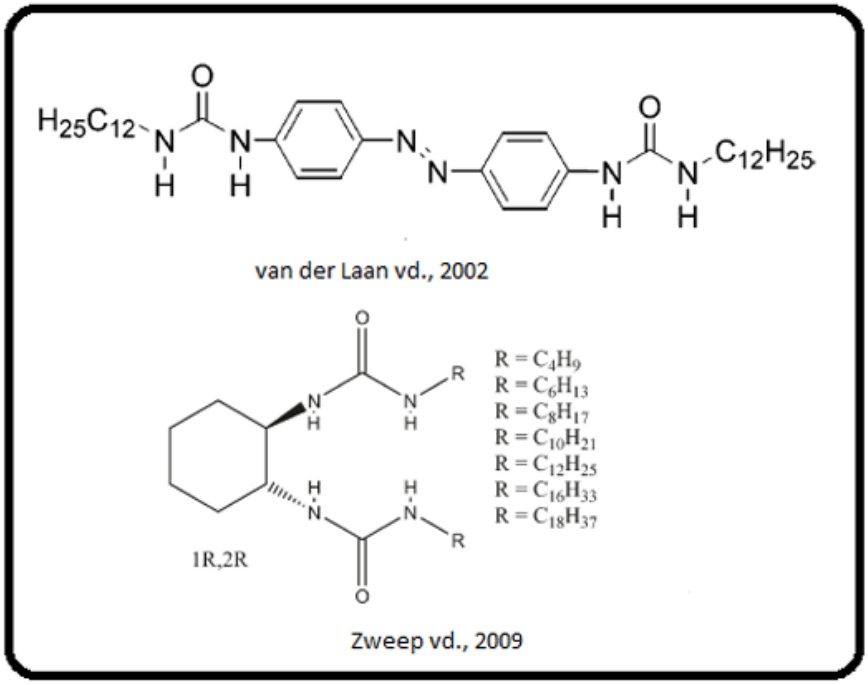

Figure 1.14. Examples of bis-urea organogelator molecules

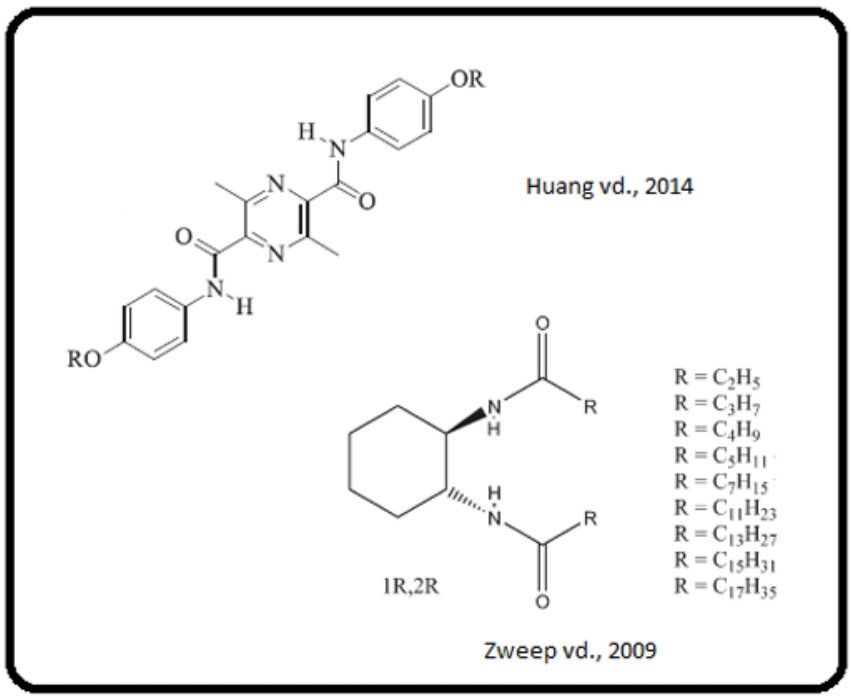

Figure 1.15. Examples of bis-amide organogelator molecules

Some bis-carbamates have also been reported to self-assemble via hydrogen bonding and form gel structures (Escuder et al., 2005; Khanna et al., 2006; Khanna et al., 2009; Khan and Sundararajan, 2011). In a previous study by Demir-Ordu and her coworkers (TÜBİTAK 3501-109T919, Demir-Ordu et al., 2015), achiral bis[N-(*p*-aryl)carbamoyloxy]alkanes (Figure 1.16, a) were found to form gels in a three-dimensional network structure (Figure 1.16, b) with hydrogen bonding, π-π and van-der Waals interactions.

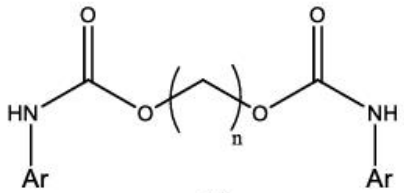

(a)

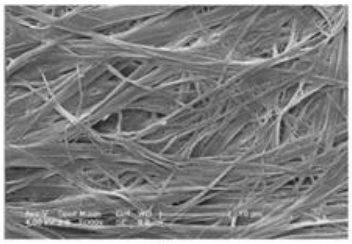

(b)

n= 3, 4, 5, 6

Ar= α- naphthyl, *p*-tolyl, *p*-methoxyphenyl, *p*-ethylphenyl, *p*-ethoxyphenyl, *p*-propilphenyl, *p*-butylphenyl, *p*-butoxyphenyl, *p*-hexylphenyl, *p*-hexylphenoxyphenyl

Figure 1.16. (a) Achiral molecules obtained in TÜBİTAK 3501, 109T919 project (1,6-Bis[N-(*p*-aryl)-carbamoyloxy]hexane, 1,5-Bis[N-(*p*-aryl)-carbamoyloxy]pentane, 1,4-Bis[N-(*p*-aryl)-carbamoyloxy]butane, 1,3-Bis[N-(*p*-aryl)-carbamoyloxy]propane), (b) SEM image of the network structure of *p*-hexyloxyphenyl derivative in toluene gel (Demir-Ordu et al., 2015).

While gelation properties are related to the structures present in organogelator molecules, they are also related to the orientation of these structures in three dimensions. Therefore, in chiral molecules, chirality is an important factor affecting self-assembly. The presence of chirality in the gelator molecule can promote or inhibit gel formation by affecting the molecular arrangement. In some cases, racemic mixtures showed weaker gelation properties than their pure enantiomers. For example, Hirst et al. (2004) reported a two-component mixture of D- and L-lysine based peptides and aliphatic diamines. They studied dendritic organogelators (Figure 1.16 (a)) to investigate the effect of chirality on the hydrogen bonded self-assembly of these compounds and to find how parameters

such as gel formation and gel strength are affected. The addition of an enantiomer (D,D,D) to the gel structure formed by its mirror reflection (L,L,L) disrupted the helix structured-fiber formation and thus reduced the gelling property.

Chiral organogels have attracted considerable attention in recent years due to their applications in chiral recognition. In the formation of supramolecular organogels, the chirality in the structure of the molecule is transferred to the nano- or meso-sized gel structure during self-assembly and chiral gels are formed. However, the rules regarding this transfer are still unclear and the subject is not clarified. There are a limited number of studies on chiral recognition in the literature.

de Loos and his coworkers (2001) first studied the self-assembly of bis-urea compounds with two stereogenic centers (Figure 1.17) in solution and found the effect of chirality on the self-assembly mechanism and suggested that this mechanism could be used for chiral recognition in gels. This study, for example, revealed that (R)-2 is entrapped by different interactions in (S)-1 and (R)-1 gels obtained in 1-butanol and pioneered chiral recognition studies.

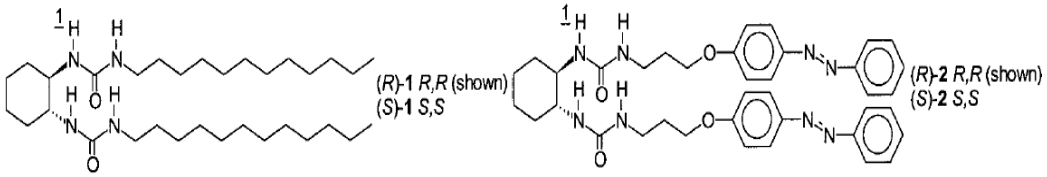

Figure 1.17. Bis-urea compound structures with two stereogenic centers (de Loos et al., 2001)

Tripathi and his coworkers (2012) found that organogelators composed of L-phenylalanine showed selectivity towards tetrabutylammonium salts of (R)- and (S)-mandelic acid in DMSO/$CHCl_3$ (Figure 18a). The solution containing chiral organogelator formed gels with (R)-mandelate but not with (S)-mandelate (Figure 18b-d).

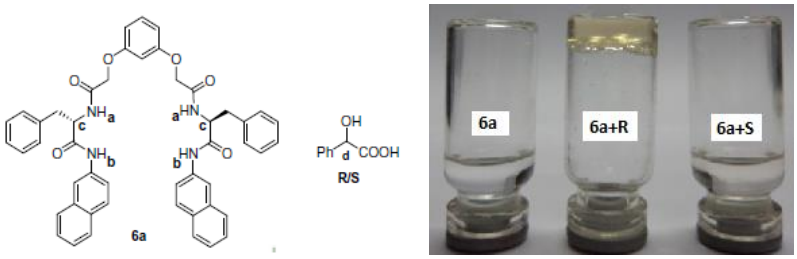

(a) (b) (c) (d)

Figure 1.18. (a) Structures of L-phenylalanine organogelator and mandelic acid, (b) solution in DMSO/$CHCl_3$, (c) Gel structure formed by the addition of (R)-mandelate, (d) Solution formed by addition of (S)-mandelate (Tripathi et al., 2012)

Edwards and Smith (2014) found that the formation of a fiber-structured, lysine-based, two-component dendrimeric gel (Figure 1.19 a, G2-Lys+C6S or G2-Lys+C6R) is affected by the chirality of the components. In instances where the amine compound used as the second component was R (Figure 1.19 a, C6R), the gel formed was found to be much more thermally stable. This difference was explained by the orientation of methyl in the chiral center, hence the difference in chirality. SEM and TEM studies also revealed that both gels were morphologically different. In the selectivity studies, the chiral gel consisting of a lysine-based molecule and 100% C6S amine took the (R)-amine compound (C6R) into the gel structure while C6S passed into the solution (Figure 1.19b). The presence of such a substitution between two chiral amines has shown that such gels can be used in chiral recognition. Based on this study, achiral and different chiral amine systems were investigated with a lysine-based molecule and the effects of chirality on gel thermodynamics were also studied (Edwards and Smith, 2018).

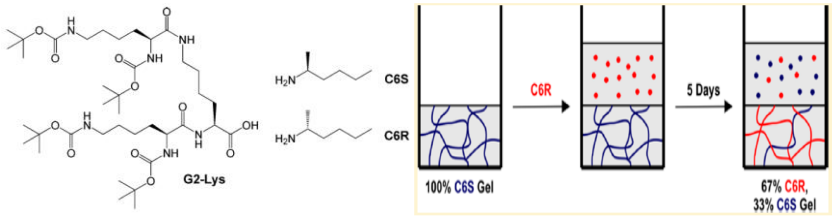

(a) (b)

Figure 1.19. (a) Two-component dendrimeric gelator structure, (b) Gel structure selectively absorbs C6R compound (Edwards and Smith, 2018)

The aim of the project was to synthesize eight chiral 1,(3S)-Bis[N-(*p*-aryl)-carbamoyloxy]butane compounds and to study their organogelation abilities by examining the influence of the length of the *p*-alkyl or *p*-alkoxy substitution on gelation. The obtained organogels will be examined for the purpose of chiral recognition mentioned above in a future work.

Table 1.2. General structure of the compounds (1,(3S)-Bis[N-(*p*-aryl)-carbamoyloxy]butanes) synthesized within the scope of the project

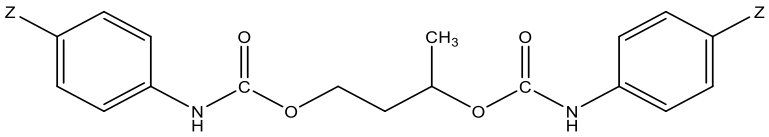

Compound No	-Z
S-Hex	-hexyl
S-O-Hex	-hexyloxy
S-Hep	-heptyl
S-O-Hep	-heptyloxy
S-Oct	-octyl
S-O-Oct	-octyloxy
S-Dec	-decyl
S-O-Dec	-decyloxy

2. MATERIALS and METHOD

^{1}H-NMR and ^{13}C-NMR spectra were obtained using JEOL NMR spectrometers (400 MHz for proton and 100 MHz for carbon) at room temperature. All chemical shifts (δ) are expressed in parts per million (ppm), relative to TMS; coupling constants (J) are reported in Hertz (Hz). The following abbreviations are used for the NMR signals: s= singlet, d= doublet, t= triplet, q= quartet, m = multiplet.

Infrared spectra were acquired using a SHIMADZU FTIR-8400S spectrometer (either in KBr pellet form or neat).

High resolution mass spectra were run on a Waters Lct Premier XE oa-TOF Mass Spectrometer, on TOF-LC-MS mass spectrometer.

Melting points were determined on a MELTEMP apparatus and uncorrected.

2.1 The synthesis of *p*-aryl isocyanates (A_1-A_5)

2.1.1 The General Procedure

S-Hex, **S-Hep**, **S-Okt**, **S-Des** and **S-O-Hex** derivatives (Scheme 2.1) were obtained from the reaction of (S)-(+)-1,3-Butanediol with *p*-substituted phenyl isocyanates in toluene in a reflux conditions. Because of this, first *p*-substituted phenyl isocyanates were synthesized by Curtis Rearrangement. For this purpose, 1.4 eq. sodium azide (NaN_3) is weighed into a single-necked flask. Toluene and 1 eq *p*-aryl benzoyl chloride are added and refluxed for eleven hours. The solution is brought to room temperature and the excess sodium azide in the solution is separated by filtration. The toluene in the solution is completely removed by vacuum distillation. The isocyanates obtained from the reaction are identified by the IR spectrum.

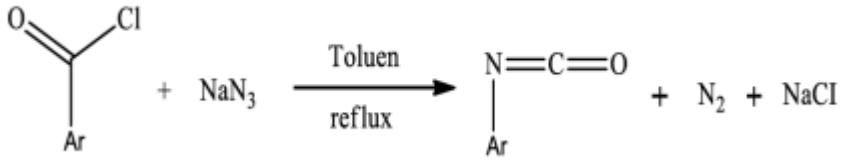

Scheme 2.1. General synthesis of *p*-Substituted phenyl isocyanates (A_1: Ar: *p*-hexylphenyl, A_2: Ar: *p*-hexyloxyphenyl, A_3: Ar: *p*-heptylphenyl, A_4: Ar: *p*-octylphenyl, A_5: Ar: *p*-decylphenyl*)*

2.2 The General Synthesis of 1,(3S)-Bis[N-(*p*-aryl)-carbamoyloxy]butane Compounds

2.2.1 The Synthesis of 1,(3S)-Bis[N-(*p*-aryl)-carbamoyloxy]butane Compounds (with the use of isocyanate)

1 eq of (S)-(+)-1,3-butanediol was taken into a round-bottomed flask and 2.1-2.3 eq of *p*-aryl isocyanate was added. After addition of toluene, the mixture was refluxed for 24 hours (Scheme 2.2). At the end of the reaction, toluene was removed with a rotary evaporator and a yellow-white precipitate was obtained. The resulting precipitate was purified by recrystallization in ethanol and the melting point determination was made for the obtained pure substances (white solid). IR, HRMS and $^{1}H/^{13}C$ NMR analyses were performed for structure characterization. Due to the chiral nature of the substances, the specific rotation angles were determined with a polarimeter.

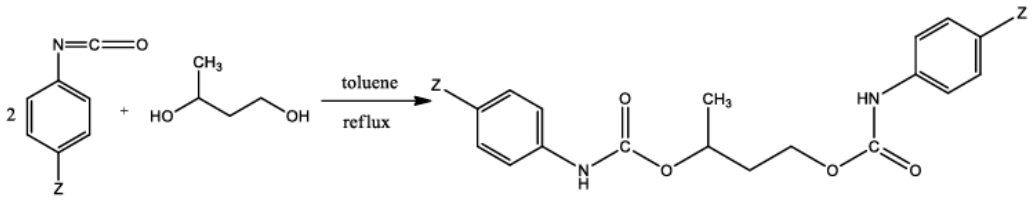

Z: hexyl, hexyloxy, heptyl, octyl, decyl

Scheme 2.2. Synthesis of 1,(3S)-Bis[N-(*p*-aryl)-carbamoyloxy]butane compounds

2.3 The Synthesis of 1,(3S)-Bis[N-(*p*-aryl)-carbamoyloxy]butane Compounds (with the use of *p*-benzoic acid)

2.3.1 General Procedure

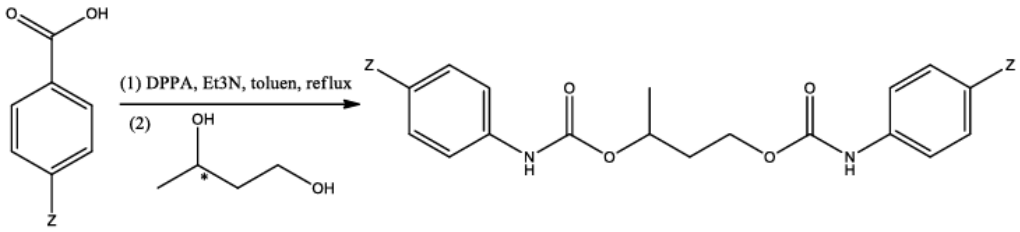

Z: *p*-octyloxy, *p*-heptyloxy and *p*-decyloxy

Scheme 2.3. Synthesis of *p*-heptyloxyphenyl (S-O-Hep), *p*-octyloxyphenyl (S-O-Oct), and *p*-decyloxyphenyl (S-O-Dec) derivatives

In a round bottomed two-necked flask, p-substituted benzoic acid (2 eq), diphenyl phosphoryl azide (DPPA) (2.2 eq), triethyl amine (2.2 eq) and dry toluene were mixed under nitrogen atmosphere and refluxed for 1 hour. Then (S)-(+)-1,3-Butanediol (1 eq) was added to the reaction mixture and refluxed for another 24 hours. At the end of the reaction, some toluene was evaporated using a rotary evaporator and the mixture was concentrated. The resulting solid was dissolved with dichloromethane and washed first with 1 M HCl solution and then with saturated $NaHCO_3$ solution. The resulting dichloromethane phase was removed with a rotary evaporator to obtain a solid. This solid was purified by recrystallization in ethanol. The melting point was determined for the pure materials (white solid) obtained. IR, HRMS and ^{1}H-^{13}C NMR analyses were performed for structure characterization. Since the substances are chiral, their specific rotations were determined by polarimetry.

2.4 Test Tube Inversion (Inverse Flow) Method and Determination of Minimum Gelation Concentration (MGC)

The minimum gel concentration (MGC) is the lowest concentration in a given mixture of a gelling agent and a solution that is considered to be the starting point of gelation. This concentration is the minimum amount necessary for gelation to take place. That is, if the gelling agent is not in sufficient quantity, no gel structure is observed in the solution and the mixture remains liquid.

Whether the gel phenomenon occurs between solution and precipitation depends on many factors. The most important factor is the molecular structure that

ensures gelation. The second effect is the nature of the solvent used in gelation. If the compound dissolves in a solvent without the application of heat, this solvent is not suitable for gelling. If dissolution does not occur despite the application of heat, it will also not be suitable for gelation. For this reason, dissolution must be in balance between the two; self-assembly must occur through cooling while the hot solution is kept at, RT as a result and the solvent is entrapped in a three-dimensional network structure (Figure 2.1). In this project, the tube inversion method will be used to determine whether gelation occurs. (Suzuki et al., 2008; Zweep et al., 2009; Demir-Ordu et al., 2015) . For this purpose, a certain amount of substance is taken into a bottle of 45x14.75 mm dimensions, 1 ml of solvent is added and the bottle mouth is tightly closed with a screw cap. The vial is then heated around the boiling point of the solvent to dissolve the substance to be tested. After obtaining the solution, the bottle is kept in a certain place at room temperature without being moved (Figure 2.1, t = 0). At the end of one hour, the flow is checked by turning the bottle upside down to determine whether gelation has occurred (Figure 2.1, t= 1 hour). The absence of flow indicates that gelation is complete. For gel stability, the bottle is left at room temperature for 24 hours. The solvents to be used in the gelation test consist of basic organic solvents in our laboratory, esters such as isopropyl palmitate and isopropyl myristate used in the pharmaceutical industry, and vegetable oils.

Figure 2.1. Organogelation stages (t: 0 min, hot solution; t: start of intense gelation after 1 min; completion of gelation after t=2 min)

3. RESULTS

3.1 Synthesis of *p*-Aryl Isocyanates (A_1-A_5)

3.1.1 *p*-Hexylphenyl Isocyanate, A_1

According to the general procedure (2.1.1) *p*-phenyl hexyl isocyanate was prepared by using 0,81 g (12,46 mmol) of sodium azide, 1.94 mL (8,90 mmol) of *p*-hexylbenzoyl chloride and 20 mL of toluene.

Yield: 1,61 g (89,14%), IR (püre, cm^{-1}) = 2258 cm^{-1} (-N=C=O)

3.1.2 *p*-Hexyloxyphenyl Isocyanate, A_2

According to the general procedure (2.1.1) *p*-hexyloxy isocyanate was prepared by using 1.89 gr (0.029 mol) of sodium azide, 4.6 ml (0.021 mol) of *p*-hexyloxybenzoyl chloride and 30 mL of toluene.

Yield: 4.48 g, %98, IR (neat, cm-1): 2276 cm^{-1}

3.1.3 *p*-Heptylphenyl Isocyanete , A_3

According to the general procedure (2.1.1) *p*-heptyl phenyl isocyanate was prepared by using 0,76 g (11,73 mmol) of sodium azide, 2,00 mL (8,38 mmol) of *p*-heptylbenzoyl chloride and 20 mL of toluene.

Yield: 1,72 g (94,56%), IR (püre, cm^{-1}) = 2238 cm^{-1}

3.1.4 *p*-Octylphenyl Isocyanate, A_4

According to the general procedure (2.1.1) *p*-octylphenyl isocyanate was prepared by using 0.36 g (5.54 mmol) of sodium azide, 0.98 mL (3,96 mmol) of *p*-octylbenzoyl chloride and 20 mL of toluene.

Yield: 0.73 g (80,0%), IR (püre, cm^{-1}) = 2223 cm^{-1} (-N=C=O)

3.1.5 *p*-Decylphenyl Isocyanate, A_5,

According to the general procedure (2.1.1) *p*-decylphenyl isocyanate was prepared by using 0,32 g (4,99 mmol) of sodium azide, 0,98 mL (3,56 mmol) of *p*-heptylbenzoyl chloride and 20 mL of toluene.

Yield: 0,8924 g (96,62%), IR (pure, cm^{-1})= 2257 cm^{-1} (-N=C=O)

3.2 The Synthesis of 1,(3S)-Bis[N-(*p*-aryl)-carbamoyloxy]butane Compounds (with the use of *p*-aryl isocyanates)

3.2.1 1,(3S)-Bis[N-(*p*-hexylphenyl)- carbamoyloxy]butane, S-Hex

According to the general procedure 2.2.1, 1,(3S)-Bis[N-(*p*-hexylphenyl)-carbamoyloxy]butane, **S-Hex** was prepared by using 1,61 g (7,92 mmol) of *p*-Hexyl phenyl isocyanate, A_1 and 0,31 g (S)-(+)-1,3-butanediol in 25 ml of toluene.

White solid, yield: 1,582 g (92,27%) Melting point: 123.0-124.0 ^{0}C, $[\propto]^{22}_D$= +36.09^0 (c=1.0, $CHCl_3$).

IR (KBr): 3345, 3032, 2953, 2924, 2855, 1699 cm^{-1} (Figure. 3.1).

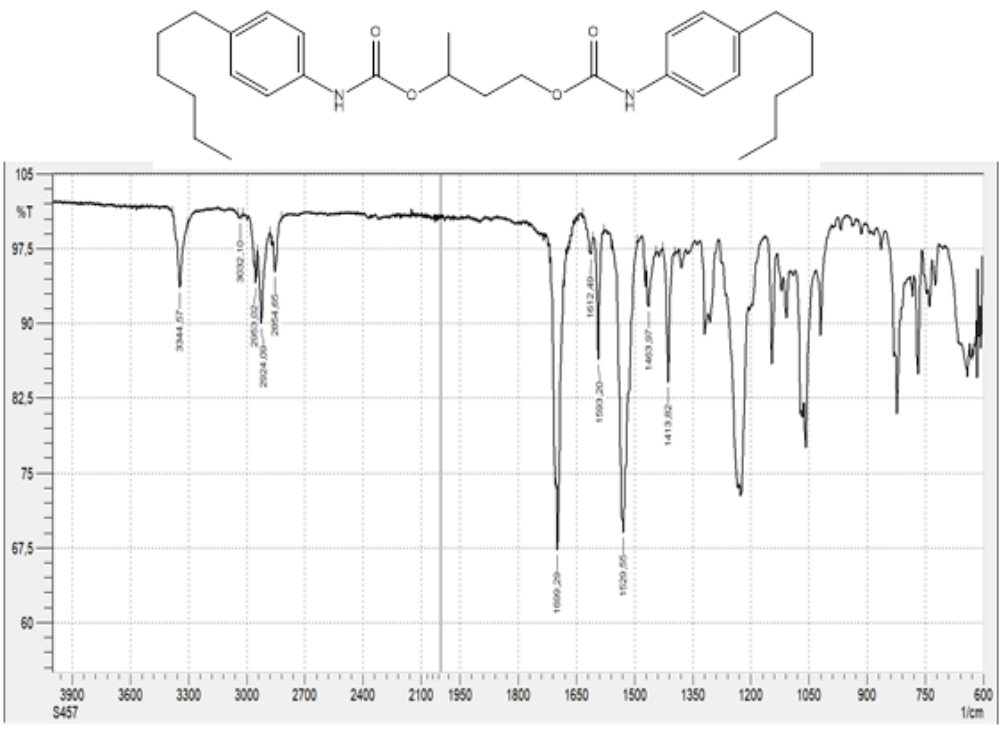

Figure 3.1. IR spectrum of compound **S-Hex**.

^{1}H NMR (300 MHz, $CDCl_3$): δ= 0.80 (t, ^{3}J= 6,6 Hz, 6H, CH_3), 1.18-1,24 (br m, 12H, CH_2), 1.27 (d, ^{3}J= 6,3 Hz, 3H, CH_3), 1.45-1,55 (m, 4H, CH_2), 1.85-1,97 (m, 2H, CH_2), 2.47 (t, ^{3}J= 7,6 Hz, 4H, CH_2), 4.10-4.27 (m, 2H, OCH_2), 4.95-5.05 (m, 1H, OCH), 6.47 (br s, 1H, NH), 6.49 (br s, 1H, NH), 7.02 (d, ^{3}J= 8,0 Hz, 2H, CH), 7.03 (d, ^{3}J= 8,0 Hz, 2H, CH), 7.16 (d, ^{3}J= 8,0 Hz, 2H, CH), 7.19 (d, ^{3}J= 8,0 Hz, 2H, CH) (Figure 3.2).

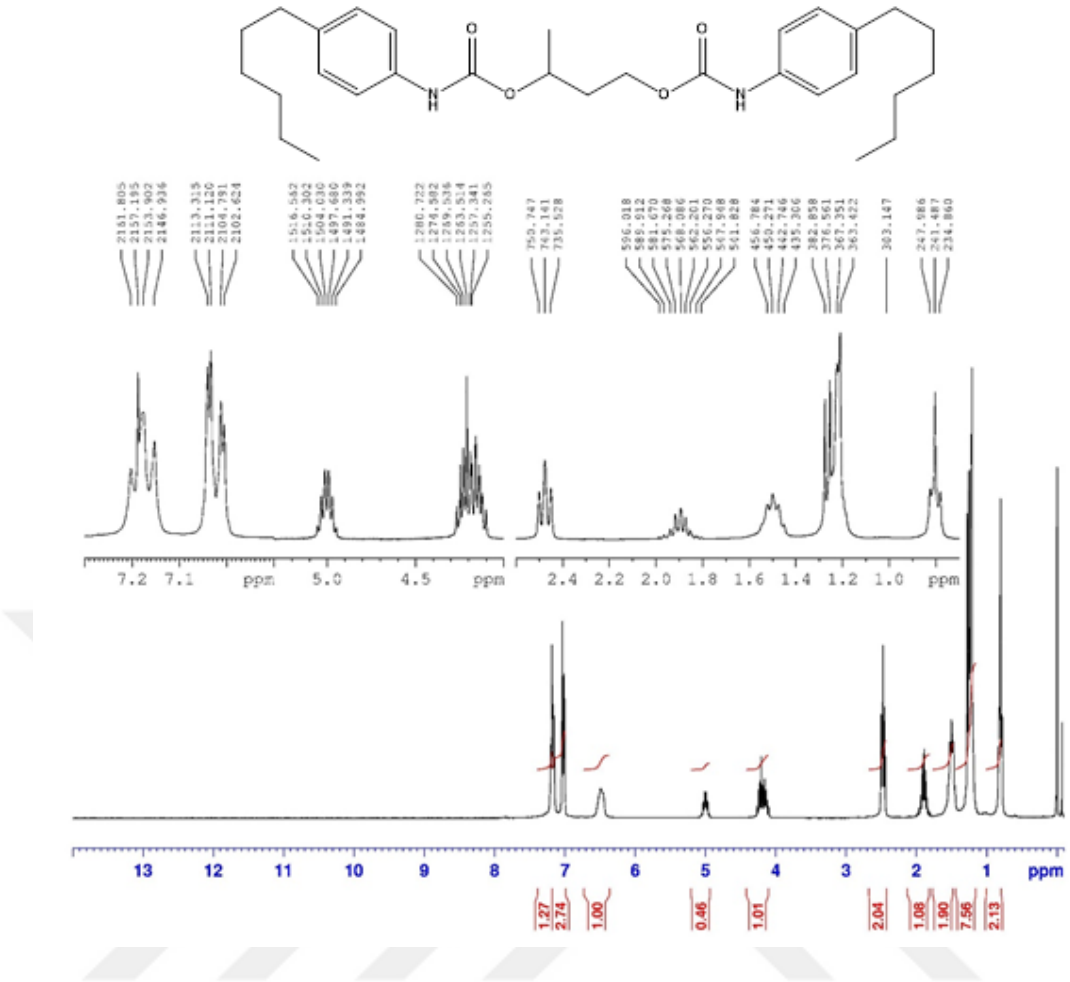

Figure 3.2. 300 MHz ^{1}H NMR spectrum of compound **S-Hex** in $CDCl_3$.

^{13}C NMR (75 MHz, $CDCl_3$): δ= 153.5, 153.2, 138.2, 135.4, 135.3, 128.9, 128.8, 118.8, 68.9, 61.6, 35.3, 31.9, 31.7, 31.5, 28.9, 22.6, 20.4, 14.1 (Figure 3.3).

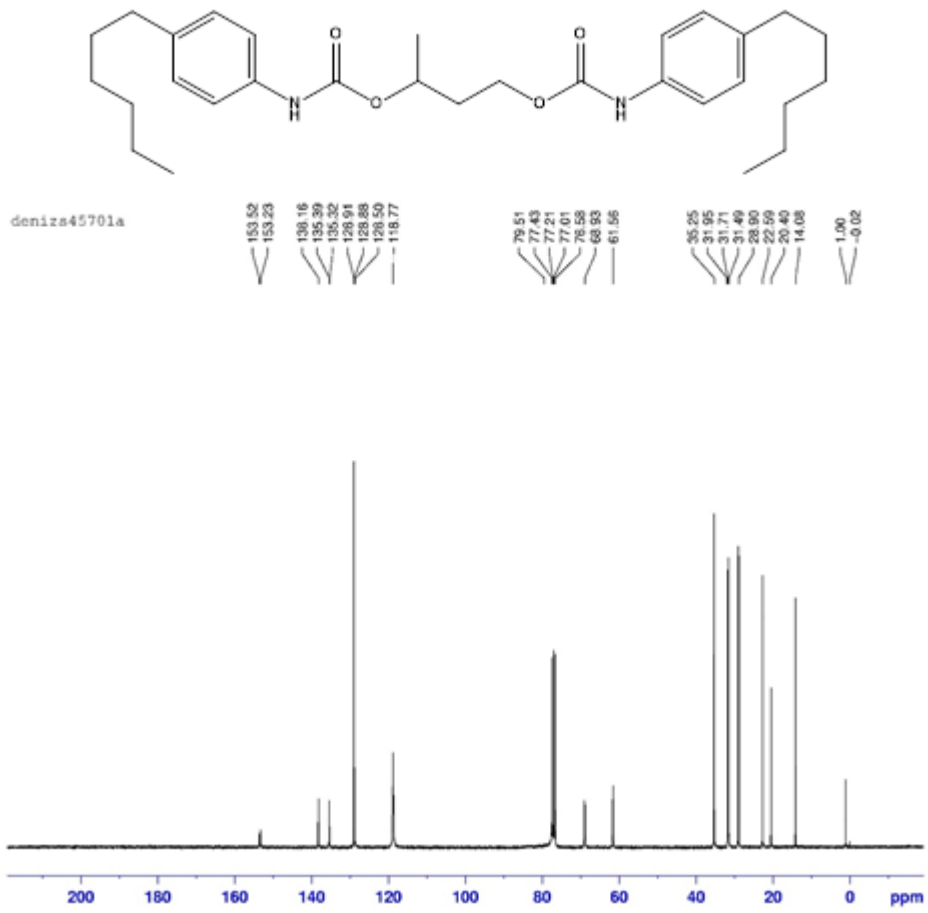

Figure 3.3. 75 MHz ^{13}C NMR spectrum of compound **S-Hex** in $CDCl_3$.

MS (HRMS): calculated for $C_{30}H_{44}N_2O_4$: 497,3379 $(M+H)^+$. Found 497,3381 $(M+H)^+$ (Figure 3.4).

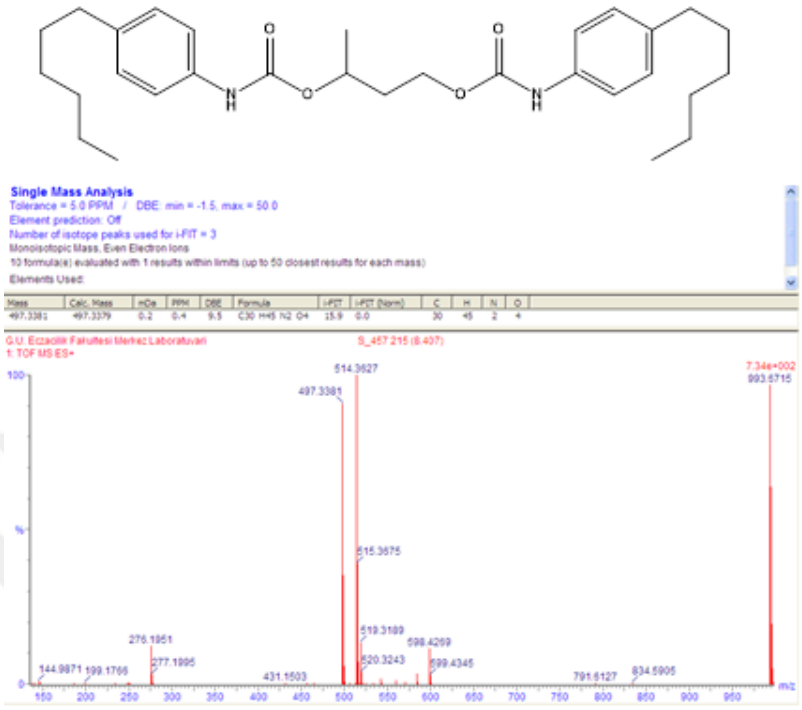

Figure 3.4. HRMS result of S-Hex.

3.2.2 1,(3S)-Bis[N-(*p*-hexyloxyphenyl)-carbamoyloxy]butane , S-O-Hex

According to the general procedure 2.2.1, 1,(3S)-Bis[N-(*p*-hexyloxyphenyl)-carbamoyloxy]butane, **S-O-Hex** was prepared by using 1,73 g (7,88 mmol) of *p*-hexyloxyphenyl isocyanate, A_2 and 0,31 g (3.43 mmol) (S)-(+)-1,3-butanediol in 25 ml of toluene.

White solid yield: : 1,36 g (75%); Melting point: 155.7-157.5 ^{0}C, $[\propto]^{22}_D$= +16.07 ^{0} (c=1.0, $CHCl_3$).

IR (KBr): 3336, 3032, 2929, 2873, 1695 cm^{-1} (Figure 3.5).

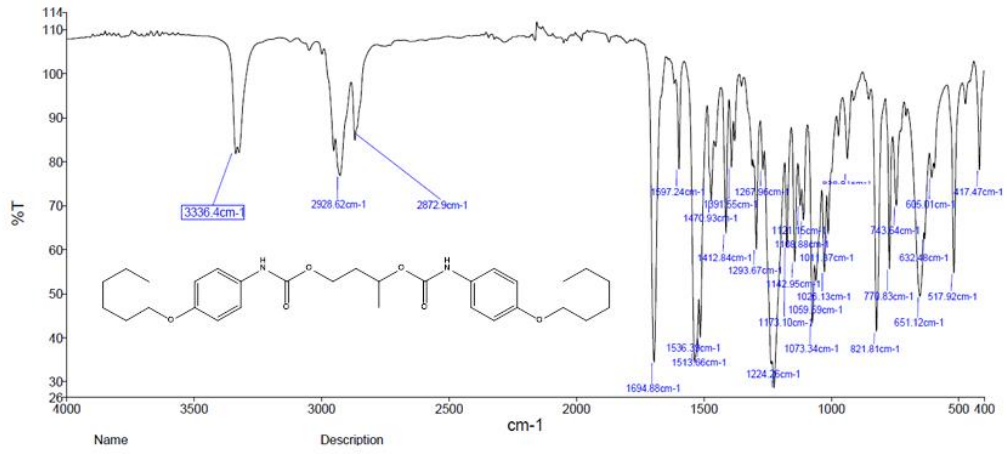

Figure 3.5. IR spectrum of compound **S-O-Hex**.

^{1}H NMR (400 MHz, $CDCl_3$): δ= 0.93 (t, ^{3}J= 8,0 Hz, 6H, CH_3), 1.34-1,37 (br m, 8H (CH_2)+3H (CH_3)), 1.43-1,50 (m, 4H, CH_2), 1.74-1,81 (m, 4H, CH_2), 1.90-2.04 (m, 2H, CH_2), 3,93 (t, ^{3}J= 8,0 Hz, 4H, CH_2), 4.19-4.33 (m, 2H, OCH_2), 5.04-5.12 (m, 1H, OCH), 6.57 (br s, 1H, NH), 6.63 (br s, 1H, NH), 6.85 (d, ^{3}J= 8,0 Hz, 2H, CH), 6.86 (d, ^{3}J= 8,0 Hz, 2H, CH), 7.28 (d, ^{3}J= 8,0 Hz, 4H, CH) (Figure 3.6).

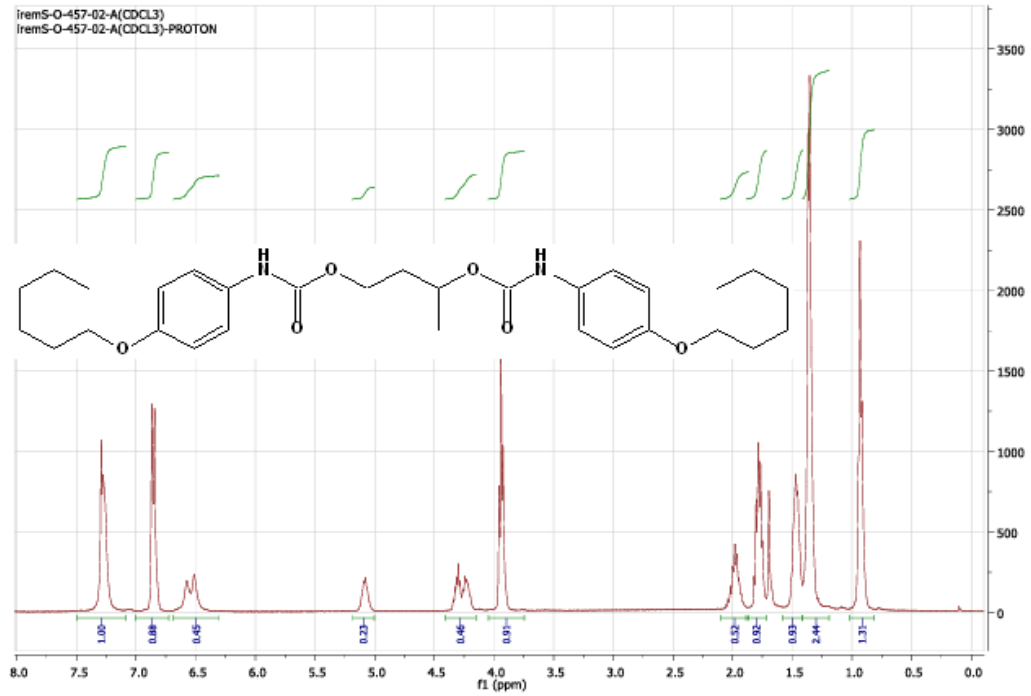

Figure 3.6. 400 MHz ^{1}H NMR spectrum of compound **S-O-Hex** in $CDCl_3$.

^{13}C NMR (100 MHz, $CDCl_3$): δ= 155.5, 153.9, 153.5, 130.7,120.6, 114.9, 68.8, 68.3, 61.5, 35.3, 31.6, 29.3, 25.7, 22.6, 20.5, 14.1 (Figure 3.7).

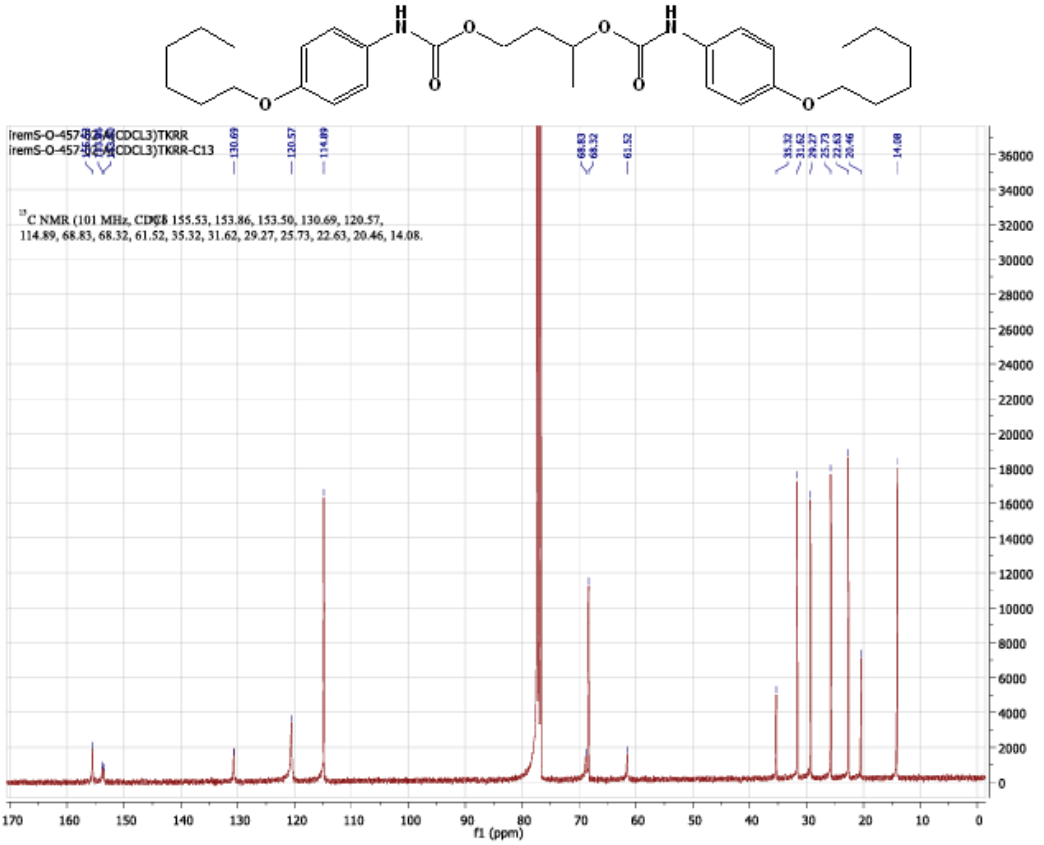

Figure 3.7. 100 MHz ^{13}C NMR spectrum of compound **S-O-Hex** in $CDCl_3$.

MS (HRMS): m/z calculated for $C_{30}H_{44}N_2O_6$: 529,3278 $(M+H)^+$; found: 529,3266 $(M+H)^+$ (Figure 3.8).

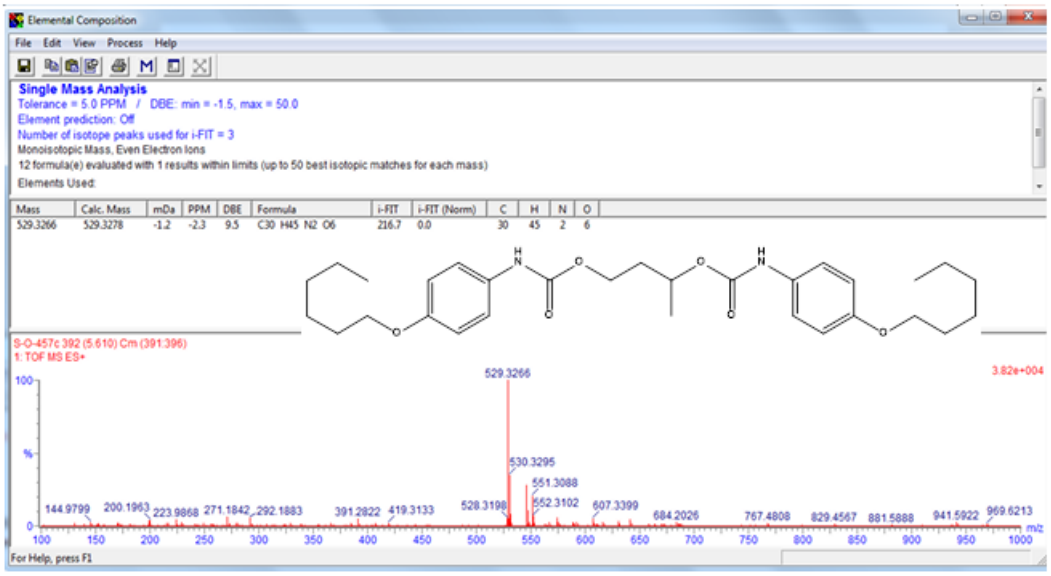

Figure 3.8. HRMS result of compound **S-O-Hex**.

3.2.3 1,(3S)-Bis[N-(*p*-heptylphenyl)-carbamoyloxy]butane , S-Hep

According to the general procedure (2.2.1), 1,(3S)-Bis[N-(*p*-heptylphenyl)-carbamoyloxy]butane , **S-Hep** was prepared by using 1,72 g (7,92 mmol) of *p*-hexylphenyl isocyanate, A_3 and 0,31 g (S)-(+)-1,3-butanediol in 25 ml of toluene.

White solid, yield: 0.71 g (93%) Melting point: 122.3-123.7 ^{0}C, $[\propto]_D^{22}$= +39.51^0 (c=1.0, $CHCl_3$).

IR (KBr): 3311, 3036, 2953, 2922, 2849, 1699 cm^{-1} (Figure 3.9).

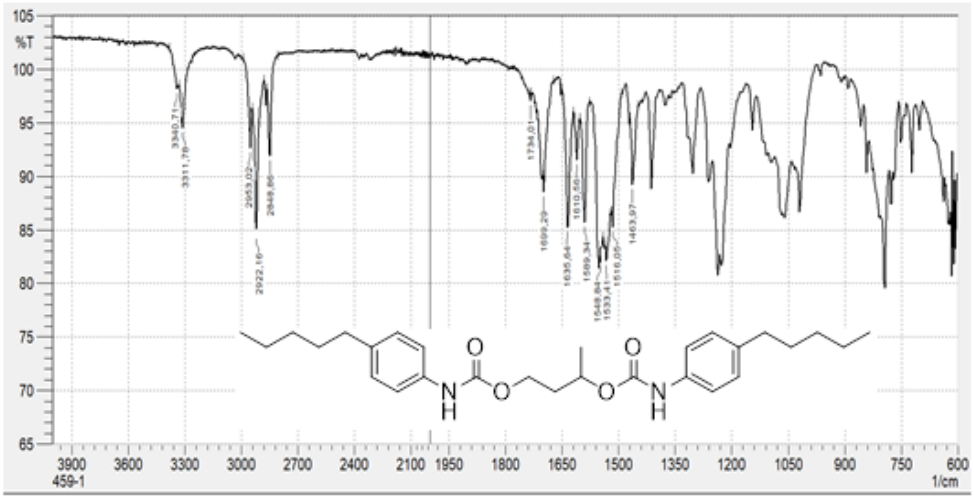

Figure 3.9. IR spectrum of compound **S-Hep**.

^{1}H NMR (300 MHz, $CDCl_3$): δ= 0.80 (t, ^{3}J= 6,9 Hz, 6H, CH_3), 1.18-1,22 (br m, 16H, CH_2), 1.27 (d, ^{3}J= 6,3 Hz, 3H, CH_3), 1.45-1,55 (m, 4H, CH_2), 1.85-1,94 (m, 2H, CH_2), 2.47 (t, ^{3}J= 7,6 Hz, 4H, CH_2), 4.10-4.27 (m, 2H, OCH_2), 4.95-5.05 (m, 1H, OCH), 6.45 (s, 1H, NH), 6.49 (s, 1H, NH), 7.02 (d, ^{3}J= 8,0 Hz, 2H, CH), 7.03 (d, ^{3}J= 8,0 Hz, 2H, CH), 7.16 (d, ^{3}J= 8,0 Hz, 2H, CH), 7.19 (d, ^{3}J= 8,0 Hz, 2H, CH) (Figure 3.10).

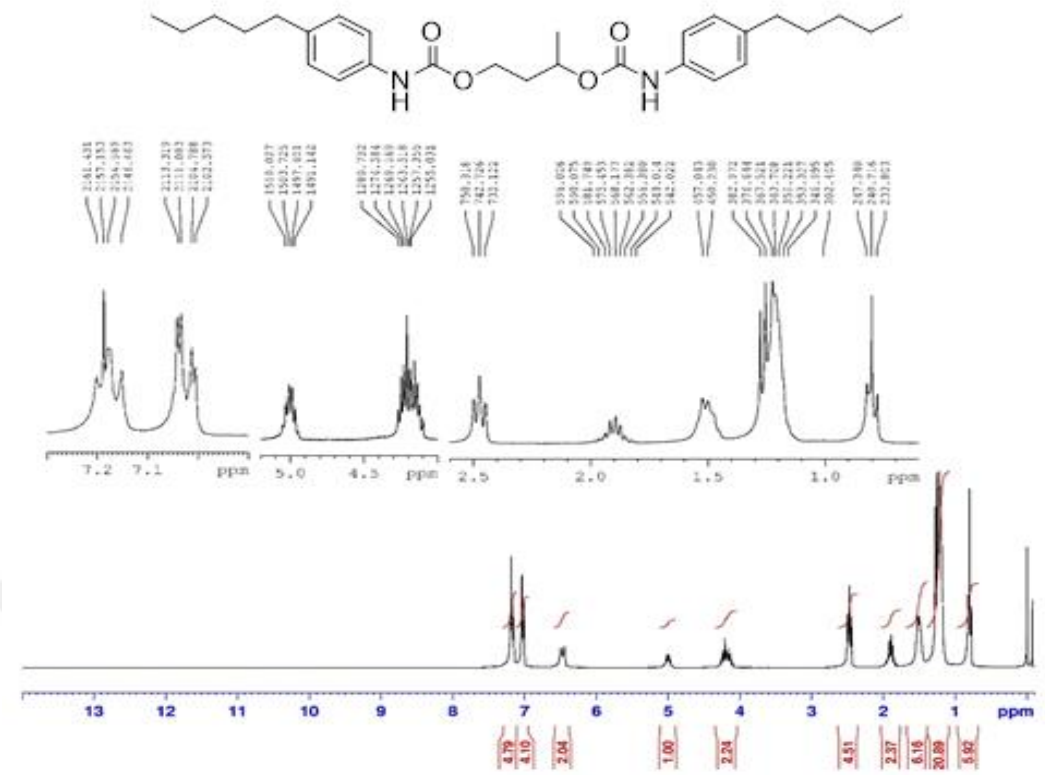

Figure 3.10. 400 MHz ^{1}H NMR spectrum of compound **S-Hep** in $CDCl_3$.

^{13}C NMR (75 MHz, $CDCl_3$): δ= 153.6, 153.3, 138.1, 135.4, 135.3, 128.9, 128.8, 118.8, 68.9, 61.6, 35.3, 31.8, 31.5, 29.2, 29.1, 23.4, 22.7, 20.4, 14.1 (Figure 3.11).

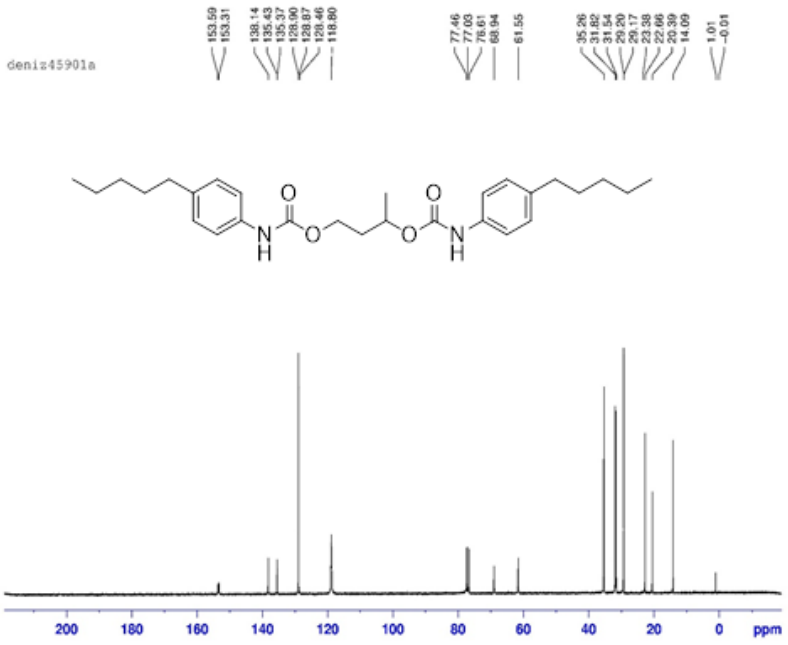

Figure 3.11. 75 MHz ^{13}C NMR spectrum of compound **S-Hep** in $CDCl_3$.

MS (HRMS): m/z calculated for $C_{32}H_{48}N_2O_4$: 525,3692 $(M+H)^+$; found: 525,3690 $(M+H)^+$ (Figure 3.12).

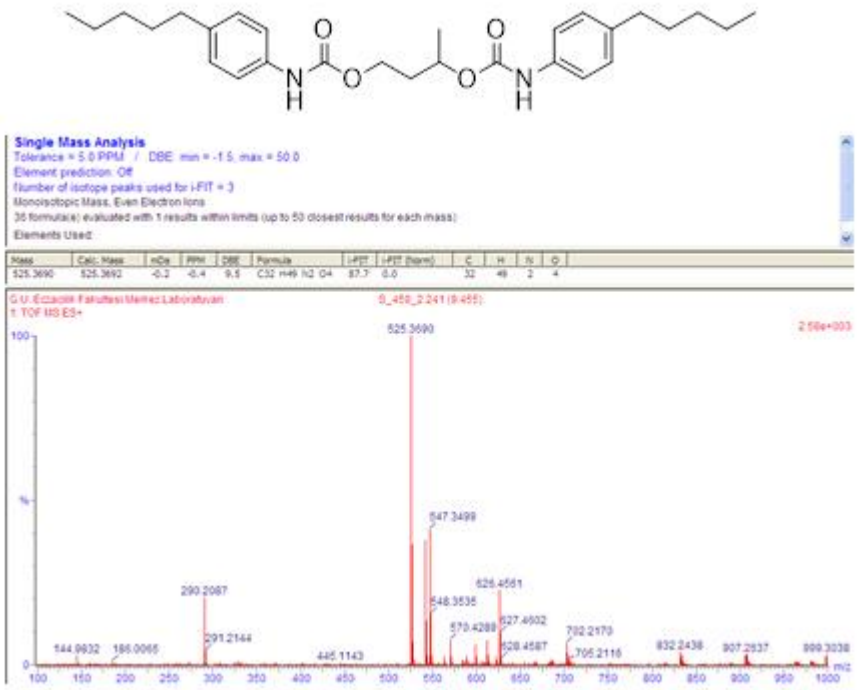

Figure 3.12. HMRS result of compound **S-Hep**.

3.2.4 1,(3S)-Bis[N-(*p*-octylphenyl)-carbamoyloxy]butane, S-Oct

According to the general procedure 2.2.1, 1,(3S)-Bis[N-(*p*-octylphenyl)-carbamoyloxy]butane, **S-Oct** was prepared by using 0.73 g (3.17 mmol) of *p*-octylphenyl isocyanate, A_3 and 0.12 g (1.38 mmol) (S)-(+)-1,3-butanediol in 10 ml of toluene.

White solid, yield: 0.70 g (92%); Melting Point: 118.1-119.1 ^{0}C, $[\propto]_D^{22}$= +32.25 ^{0} (c=1.0, $CHCl_3$).

IR (KBr): 3347, 3040, 2957, 2922, 2849, 1699 cm^{-1} (Figure 3.13).

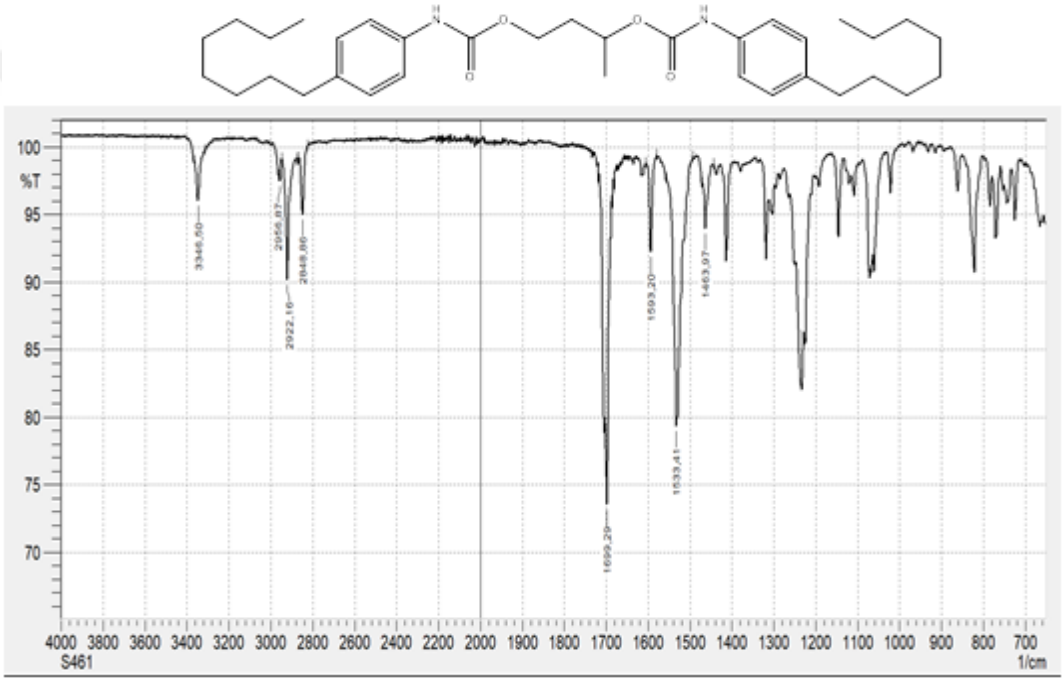

Figure 3.13. IR spectrum of compound **S-Oct**.

^{1}H NMR (300 MHz, $CDCl_3$): δ= 0.80 (t, ^{3}J= 6,9 Hz, 6H, CH_3), 1.19-1,22 (br m, 20H, CH_2), 1.27 (d, ^{3}J= 6,3 Hz, 3H, CH_3), 1.46-1,52 (br m, 4H, CH_2), 1.85-1,94 (m, 2H, CH_2), 2.47 (t, ^{3}J= 7,4 Hz, 4H, CH_2), 4.10-4.27 (m, 2H, OCH_2), 4.95-5.05 (m, 1H, OCH), 6.43 (s, 1H, NH), 6.47 (s, 1H, NH), 7.02 (d, ^{3}J= 8,0 Hz, 2H, CH), 7.03 (d, ^{3}J= 8,0 Hz, 2H, CH), 7.16 (d, ^{3}J= 8,0 Hz, 2H, CH), 7.19 (d, ^{3}J= 8,0 Hz, 2H, CH) (Figure 3.14).

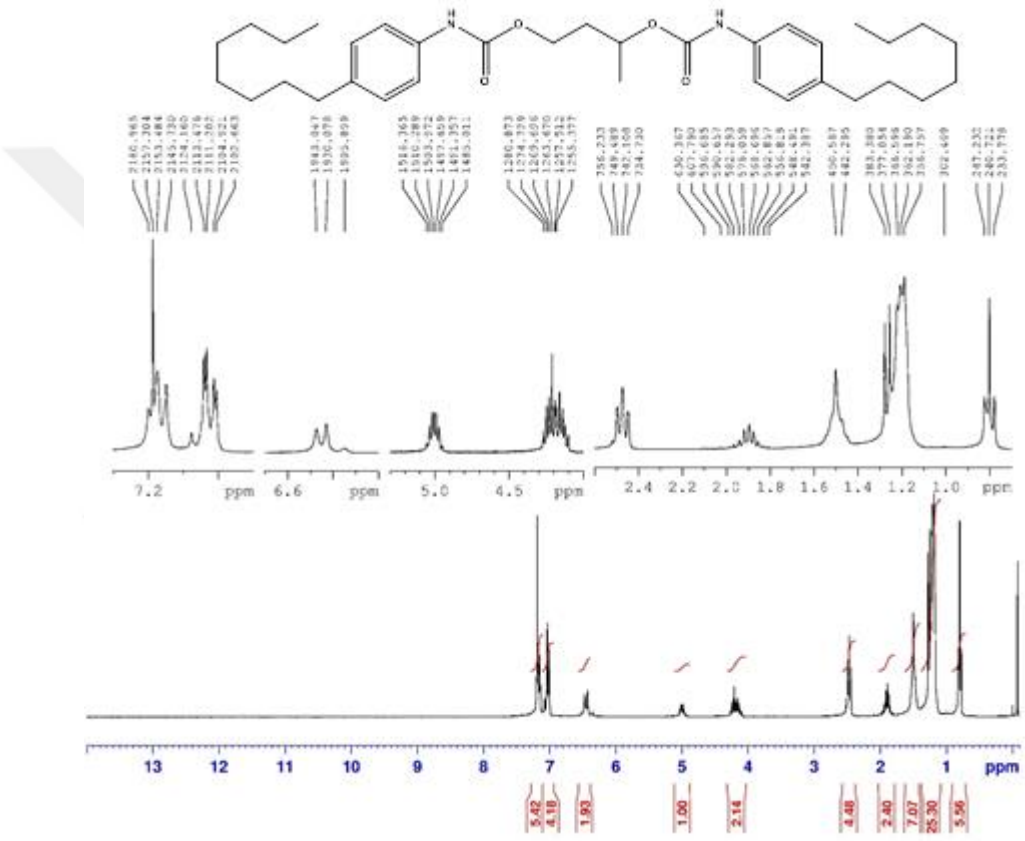

Figure 3.14. 300 MHz ^{1}H NMR spectrum of compound **S-Oct** in $CDCl_3$.

^{13}C NMR (75 MHz, $CDCl_3$): δ= 153.5, 153.2, 138.2, 135.4, 135.3, 129.3, 128.9, 118.8, 68.9, 61.6, 35.3, 31.9, 31.5, 29.5, 29.3, 22.7, 20.4, 14.1 (Figure 3.15).

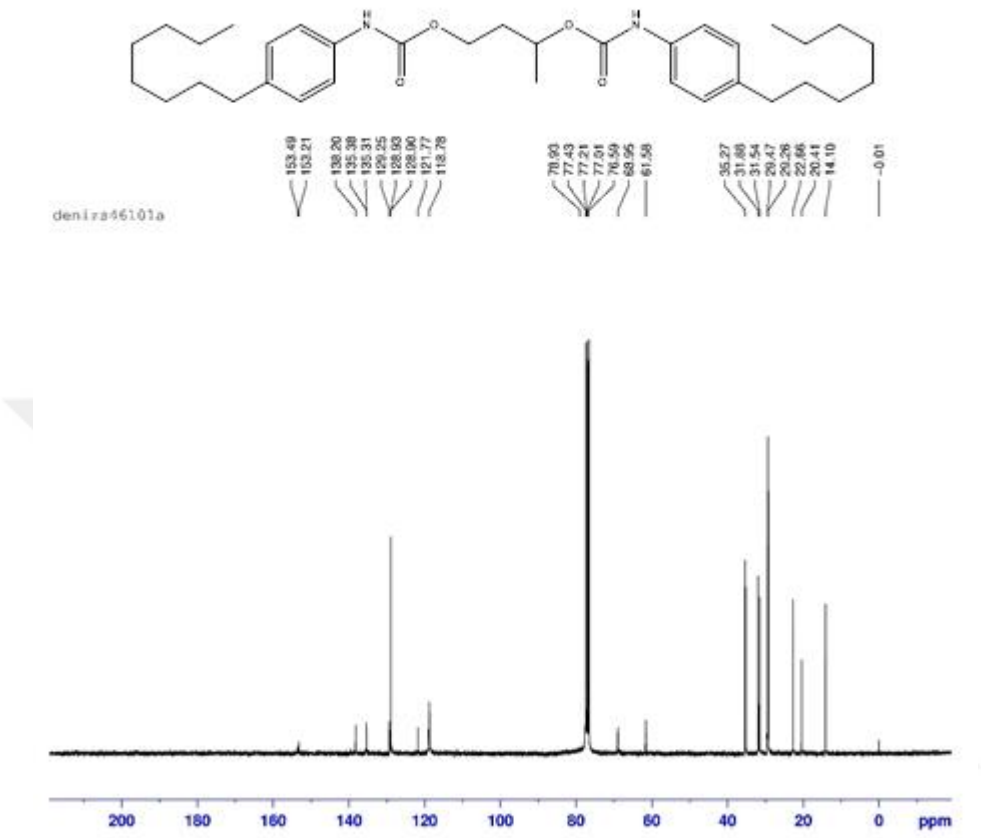

Figure 3.15. 75 MHz ^{13}C NMR spectrum of compound **S-Oct** in $CDCl_3$.

MS (HRMS): m/z calculated for $C_{34}H_{52}N_2O_4$: 553,4005 $(M+H)^+$; found: 553,4010 $(M+H)^+$ (Figure 3.16).

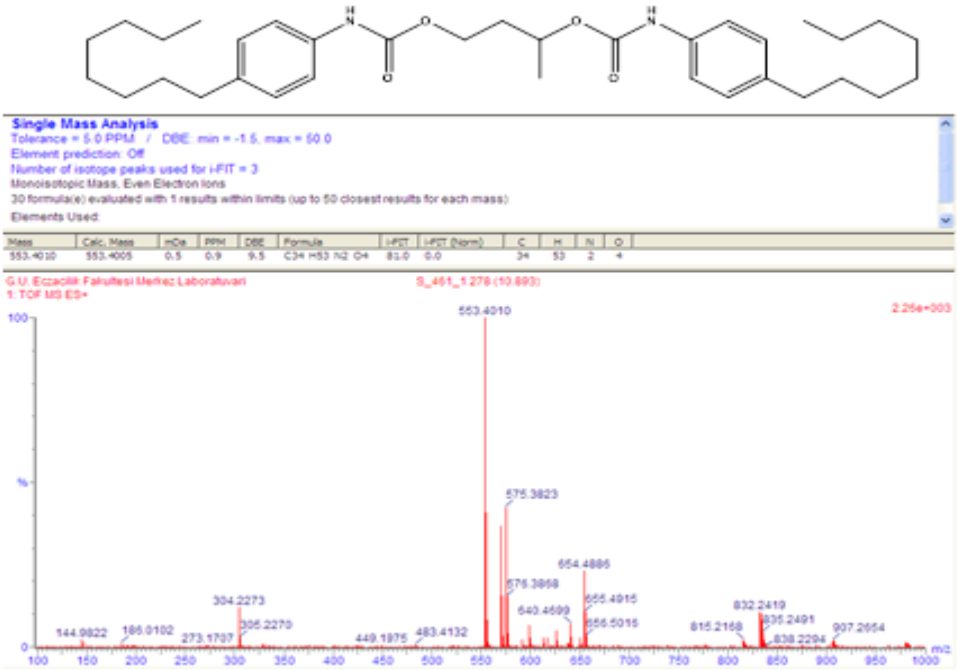

Figure 3.16. HRMS result of compound **S-Oct**.

3.2.5 1,(3S)-Bis[N-(*p*-decylphenyl)-carbamoyloxy]butane, S-Dec

According to the general procedure 2.2.1, 1,(3S)-Bis[N-(*p*-decyphenyl)-carbamoyloxy]butane, **S-Dec** was prepared by using 0,74 g (2,85 mmol) of *p*-decylphenyl isocyanate, A_5 and 0,13 g (S)-(+)-1,3-butanediol in 25 ml of toluene.

White solid, yield: 0,64 g (85%) Melting point: 113.8-115.8 ^{0}C, $[\propto]_D$ ^{22}= +32.78 ^{0} (c=1.0, $CHCl_3$).

IR (KBr): 3348, 3036, 2957, 2918, 2847, 1699 cm^{-1} (Figure 3.17).

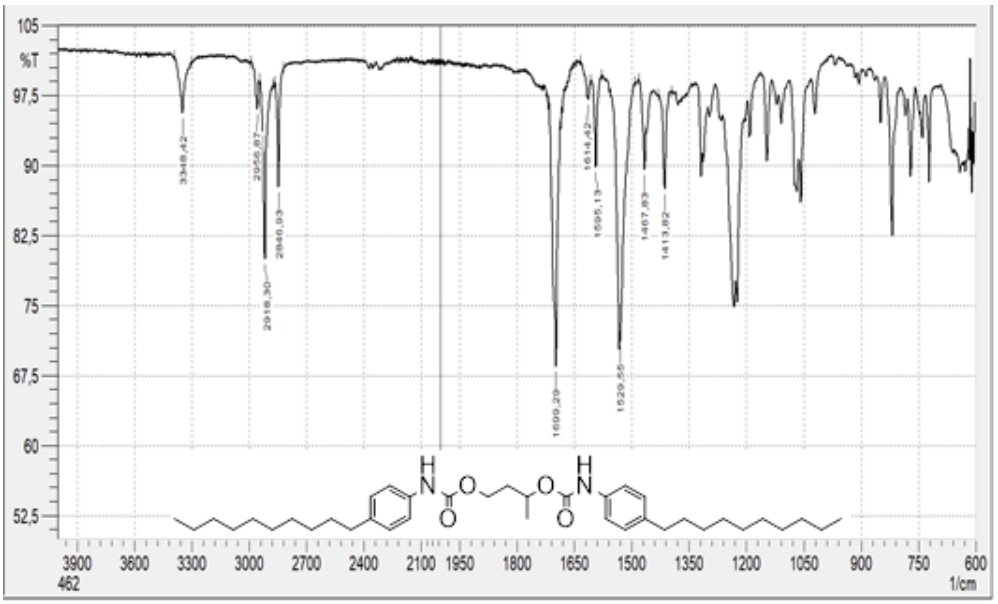

Figure 3.17. IR spectrum of compound **S-Dec.**

^{1}H NMR (300 MHz, $CDCl_3$): δ= 0.87 (t, ^{3}J= 6,9 Hz, 6H, CH_3), 1.25-1,29 (br m, 28H, CH_2), 1.34 (d, ^{3}J= 6,6 Hz, 3H, CH_3), 1,52-1.63 (br m, 4H, CH_2), 1.92-2.01 (m, 2H, CH_2), 2.54 (t, ^{3}J= 7,5 Hz, 4H, CH_2), 4.17-4.34 (m, 2H, OCH_2), 5.02-5.12 (m, 1H, OCH), 6.54 (s, 1H, NH), 6.56 (s, 1H, NH), 7.09 (d, ^{3}J= 8,0 Hz, 2H, CH), 7.10 (d, ^{3}J= 8,0 Hz, 2H, CH), 7.24 (d, ^{3}J= 8,0 Hz, 2H, CH), 7.26 (d, ^{3}J= 8,0 Hz, 2H, CH) (Figure 3.18).

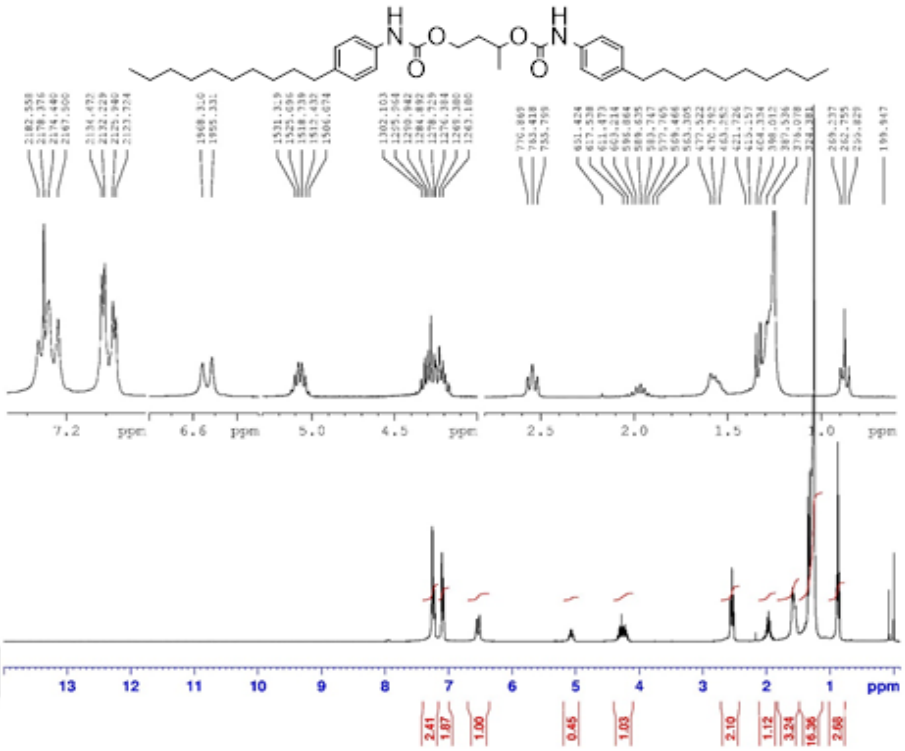

Figure 3.18. 300 MHz ^{1}H NMR spectrum of compound **S-Dec** in $CDCl_3$.

^{13}C NMR (75 MHz, $CDCl_3$): δ= 153.6, 153.3, 138.2, 135.4, 135.3, 129.6, 129.3, 128.9, 128.8, 118.8, 68.9, 61.6, 36.0, 35.3, 35.1, 31.9, 31.6, 31.2, 29.6, 29.5, 29.3, 29.2, 22.7, 20.4, 20.2, 14.1 (Figure 3.19).

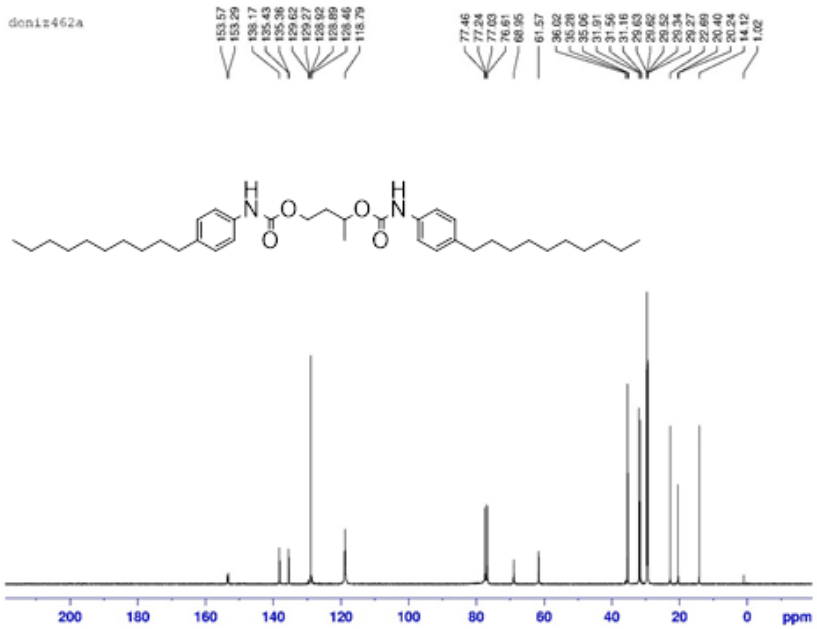

Figure 3.19. 75 MHz ^{13}C NMR spectrum of compound **S-Dec** in $CDCl_3$.

MS (HRMS): m/z calculated $C_{38}H_{60}N_2O_4$: 609,4631 $(M+H)^+$; found: 609,4627 $(M+H)^+$ (Figure 3.20).

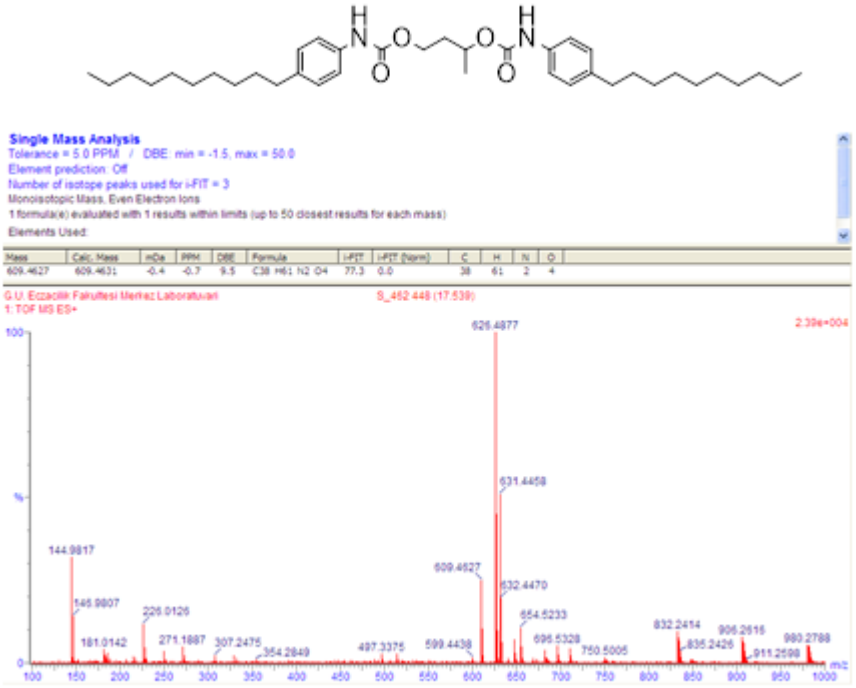

Figure 3.20. HRMS of compound **S-Dec**.

3.3 The Synthesis of 1,(3S)-Bis[N-(*p*-aryl)-carbamoyloxy]butane Compounds (with the use of *p*-benzoic acid)

3.3.1 1,(3S)-Bis[N-(*p*-heptyloxyphenyl)-carbamoyloxy]butane, S-O-Hep

According to the general procedure 2.3.1, 1,(3S)-Bis[N-(*p*-heptyloxyphenyl)-carbamoyloxy]butane, **S-O-Hep** was prepared by using 1.50 g of *p*-heptlyoxy benzoic acid, 1,49 ml of diphenylphosphoryl azide and 0,97 ml of (S)-(+)-1,3-butanediol in 10 ml of toluene.

White solid, yield: 1,56 g (88%) Melting point: 148.8-149.8 ^{0}C, $[\propto]^{22}_{D}$: $+26.08^{0}$ (c=1.0, $CHCl_3$).

IR (KBr): 3337, 3033, 2923, 2861, 1695 cm^{-1} (Figure 3.21)

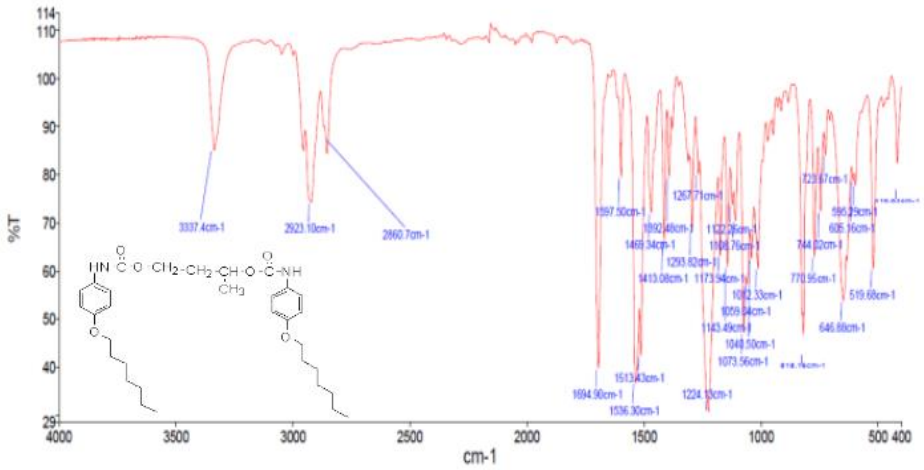

Figure 3.21. IR spectrum of compound **S-O-Hep**.

^{1}H NMR (400 MHz, $CDCl_3$): δ= 0.92 (t, ^{3}J= 8,0 Hz, 6H, CH_3), 1.33-1,36 (br m, 12H (CH_2)+3H (CH_3)), 1.44-1,48 (m, 4H, CH_2), 1.75-1,82 (m, 4H, CH_2), 1.91-2.05 (m, 2H, CH_2), 3,94 (t, ^{3J}= 8,0 Hz, 4H, CH_2), 4.20-4.34 (m, 2H, OCH_2), 5.06-5.11 (m, 1H, OCH), 6.53 (br s, 1H, NH), 6.60 (br s, 1H, NH), 6.85 (d, ^{3}J= 8,0 Hz, 2H, CH), 6.86 (d, ^{3}J= 8,0 Hz, 2H, CH), 7.26 (d, ^{3}J= 8,0 Hz, 4H, CH) (Figure 3.22).

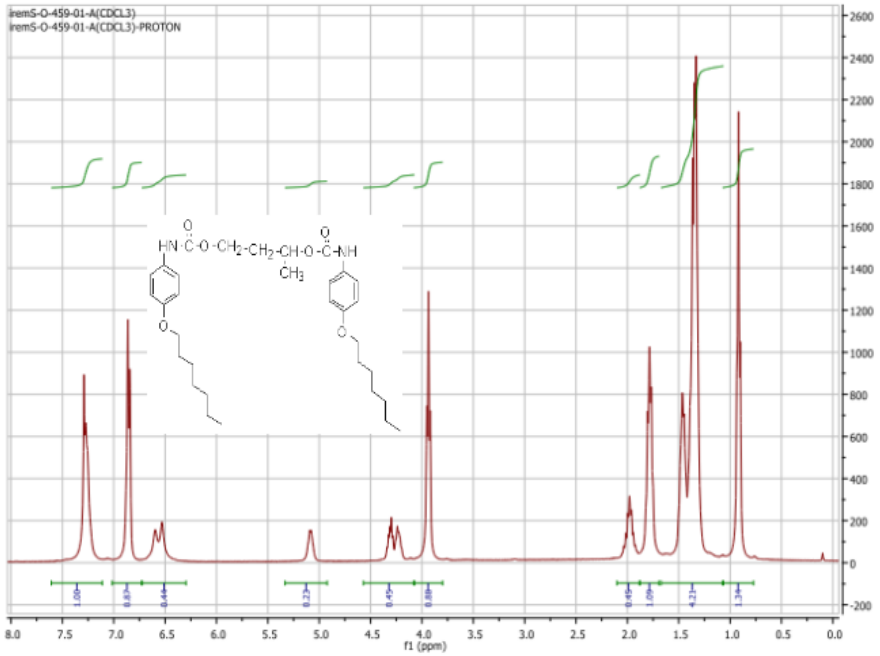

Figure 3.22. 400 MHz ^{1}H NMR spectrum of compound **S-O-Hep** in $CDCl_3$.

^{13}C NMR (100 MHz, $CDCl_3$): δ= 155.5, 153.9, 153.6, 130.7, 123.9, 120.6, 115.1, 114.9, 114.8, 68.9, 68.3, 61.5, 35.3, 31.8, 29.3, 29.1, 26.0, 22.6, 20.5, 14.1 (Figure 3.23).

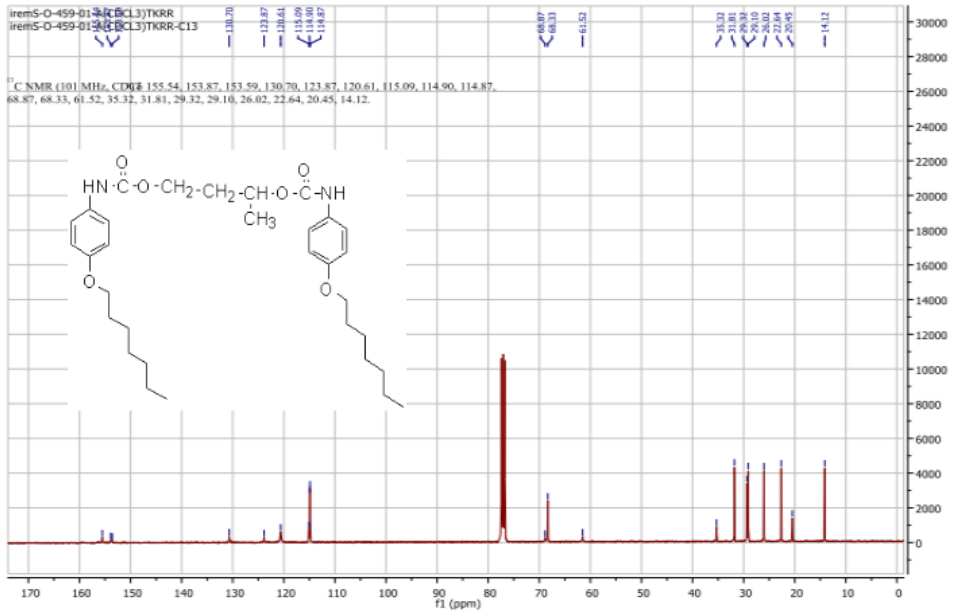

Figure 3.23. 100 MHz ^{13}C NMR spectrum of compound **S-O-Hep** in $CDCl_3$.

MS (HRMS): m/z calculated for $C_{32}H_{48}N_2O_6$: 557,3591 $(M+H)^+$; found: 557,3571 $(M+H)^+$ (Figure 3.24).

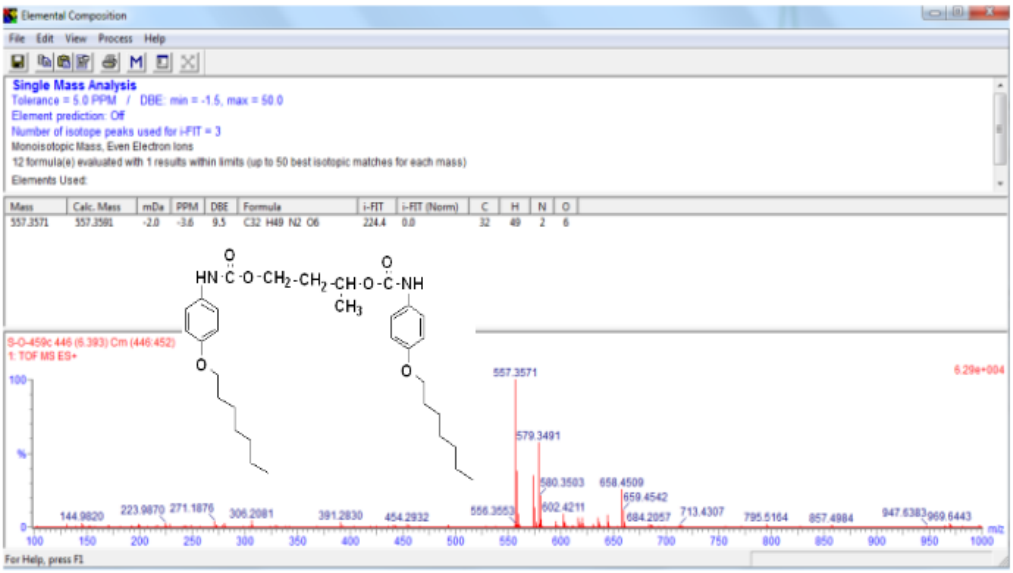

Figure 3.24 HRMS of compound **S-O-Hep**.

3.3.2 1,(3S)-Bis[N-(*p*-octyloxyphenyl)- carbamoyloxy]butane, S-O-Oct

According to the general procedure 2.3.1, 1,(3S)-Bis[N-(*p*-octyloxyphenyl)-carbamoyloxy]butane, **S-O-Oct** was prepared by using 2,00 g of *p*-octylyoxy benzoic acid, 1,89 ml of diphenylphosphoryl azide, 1,22 ml of triethylamine and 0,35 ml of (S)-(+)-1,3-butanediol in 10 ml of toluene.

White solid, yield: 1,96 g (83,90%) Melting point: 149.0-150.5 ^{0}C, $[\propto]_D$ ^{22}= +30.04^0 (c=1.0, $CHCl_3$).

IR (KBr): 3339, 3325, 2978, 2930, 1694 cm^{-1} (Figure 3.25).

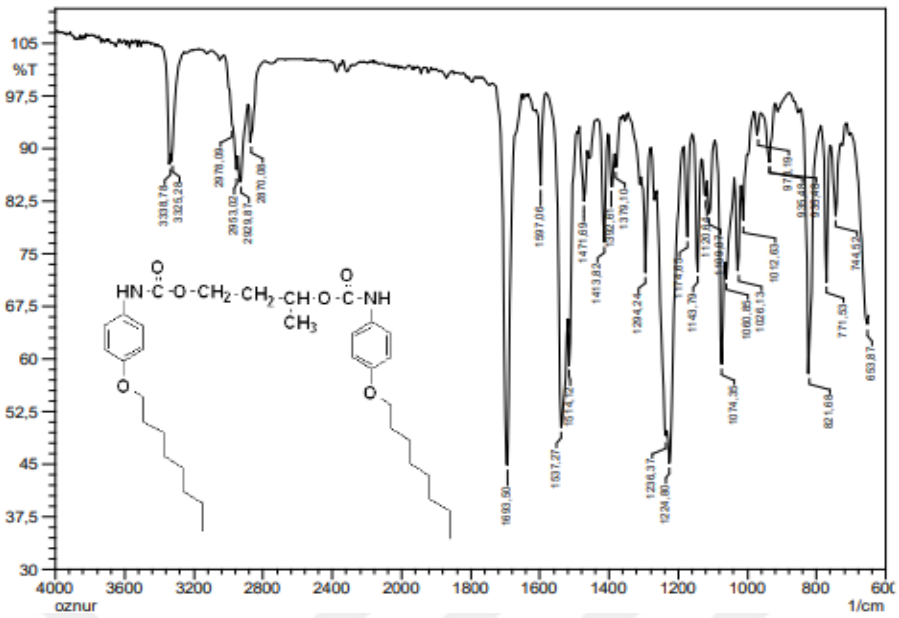

Figure 3.25. IR Spectrum of compound **S-O-Oct**.

^{1}H NMR (400 MHz, $CDCl_3$): δ= 0.91 (t, ^{3}J= 8,0 Hz, 6H, CH_3), 1.31-1,34 (br m, 16H (CH_2)), 1.36 (d, ^{3}J= 6,0 Hz,3H (CH_3)), 1.43-1,51 (m, 4H, CH_2), 1.75-1,82 (m, 4H, CH_2), 1.91-2.05 (m, 2H, CH_2), 3,94 (t, ^{3}J= 8,0 Hz, 4H, CH_2), 4.20-4.34 (m, 2H, OCH_2), 5.04-5.13 (m, 1H, OCH), 6.51 (br s, 1H, NH), 6.57 (br s, 1H, NH), 6.85 (d, ^{3}J= 8,0 Hz, 2H, CH), 6.86 (d, ^{3}J= 8,0 Hz, 2H, CH), 7.26 (d, ^{3}J= 8,0 Hz, 4H, CH) (Figure 3.26).

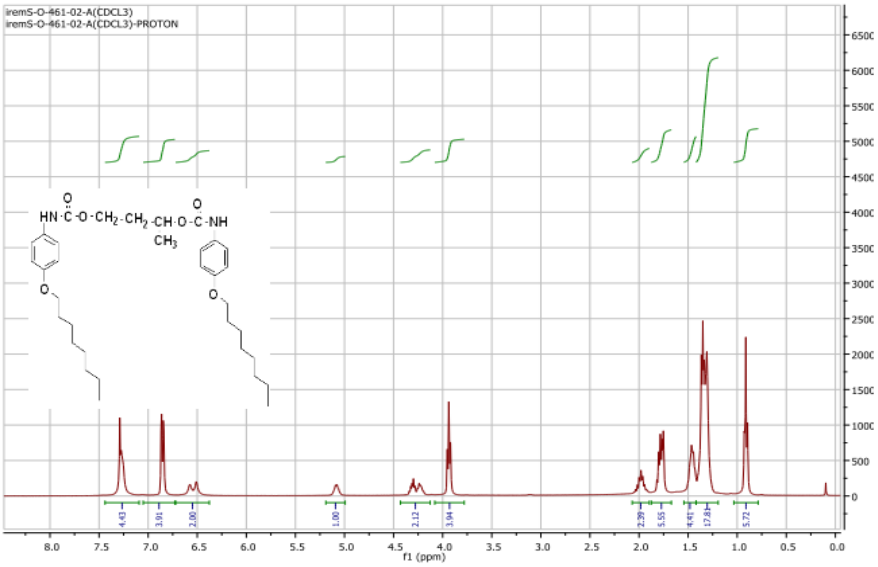

Figure 3.26. 400 MHz ^{1}H NMR spectrum of compound **S-O-Oct** in $CDCl_3$.

^{13}C NMR (100 MHz, $CDCl_3$): δ= 155.5, 153.8, 153.5, 130.7, 120.6, 114.9, 114.8, 68.8, 68.3, 61.5, 35.3, 31.8, 29.4, 29.3, 29.2, 26.1, 22.7, 20.5, 14.1 (Figure 3.27).

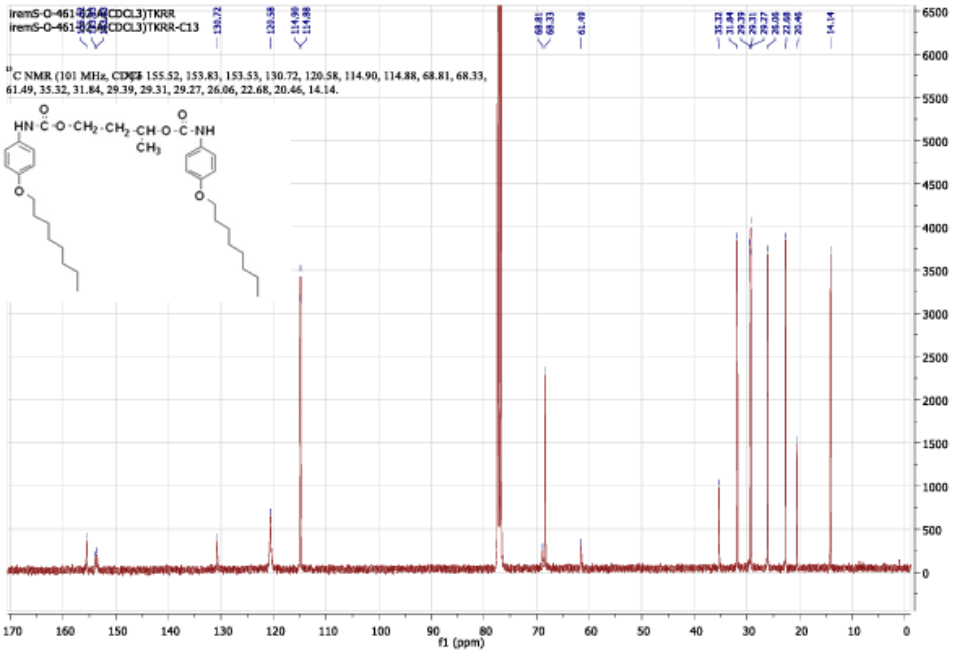

Figure 3.27. 100 MHz ^{13}C NMR spectrum of compound **S-O-Oct** in $CDCl_3$.

MS (HRMS): m/z calculated for $C_{34}H_{52}N_2O_6$: 585,3904 (M+H)+; found: 585,3903 $(M+H)^+$ (Figure 3.28).

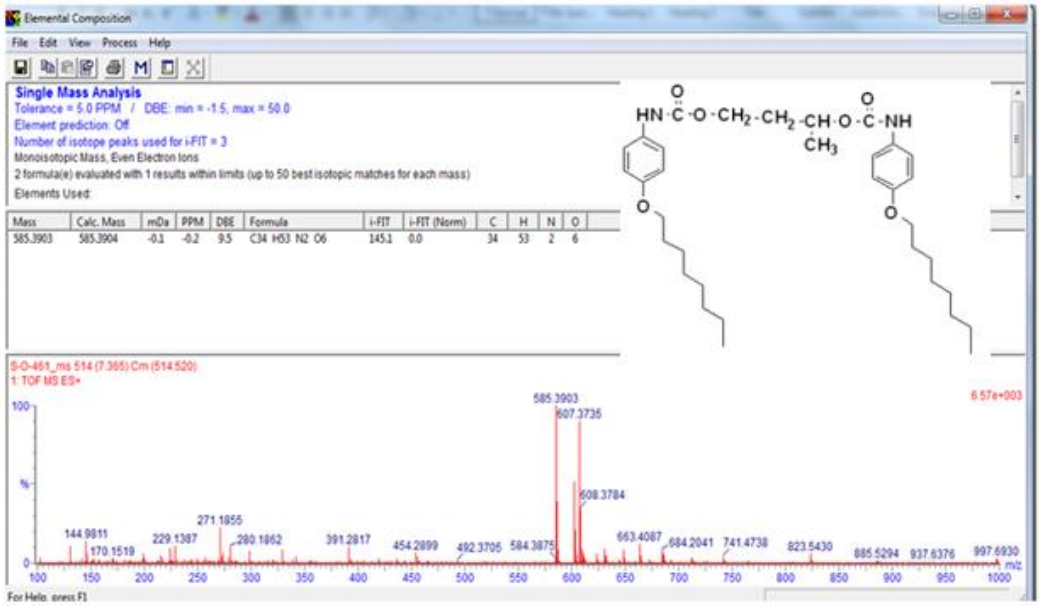

Figure 3.28. HRMS result of compound **S-O-Oct**.

3.3.3 1,(3S)-Bis[N-(*p*-decyloxyphenyl)-carbamoyloxy]butane, S-O-Dec

According to the general procedure 2.3.1, 1,(3S)-Bis[N-(*p*-decyloxyphenyl)-carbamoyloxy]butane, **S-O-Dec** was prepared by using 2,00 g of *p*-decyl benzoic acid, 1,70 ml of diphenylphosphoryl azide, 1,10 ml of triethylamine and 0,32 ml of (S)-(+)-1,3-butanediol in 10 ml of toluene.

White solid, yield: 1,88 g (81,66%) Melting point: 132.0-134.0 ^{0}C, $[\propto]_D$ ^{22}= +28.09 ^{0} (c=1.0, CHCl3).

IR (KBr): 3344, 3033, 2954, 2919, 2851, 1695 cm^{-1} (Figure 3.29).

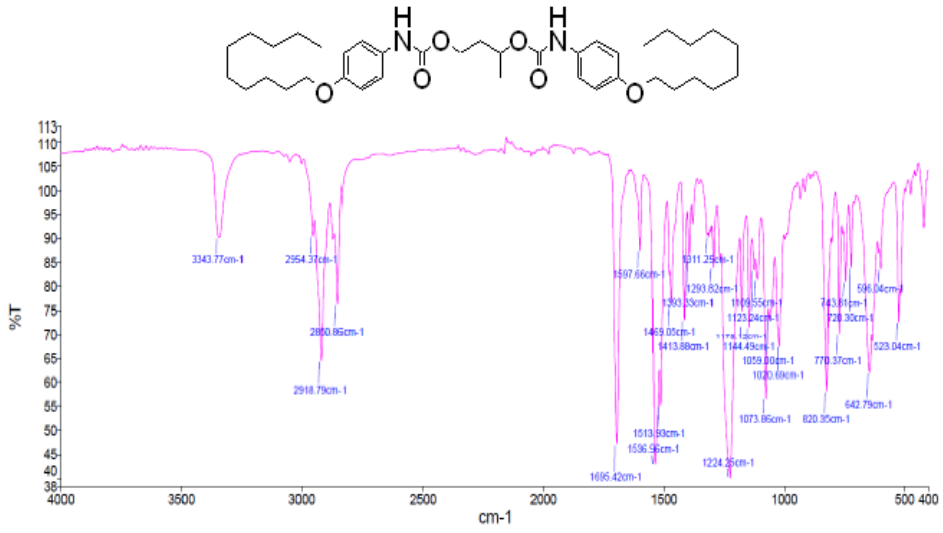

Figure 3.29. IR Spectrum of compound **S-O-Dec**.

^{1}H NMR (400 MHz, $CDCl_3$): δ= 0.91 (t, ^{3}J = 8,0 Hz, 6H, CH_3), 1.30-1,33 (br m, 24H (CH_2)), 1.36 (d, ^{3}J = 8,0 Hz,3H (CH_3)), 1.43-1,51 (m, 4H, CH_2), 1.75-1,82 (m, 4H, CH_2), 1.91-2.05 (m, 2H, CH_2), 3,94 (t, ^{3}J = 8,0 Hz, 4H, CH_2), 4.20-4.34 (m, 2H, OCH_2), 5.05-5.12 (m, 1H, OCH), 6.50 (br s, 1H, NH), 6.56 (br s, 1H, NH), 6.85 (d, ^{3}J = 8,0 Hz, 2H, CH), 6.86 (d, ^{3}J = 8,0 Hz, 2H, CH), 7.26 (d, ^{3}J = 8,0 Hz, 4H, CH) (Figure 3.30).

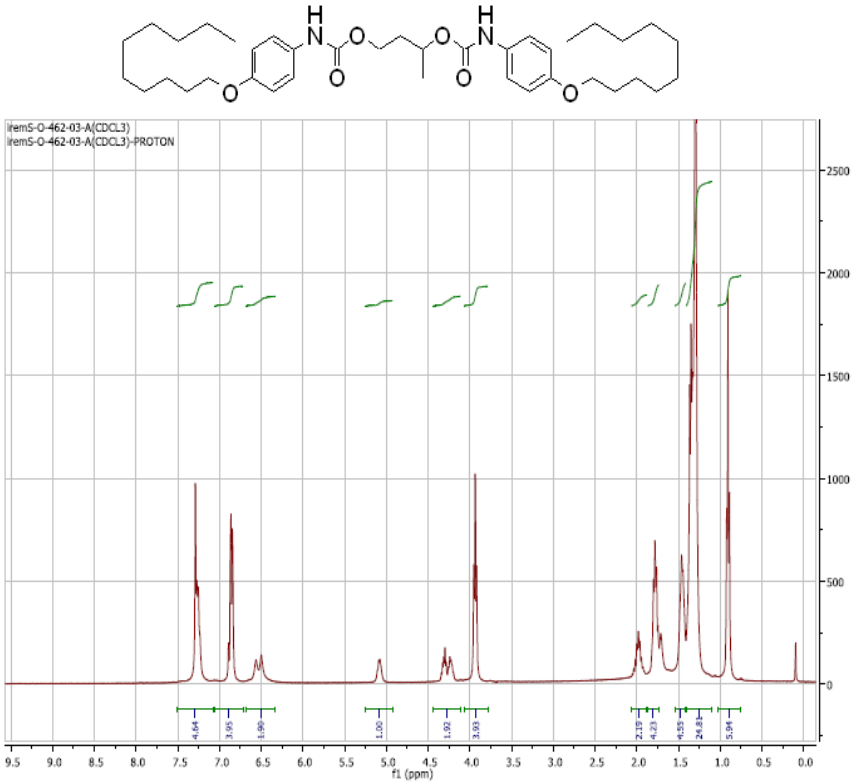

Figure 3.30. 400 MHz ^{1}H NMR spectrum of compound **S-O-Dec** in $CDCl_3$.

^{13}C NMR (100 MHz, $CDCl_3$): δ= 155.6, 153.8, 153.5, 130.7, 124.1, 120.6, 115.2, 115.0, 114.9, 68.9, 68.4, 61.5, 35.4, 31.9, 29.6, 29.5, 29.4, 29.3, 26.1, 22.7, 20.4, 14.1 (Figure 3.31).

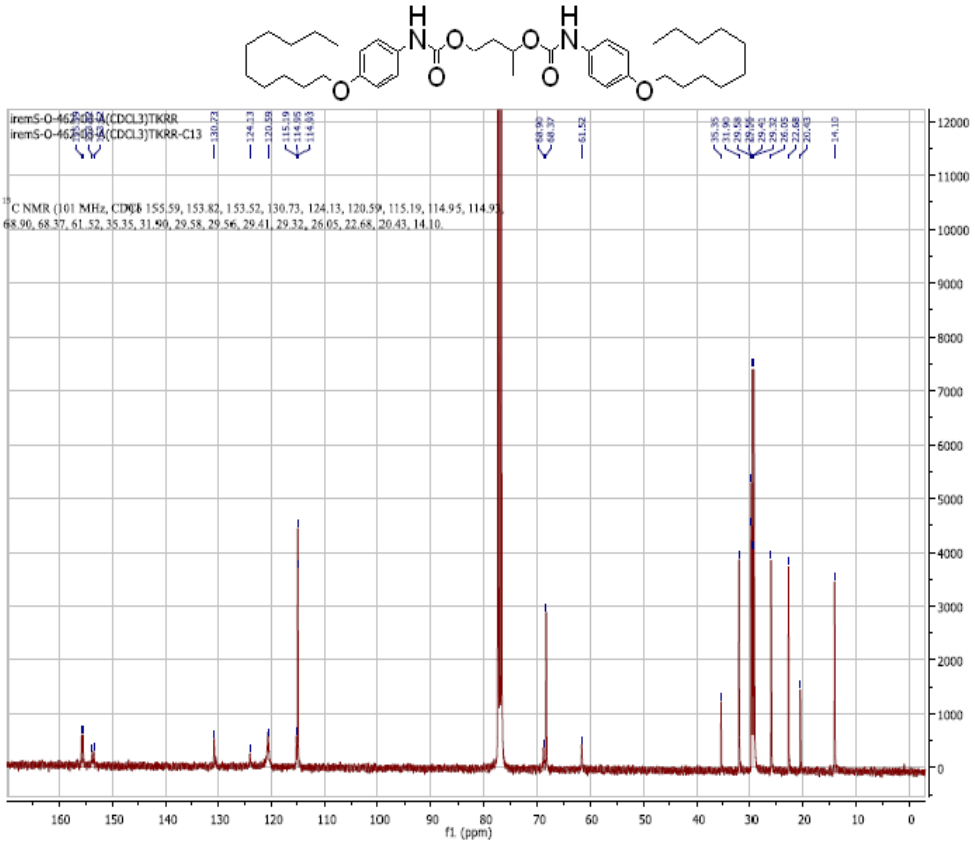

Figure 3.31. 100 MHz ^{13}C NMR spectrum of compound **S-O-Dec** in $CDCl_3$.

MS (HRMS): m/z calculated for $C_{38}H_{60}N_2O_6$: 641,4530 $(M+H)^+$; found: 641,4510 $(M+H)^+$ (Figure 3.32).

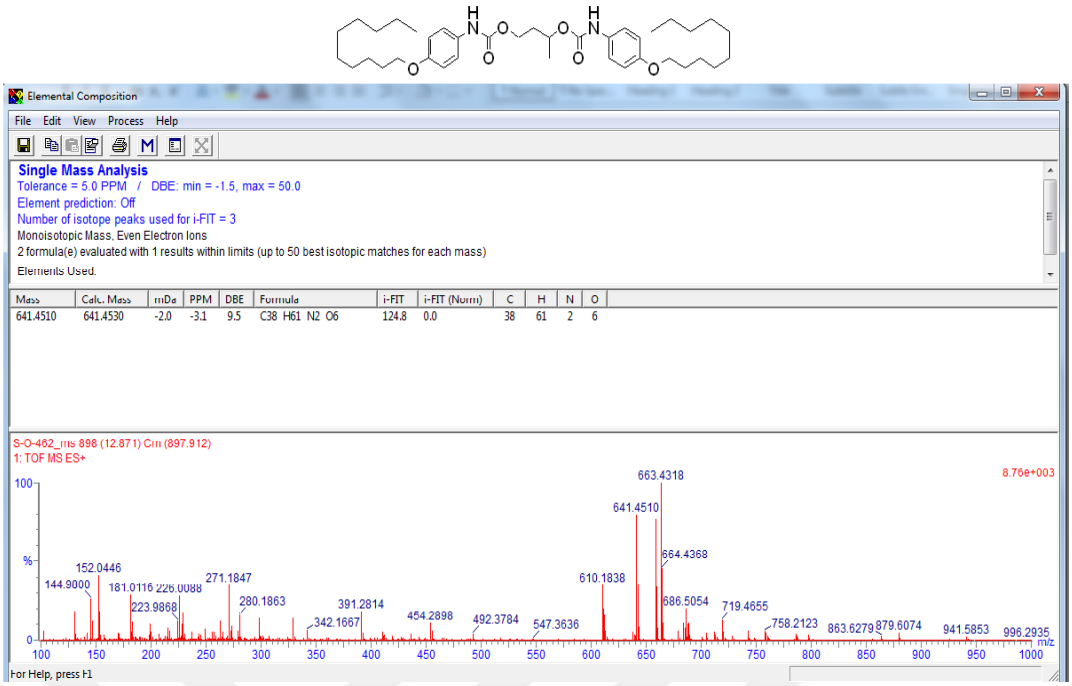

Figure 3.32. HRMS of compound **S-O-Dec**.

4. DISCUSSION

4.1 The Synthesis of 1,(3S)-Bis[N-(*p*-aryl)-carbamoyloxy]butane Compounds

The aim of this study was to synthesize new biscarbamate derivatives and investigate their gelation properties in different organic solvents.

The synthesis of bis-carbamate derivatives, namely **S-Hex**, **S-O-Hex**, **S-Hep**, **S-Oct**, and **S-Dec**, was performed in two stages (see Schemes 2.1 and 2.2). In the initial step (2.1.1), *p*-aryl isocyanates were successfully prepared via the Curtius rearrangement and were characterized by IR spectroscopy, showing distinct isocyanate (-N=C=O) absorption bands (Fig. 4.1 and Table 4.1).

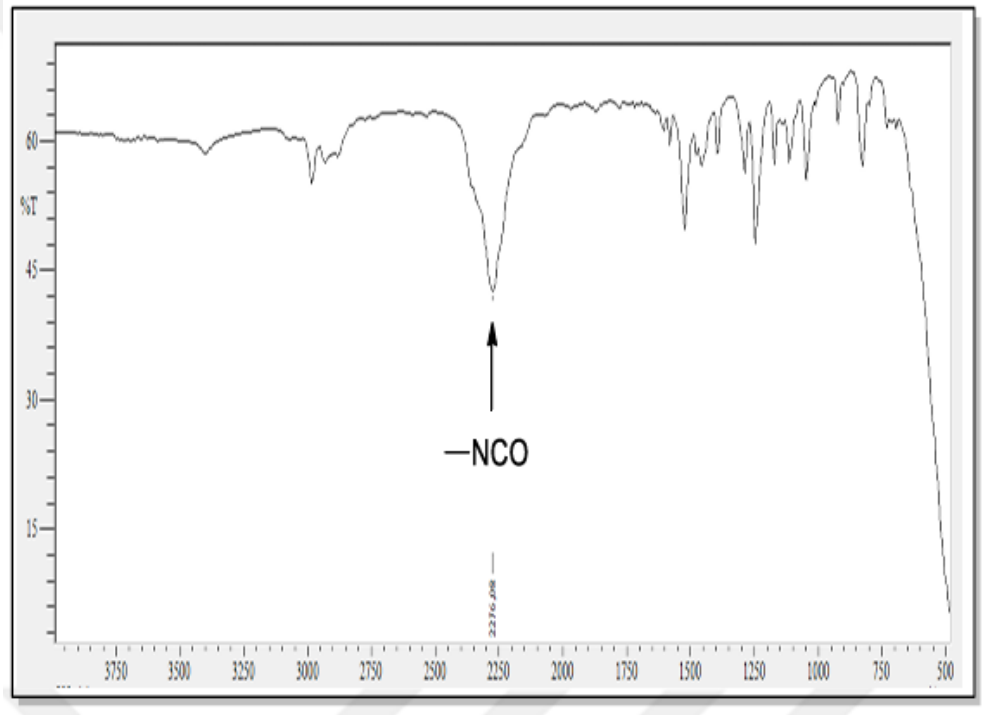

Figure 4.1. IR spectrum of *p*-hexyloxyphenyl iscoyanate.

Table 4.1. The yields of the synthesized *p*-aryl isocyanates (A_1-A_5).

Compound	Z	Yield (g/%)		IR (ν_{max}/cm^{-1})
A_1	Hexyl	0,8924	96,62	2257
A_2	Hexyloxy	4,48	98,00	2276
A_3	Heptyl	1,720	94,56	2238
A_4	Octyl	0,73	80,00	2223
A_5	Decyl	0,8924	96,62	2257

In the second step 1,(3S)-Bis[N-(p-aryl)carbamoyloxy]butanes, **S-Hex**, **S-O-Hex**, **S-Hep**, **S-Oct** and **S-Dec** were synthesized by the reaction of (S)-(+)-1,3-butanediol with *p*-aryl isocyanates in 75-93% yield according to the general procedure 2.2.1. (Table 4.2).

1,(3S)-Bis[N-(p-aryl)carbamoyloxy]butanes, **S-O-Hep**, **S-O-Oct** and **S-O-Dec** were synthesized according to the general procedure in 3.2.2 with the use of *p*-benzoic acid and DPPA. The yields and the melting points of all synthesized compounds are given in Table 4.2.

Table 4.2. The yields and the melting points of synthesized 1,(3S)-Bis[N-(p-aryl)carbamoyloxy]butanes.

Compound	Z	Yield (g/%)		Melting Point (^{0}C)
S-Hex	*p*-hexylphenyl	1,582	92,27	123.0-124.0
S-O-Hex	*p*-hexyloxyphenyl	1,360	75,00	155.7-157.5
S-Hep	*p*-heptylphenyl	0,710	93,00	122.3-123.7
S-O-Hep	*p*-heptyloxyphenyl	1,560	88,29	148.8-149.8
S-Oct	*p*-octylphenyl	0,700	92,00	118.1-119.1
S-O-Oct	*p*-octyloxyphenyl	1,960	83,90	149.0-150.5
S-Dec	*p*-decylphenyl	0,640	85,00	113.8-115.8
S-O-Dec	*p*-decyloxyphenyl	1,880	81,66	132.0-134.0

4.2 Structure Determination of 1,(3S)-Bis[N-(*p*-aryl)-carbamoyloxy]butane Derivatives

^{1}H NMR, ^{13}C NMR and IR spectroscopy were used for the structure determination of 1,(3S)-Bis[N-(*p*-aryl)-carbamoyloxy]butane compounds. Especially in the IR spectra, the observed disappearance of the cumulative -N=C=O vibrational band around 2200 cm^{-1} indicates the formation of carbamate in the first step. For all compounds, the carbamate NH stretching is observed as two broad peaks in the range 3323-3348 cm^{-1}, while the carbamate C=O stretching vibration shows a sharp peak in the range 1695-1701 cm^{-1}. The observation of two peaks for N-H functionality is due to the assymmetric nature of the structures. The IR spectrum of compound **S-O-Oct** was given as an example in Figure 4.2. As shown in the figure two NH peaks were observed at 3339 and 3325 cm^{-1}. The IR data for all compounds was tabulated in Table 4.3.

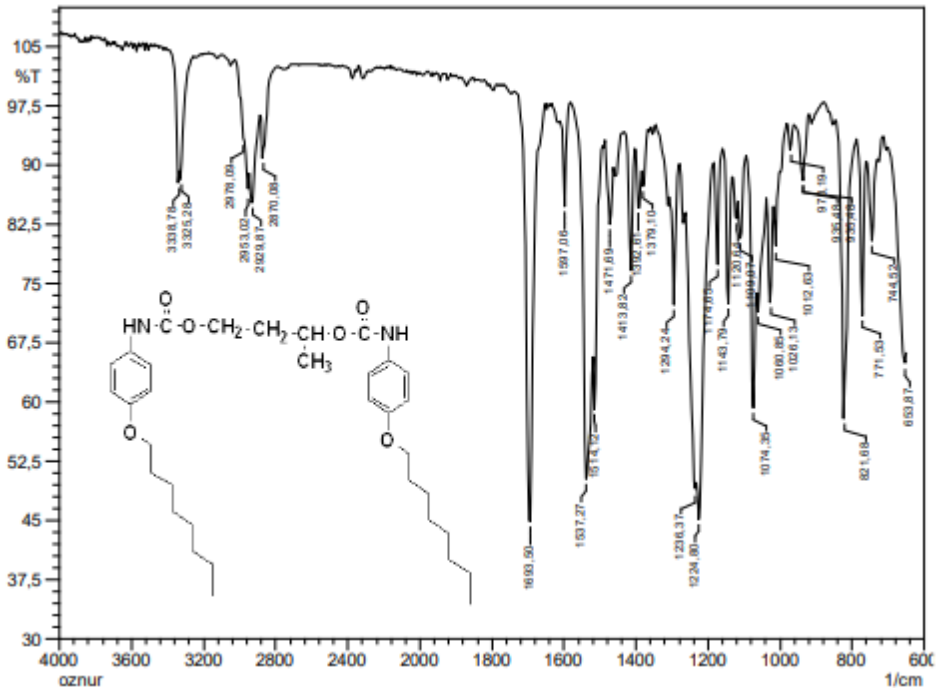

Figure 4.2. IR spectrum of compound **S-O-Oct**.

Table 4.3. IR data for the 1,(3S)-Bis[N-(*p*-aryl)-carbamoyloxy]butane compounds.

IR(ν_{max}/cm^{-1})				
Compound	**N-H**	**Ar-H**	**C-H**	**C=O**
S-Hex	3345	3032	2953-2924-2855	1699
S-O-Hex	3336	3032	2929-2873	1695
S-Hep	3311	3036	2953-2922-2849	1699
S-O-Hep	3337	3033	2923-2861	1695
S-Oct	3347	3040	2922-2849	1699
S-O-Oct	3339	3023	2978-2930	1694
S-Dec	3348	3036	2957-2918-2847	1699
S-O-Dec	3344	3033	2954-2851	1695

Full spectroscopy data for these compounds are given in Section 3. The detailed ^{1}H NMR spectrum of the *p*-octyloxy derivative (**S-O-Oct**) was chosen as an example for structure characterization. During the reaction the isocyanate function is converted to carbamate function. Therefore, the most important structure-proving signals at first glance belong to the carbamate N-H protons (a and a') observed in the range 6.43-6.63 ppm in the ^{1}H NMR spectra (Figure 4.3). Due to the molecular asymmetry, these protons are observed as individual singlet signals.

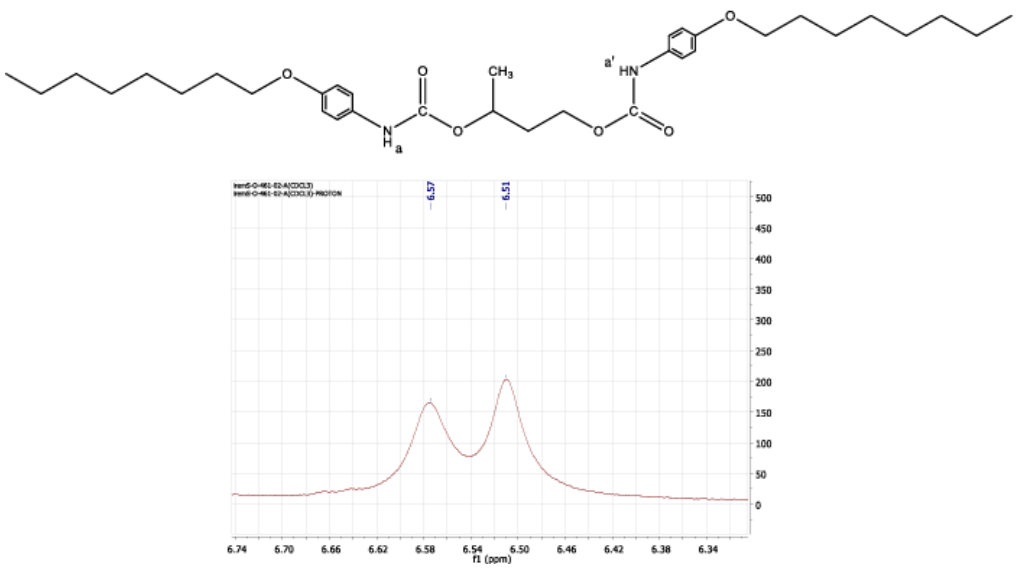

Figure 4.3. NH signals observed at 6.51 and 6.57 ppm for the *p*-Octyloxy derivative

In the aromatic region, ortho (b and b') and meta (c and c') aromatic protons were observed as doublet signals with a splitting constant of 8 Hz (Figure 4.4). Due to their proximity to the chiral center, *ortho*-b-b' protons were observed as two separate doublet signals at 6.85 and 6.86 ppm. The meta protons c,c' gave a single broader doublet signal right next to the solvent signal.

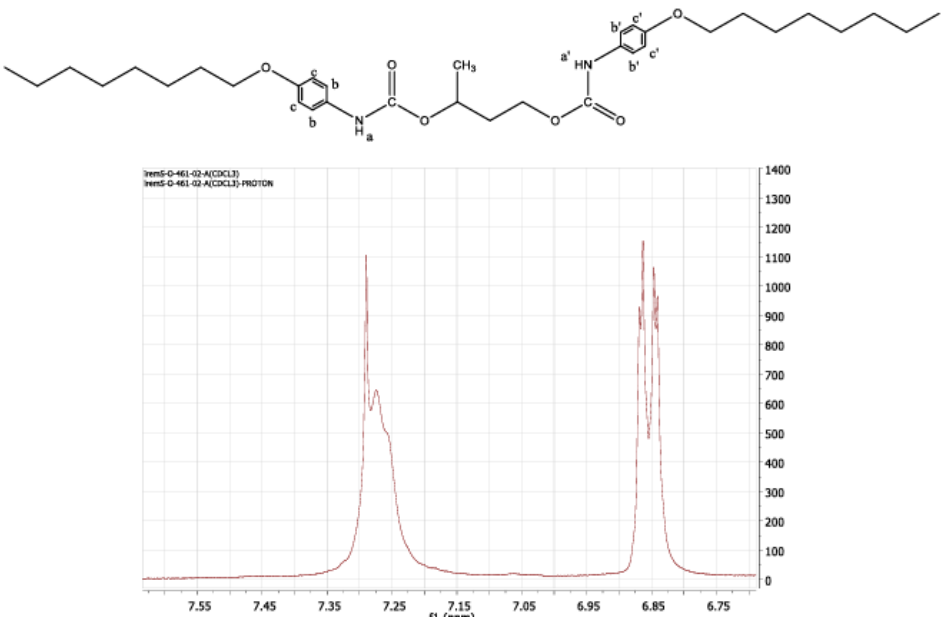

Figure 4.4. Signals observed for aromatic protons of the *p*-Octyloxy derivative

The methine proton (d) at the chiral center was observed as a multiplet signal in the range of 5.04-5.13 ppm, coupled with neighboring methyl and diastereotopic methylene protons (Figure 4.5).

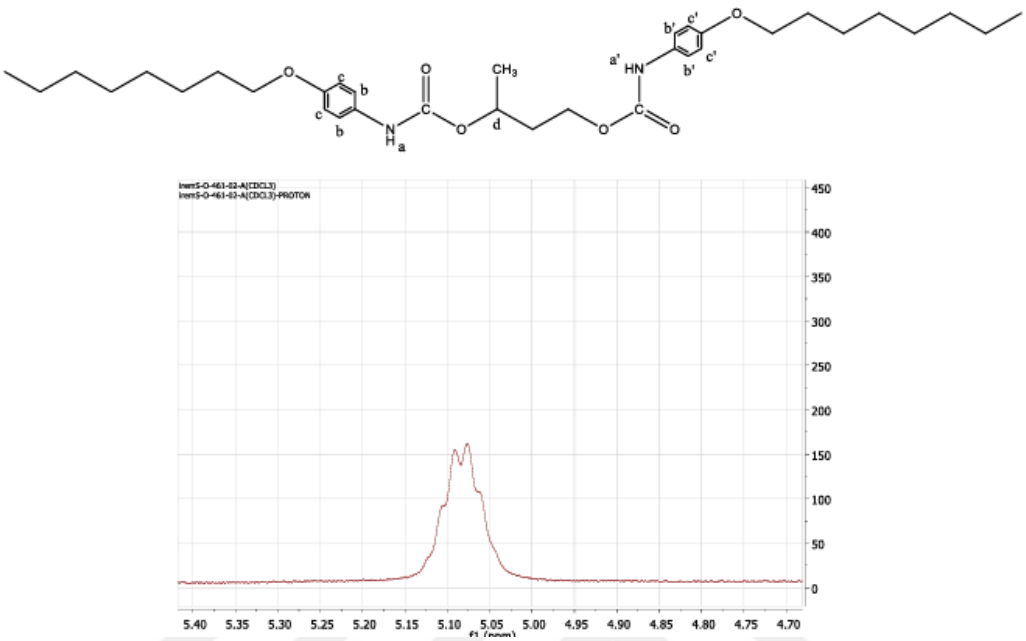

Figure 4.5. Multiplet signal observed for the proton of methine (d) of the *p*-Octyloxy derivative

Diastereotopic methylene protons (e) were observed as multiplets in the range of 1.91-2.05 ppm, with complex splitting affected by both the proton (d) at the chiral center and the neighboring diastereotopic methylene protons (f). (Figure 4.6).

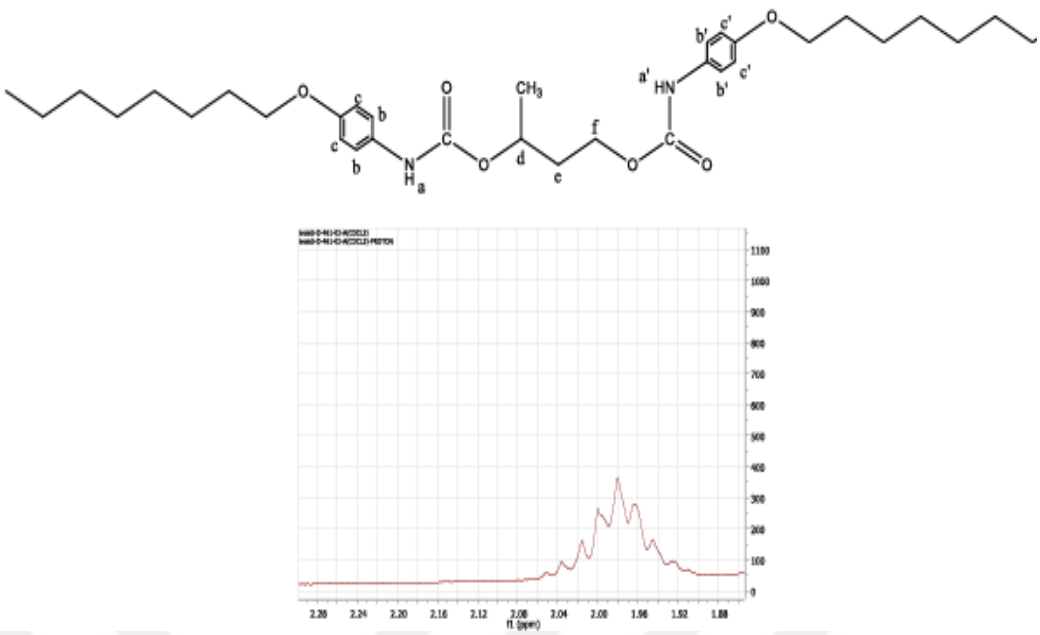

Figure 4.6. Multiplet signal observed for methylene (e) protons of the *p*-octyloxy derivatives

The diastereotopic methylene protons (f) next to the carbamate oxygen was observed as a multiplet in the range of 4.20-4.34 ppm, affected by other diastereotopic methylene protons (e) adjacent to the chiral center. The resulting AB quartet signal was again splitted by the diastereotopic methylene protons. The complex splitting resulting from the overlap of some peaks is given in Figure 4.7.

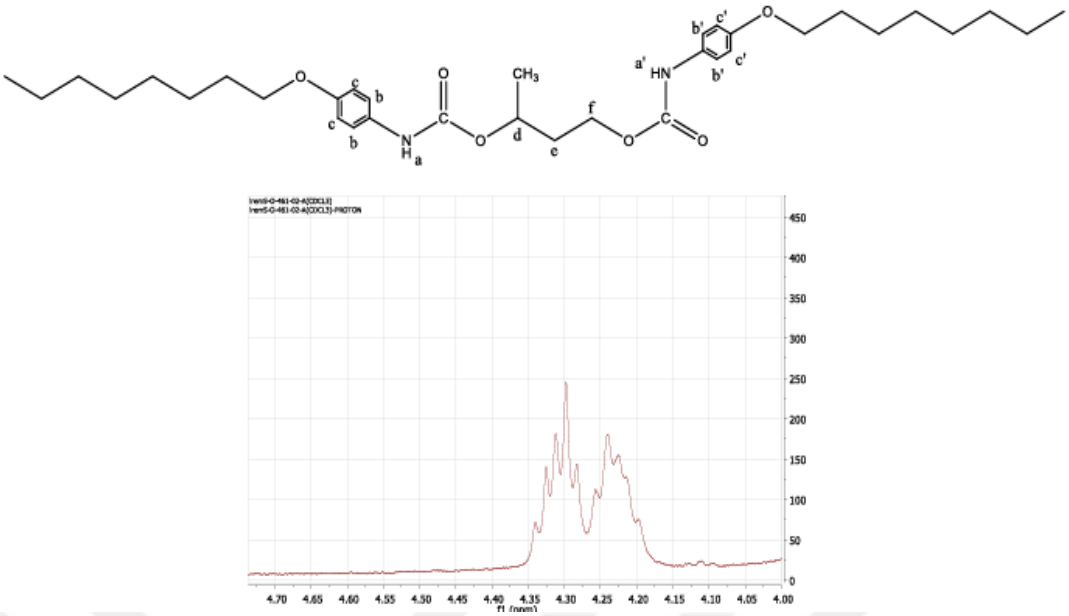

Figure 4.7. Multiplet signal observed for diastereotopic methylene (f) protons of the *p*-octyloxy derivative.

The methylene protons (h, h') in the *p*-octyloxy chain, were observed as a single triplet at 3.94 ppm due to the coupling with neighboring methylene protons (Figure 4.8).

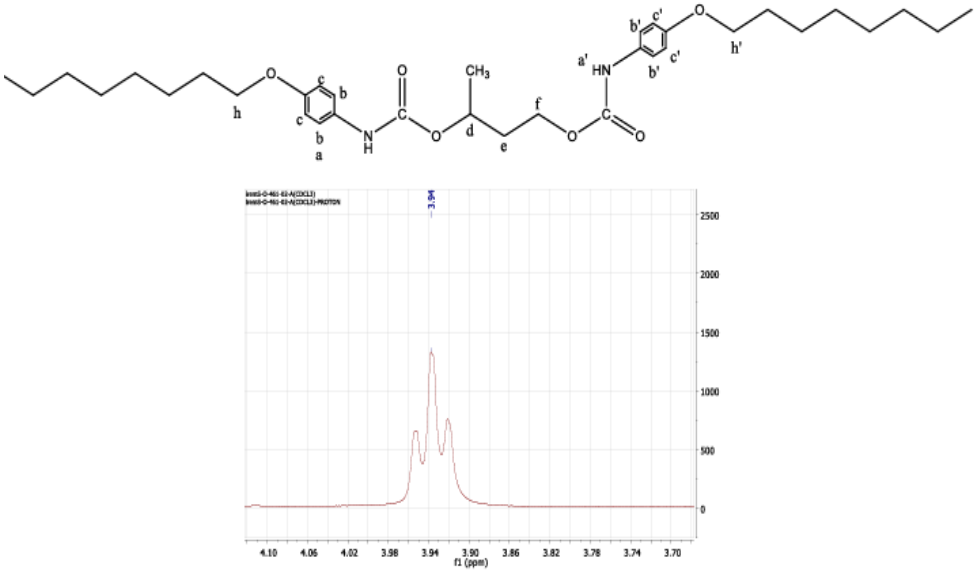

Figure 4.8. Triplet signal observed for methylene (h, h') protons of the *p*-octyloxy derivative

(i, i') protons in the *p*-octyloxy chain were coupled with neighboring methylene groups and gave a pentet (multiplet) in the range of 1.75-1.82 ppm. However, as one of the signals overlapped with the water peak in the solvent, the signal in Figure 4.9 was observed.

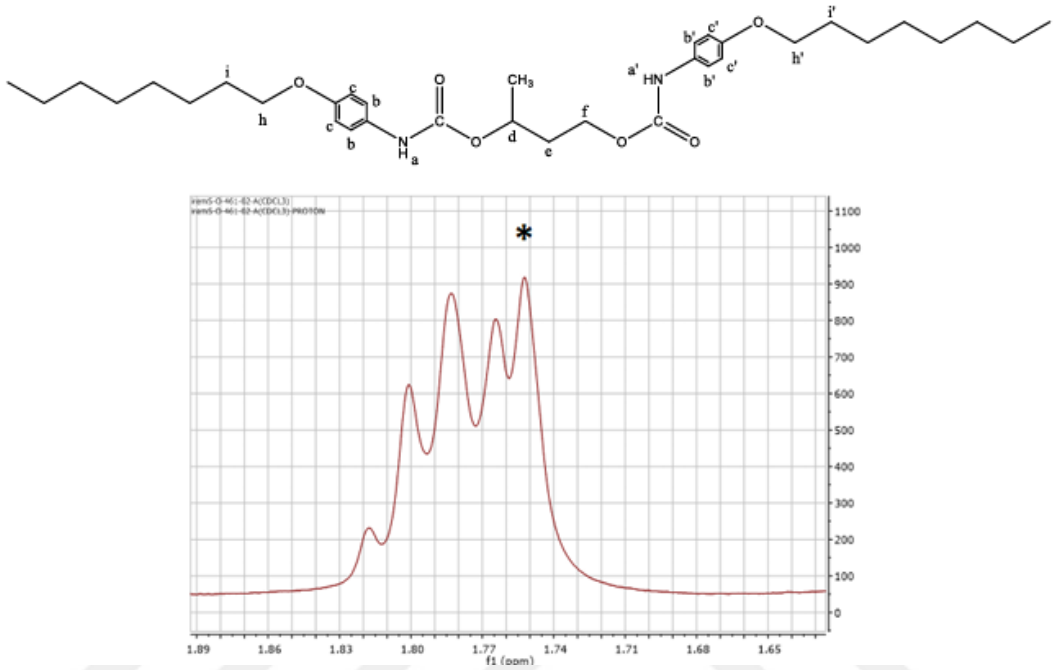

Figure 4.9. Multiplet signal observed for methylene (i, i') protons of the *p*-Octyloxy derivative, *: solvent peak.

Similarly, (j, j') protons gave a pentet (multiplet) in the range of 1.43-1.51 ppm (Figure 4.10).

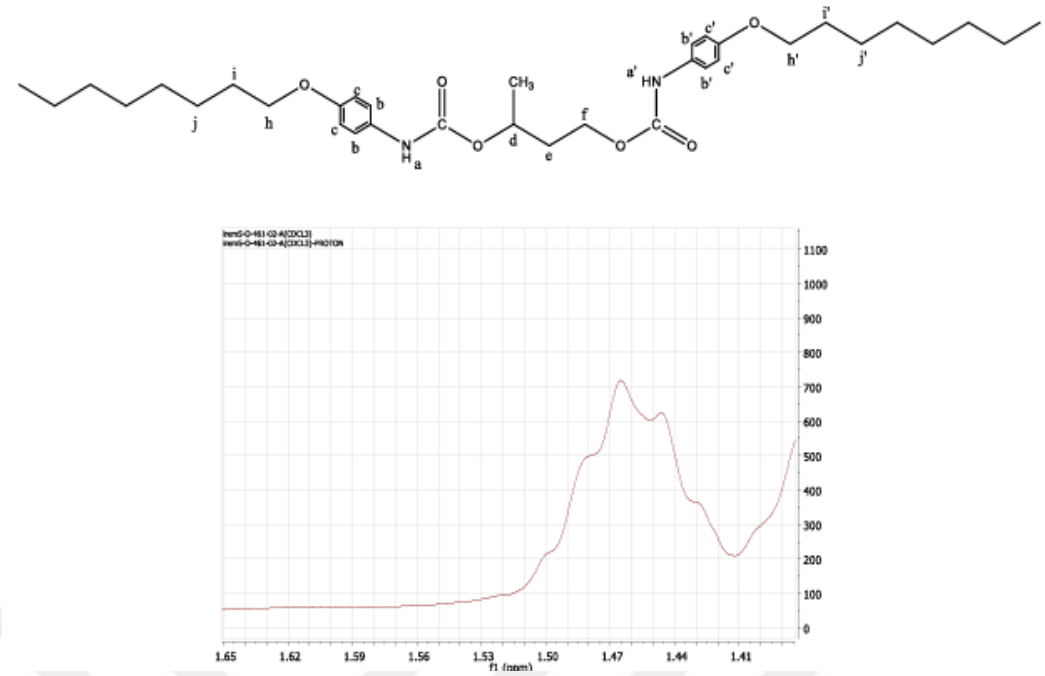

Figure 4.10. Multiplet signal observed for methylene (j, j') protons of the *p*-octyloxy derivative

For this derivative, the methyl group (g) at the chiral center (Figure 5.9) appears as a doublet signal at 1.36 ppm. For some derivatives, it could not be observed due to the signal overlapping in that area and the integral calculation could be performed together with the other peaks. Other methylene groups (k, k') in the *p*-octyloxy chain were observed as broad signals of sixteen protons at 1.31 and 1.34 ppm due to their close chemical shift values. (Figure 4.11).

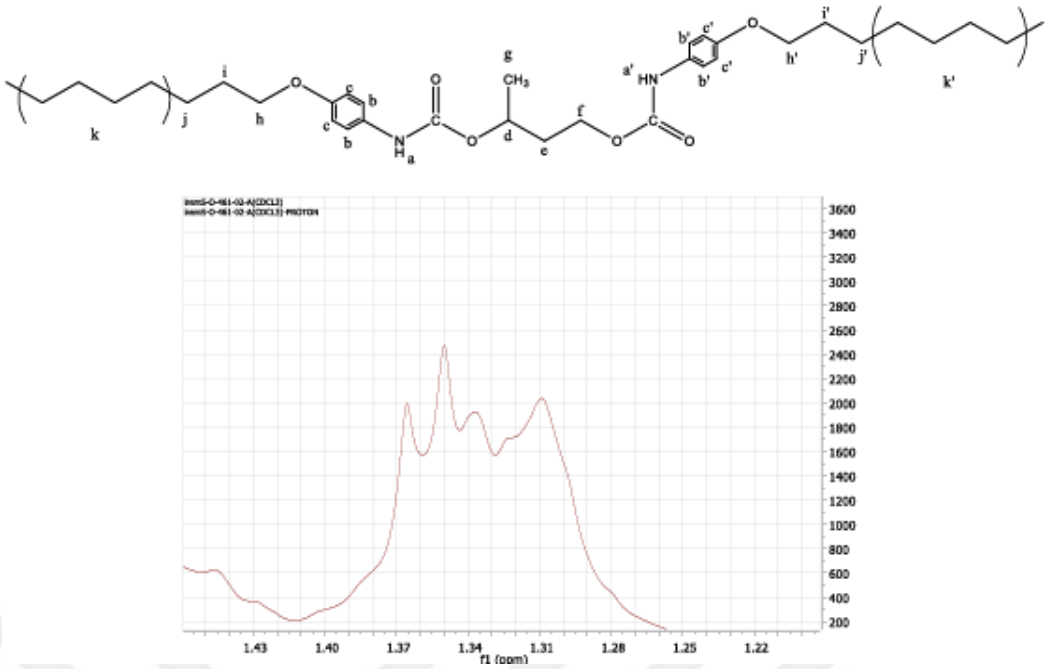

Figure 4.11. For the methyl protons (g) of the *p*-octyloxy derivative, the doublets observed at 1.36 ppm and a broad multiplet signal observed for methylene (k, k') protons.

The methyl group in the *p*-octyloxy chain (l, l') show a triplet signal equivalent to six protons at 0.91 ppm. (Figure 4.12).

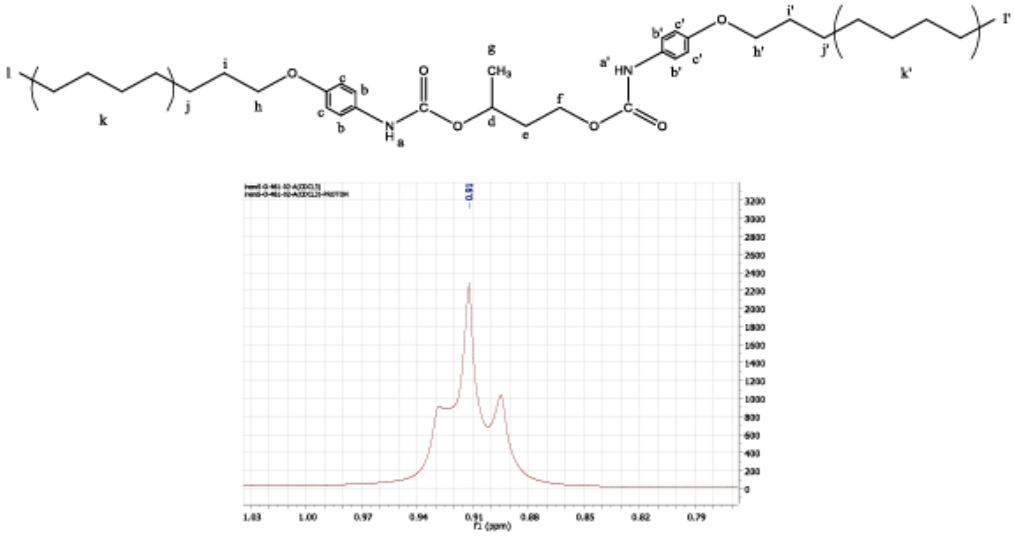

Figure 4.12. Triplet signal observed for methyl (l, l') protons of the *p*-octyloxy derivative.

In the ^{13}C NMR spectra, it was observed that some peaks were affected by asymmetry and gave separate peaks. For example, in Figure 3.13, the two carbonyls of the *p*-decyloxy derivative were observed as two separate signals at 153.8 and 153.5 ppm. The signal at 155.6 ppm is the quarternary carbon to which the *p*-decyloxy group is attached.

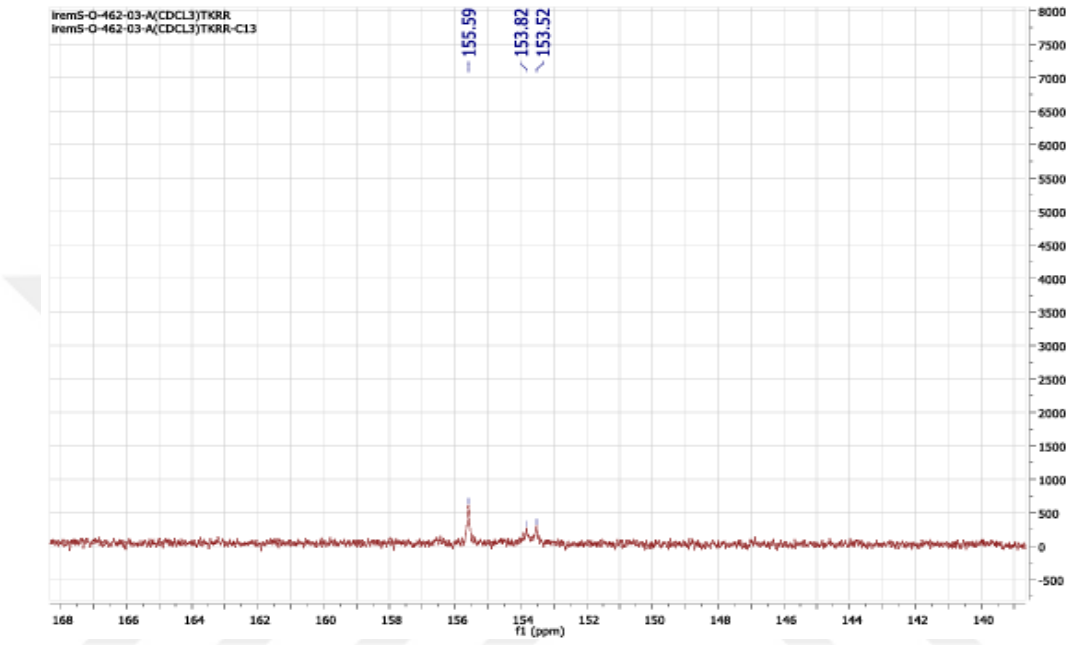

Figure 4.13. Signals observed for the quarternary carbons of the *p*-decyloxy derivatives.

4.3 Investigation of Gelling Properties of 1,(3S)-Bis[N-(*p*-aryl)-carbamoyloxy]butane derivatives in Organic Solvents

Although most of the molecules that can gel are found by chance, recent studies have shown that the molecules capable of hydrogen bonding and van der Waals interactions provide gelation (Esch et al, 1999; Laan et al., 2002; Suzuki et al., 2003; Nigawara et al., 2003; Hirst et al., 2004; Suzuki et al., 2005; Mohenmeyer et al., 2005; Lebel et al., 2006; Hardy et al., 2007; Loos et al., 2007; Li et al. 2007; Suzuki et al., 2008; Debnath et al., 2008; Zweep et al., 2009). Each compound structure given to the literature allows the mechanism of gelation to be revealed. Especially in apolar solvents, it is stated that the primary interaction is hydrogen bonding. Other interactions play a supporting and strengthening role to the primary interaction. However, since the high number of primary and secondary forces for

the self-assembly of molecules will also trigger crystal formation, all these forces should be considered in a balanced way when designing a gelling molecule. Considering that gelation is an event between solution or precipitate formation (Zweep et al., 2009; Hirst et al., 2004), it is difficult to know in advance whether a molecule will gel or not. The compounds synthesized within the scope of the project contain carbamate functional group for hydrogen bonding and *p*-alkoxy and *p*-alkylphenyl groups. It was predicted that the phenyl ring would be involved in π-π interaction and the electron donor groups attached to the phenyl ring would strengthen this interaction. Moreover, the chain length of the *p*-alkoxy or *p*-alkyl groups may have an effect on the gelation abilites and the morphology of the gel or the liquid uptake capacity of the material. The van der Waals interactions between the para-substituents are also predicted to act as secondary interactions and support the gelation process.

The effect of stereochemistry on gelation led us to design enantiomerically pure long chain *p*-alkyl and *p*-alkoxysubstituted 1,3S-Bis[N-(*p*-aryl)carbamoyloxy]butane derivatives (Figure 4.14). The starting point for the design of these molecules was the results obtained from the previously completed project supported by TÜBİTAK-3501 109T919. In this study (Demir-Ordu et al, 2015), low molecular mass organogelators based on bis-carbamates without chiral center (Figure 4.15) were found to gel toluene, xylene, ethyl laurate, n-butyl palmitate, olive oil, sunflower oil and corn oil. In these derivatives, there are two carbamate groups capable of hydrogen bonding and an aryl ring with electron donor groups. It was predicted that the electron donor groups would increase the electron density of the ring and provide better π–π interaction of the molecule and the alkyl chain in the compounds was thought to play a role in the gelation mechanism by van der Waals interactions. As a result of the project, it was determined that the factors effective in gelation were (i) the length of the alkyl chain linking the two carbamate structures (Figure 4.15, n number), (ii) the alkoxy or alkyl groups in the para position and the length of the alkyl chain, (iii) concentration and (iv) temperature. The length of the methylene chain linking the two carbamate groups was found to have an odd-even effect on gelation. Especially for *p*-alkoxy derivatives, molecules containing an odd number of methylene groups formed gels, whereas those containing an even number of methylene groups precipitated. For *p*-alkyl derivatives, decreasing this number increased gelation. This effect was

explained by another factor solubility. In particular, it was observed that the three-carbon chain between carbamate groups positively affected gelation for both *p*-alkyl and *p*-alkoxy derivatives. Especially for *p*-alkoxy derivatives, although molecules containing an odd number of methylene groups formed gels, precipitation was observed for those containing an even number of methylene groups. In addition, cryogels were obtained from *para*-alkyl derivatives at -18 ^{0}C. Among these derivatives, the *p*-hexyl derivative was found to have a nanoporous structure unlike other nanofiber structured gels. Hydrogen bonding, π-π and van der Waals interactions in gelation were proved by NMR and IR analysis. Because of these results, the designed compounds includes three-carbon spacer between the carbamate units and long alkyl/alkoxy chain on the *para*-position.

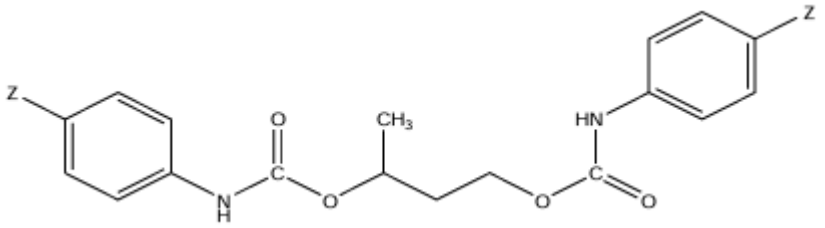

Z: hexyl, hexyloxy, heptyl, heptyloxy, octyl, octyloxy, decyl, decyloxy

Figure 4.14. Synthesized compounds within the scope of the thesis.

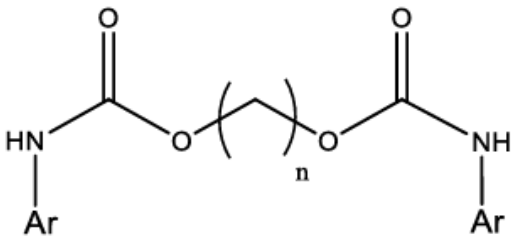

Figure 4.15. Compounds synthesized within the scope of TUBITAK-3501 109T919 project (1,6-Bis[N-(*p*-aryl)carbamoyloxy]hexane, 1,5-Bis[N-(*p*-aryl)-carbamoyloxy]pentane, 1,4-Bis[N-(*p*-aryl)carbamoyloxy]butane, 1,3-Bis[N-(*p*-aryl)-carbamoyloxy]propane).

One of the most important criteria for gelation is solubility. For this reason, solvent screening was first performed for each of the synthesized substances and a list of solvents was created by looking at the polarity index of the solvents.

4.3.1 Determination of Minimum Gelation Concentration (MGC)

In order to determine the minimum amount for gelation, a certain amount of organogelator was dissolved in 1 ml of organic solvent by heating as described in Section 2.3 and allowed to cool: at RT and -18 ^{0}C due to the effect of temperature on gelation. The solution was not moved during this process. The gelation studies for p-alkyl derivatives are given in Table 4.4. Similarly, all studies were performed at both room temperature and -18 ^{0}C for *p*-alkoxy derivatives (Table 4.5, Table 4.6, Table 4.7). Acetone, THF, DMF, methyl alcohol, diethyl ether, dichloromethane and chloroform, which are frequently used organic solvents in laboratories, are not suitable solvents for gelation since they easily dissolve compounds at room temperature. Only solution was obtained in these solvents. The synthesized compounds are insoluble in hexane, cyclohexane, pentane and petroleum ether. Therefore, these solvents were also not suitable for gelation. Afterwards, in order to change the solvent polarity, the ability of the compounds to gel was tested in n-pentanol, n-hexanol, n-heptanol, n-octanol, ethanol, ethyl acetate, acetonitrile, toluene and *p*-xylene. The results obtained are given in Table 4.5. Although alcohols such as n-pentanol, n-hexanol, n-heptanol and n-octanol did not provide gelation, gelation in toluene, *p*-xylene, ethanol and ethyl acetate was obtained for some derivatives.

In order to change the polarity, gelation studies were also performed with long chain esters, which are also used in the pharmaceutical industry. All results are given in Table 4.6. Finally, gelation studies were carried out in vegetable oils with lower polarities (Table 4.7).

Table 4.4. Gelation studies obtained for *p*-alkyl derivatives (DMSO: Dimethyl sulfoxide, NBP: n-Butyl palmitate, EL: Ethyl laurate, IPM: Isopropyl myristate, IPP: Isopropyl palmitate) (*: values in parentheses are minimum gelation concentration (MGC): mg/1 ml solvent)(ppt: precipitate, G: gel, PG: partial gel, sol: solution)

Compound No	Temperature (^{0}C)	SOLVENT							
		DMSO	Olive Oil	Corn Oil	Sunflower Oil	NBP	EL	IPM	IPP
S-Hex	RT	sol	ppt	ppt	ppt	G (21)*	sol	sol	G (50)
	-18	sol	PG	PG	PG	ppt	sol	sol	ppt
S-Hep	RT	sol	ppt	ppt	ppt	ppt	sol	ppt	G (46)
	-18	sol	G (44)	G (50)	G (34)	G (34)	ppt	G (44)	ppt
S-Oct	RT	sol	ppt	ppt	ppt	ppt	ppt	ppt	G (38)
	-18	sol	G (35)	G (47)	G (42)	G (32)	G (52)	G (50)	ppt
S-Dec	RT	sol	sol	sol	sol	ppt	ppt	ppt	G (48)
	-18	sol	G (23)	G (30)	G (28)	G (50)	ppt	G (48)	ppt

(*:NBP gel was obtained at room temperature but was stable for 6 hours)

According to the data in Table 4.4, all *p*-alkyl derivatives form stable gels in IPP only at room temperature. Only **S-Hex** NBP gel could be obtained at room temperature but remained stable for six hours. In partial gel formations, the viscosity of the solution increased but the structure tended to flow. Addition of substance did not transform the viscous structure into a gel.

For olive oil, corn oil gels increasing the length of *p*-alkyl substitution from heptyl to decyl decreased the MGC value. This result is attributed to increasing chain length, thus strengthening van der Waals interactions.

For NBP gels, a reverse affect was observed at -18 ^{0}C probably as a result of increasing solubility in NBP.

S-Hep, S-Oct and **S-Dec** derivatives were found to gel IPM only at -18 ^{0}C. The lowest MGC value was obtained for **S-Hep** derivative. Fort this solvent, increasing the *p*-alkyl chaing length from heptyl to decyl increased the solubility, hence increased the MGC value.

In IPP all derivatives formed gels at RT. Increasing the chain length from hexyl to octyl decreased the MGC value, probably due to an increase in van der Waals interactions. But for **S-Dec** derivative MGC value was found to be the highest, as a result of an increase in solubility.

Gels that could not be obtained for *p*-alkyl derivatives in some common organic solvents could be obtained for *p*-alkoxy derivatives. This can be explained by the solubility and the electron donating property of the *p*-alkoxy group that may enhance the π–π interaction (Demir-Ordu et al., 2015). In the solvents given in Table 4.5, *p*-alkyl derivatives only formed solutions due to their high solubilities.

A direct relationship between gelation property and *p*-alkyl chain length or temperature could not be observed for the solvents given in Table 4.5.

Table 4.5. Gelation studies in organic solvents for *p*-Alkoxy derivatives (*:values in parentheses are minimum gelation concentration (MGC): mg/1 ml solvent) (ppt: precipitate, G: gel, PG: partial gel, sol: solution)

Compound No	Temperature (^{0}C)	SOLVENT					
		Ethyl Acetate	**Absolute Ethanol**	***p*-xylene**	**Acetonitrile**	**Toluene**	**DMSO**
S-O-Hex	RT	ppt	PG	PG	PG	PG	sol
	-18	G (40)	G (51)	PG	PG	PG	sol
S-O-Hep	RT	ppt	PG	G (61)	G (32)	ppt	sol
	-18	ppt	G (33)	ppt	G (32)	G (61)	sol
S-O-Oct	RT	G (46)	PG	PG	PG	ppt	PG
	-18	ppt	G (52)	PG	PG	G (46)	PG
S-O-Dec	RT	ppt	ppt	G (44)	PG	G (47)	G (80)
	-18	ppt	ppt	ppt	PG	G (47)	G (80)

p-Alkoxy derivatives formed a limited number of gel structures in esters (Table 4.6). Compared to *p*-alkyl derivatives, their solubility in these solvents is limited.

p-Alkoxy derivatives formed gel structures mostly in vegetable oils (Table 4.7). Some gels were formed at both temperatures, while for others the temperature had to be cooled to -18 ^{0}C. Especially canola oil gel structure could be obtained for all derivatives.

Table 4.6. Gelation studies in esters for *p*-alkoxy derivatives (*:values in parentheses minimum gelation concentration (MGC): mg/1 ml solvent) (ppt: precipitate, G: gel, PG: partial gel)

Compound No	Temperature (^{0}C)	SOLVENT			
		EL	IPP	NBP	IPM
S-O-Hex	RT	ppt	ppt	ppt	PG
	-18	ppt	ppt	G (29)	PG
S-O-Hep	RT	ppt	PG	ppt	ppt
	-18	ppt	PG	ppt	ppt
S-O-Oct	RT	ppt	PG	PG	PG
	-18	ppt	PG	G (31)	PG
S-O-Dec	RT	G (40)	ppt	ppt	ppt
	-18	ppt	ppt	ppt	ppt

Decreasing gelation temperature from RT to -18 ^{0}C affected the gelation abilities of **S-O-Hep** in sunflower, canola and hazelnut oils. Although partial gels were obtained at RT, stable gel structures formed at -18 ^{0}C. Similarly for **S-O-Oct** and **S-O-Dec** canola oil gels were obtained at -18 ^{0}C as a result of temperature effect.

Table 4.7. Gelling studies in vegetable oils (*:values in parentheses are minimum gelation concentrations (MGC): mg/1 ml solvent) (ppt: precipitate, G: gel, PG: partial gel)

Compound No	Temperature (^{0}C)	SOLVENT			
		Olive Oil	Sunflower Oil	Canola Oil	Hazelnut Oil
S-O-Hex	RT	G (41)	G (42)	G (42)	G (43)
	-18	G (41)	G (42)	G (42)	G (43)
S-O-Hep	RT	G (63)	PG	PG	PG
	-18	G (63)	G (52)	G (42)	G (50)
S-O-Oct	RT	ppt	PG	PG	PG
	-18	ppt	PG	G (31)	PG
S-O-Dec	RT	ppt	PG	PG	PG
	-18	ppt	PG	G (43)	PG

Only **S-OHex** and **S-O-Hep** derivatives formed gel structures in olive oil and sunflower oil. Increasing the *p*-alkoxy chain length decreased the gelation behavior and for **S-O-Oct** and **S-O-Dec** derivatives only precipitation was observed.

The lowest MGC value was obtained for **S-O-Oct** derivate. The MGC values for the gelation of **S-O-Hex** and **S-O-Hep** derivatives in canola oil were obtained as the same. Increasing the *p*-alkoxy chain length decreased the gelation behavior probably due to an increase in solubility.

5. CONCLUSION

All 1,(3S)-Bis[N-(p-aryl)carbamoyloxy]butane derivatives were synthesized with yields ranging from 81% to 92%. Melting points were measured after purification, and the structures were confirmed using ^{1}H, ^{13}C NMR, IR spectroscopy, and HRMS techniques. Since the compounds have an asymmetric carbon, their specific rotations were also determined by polarimetry. Two methods were used in compound synthesis. **S-Hex**, **S-O-Hex**, **S-Hep**, **S-Oct** and **S-Des** derivatives were obtained from the reaction of (S)-(+)-1,3-Butanediol with *para* substituted phenyl isocyanates in toluene under reflux. Since some of the benzoyl chlorides used as starting materials were not commercially available, **S-O-Hep**, **S-O-Okt** and **S-O-Des** derivatives were obtained using diphenyl phosphoryl azide (DPPA) and benzoic acid.

For all 1,(3S)-Bis[N-(*p*-aryl)-carbamoyloxy]butane compounds gelation studies were performed. After purification, for all substances suitable gelling organic solvents were found. Since there is also a temperature effect on gelation, gelation studies were carried out both at room temperature and at -18 ^{0}C. *p*-Alkyl derivatives, **S-Hex**, **S-Hep**, **S-Oct** and **S-Des,** form stable gels in IPP only at room temperature. **S-O-Hex** derivative formed gel structure in ethyl acetate, absolute ethanol, n-butyl palmitate, olive oil, sunflower oil, canola oil and hazelnut oil at -18 ^{0}C. At room temperature, gels were obtained only in olive oil, sunflower oil, canola oil and hazelnut oil. The **S-O-Hep** derivative formed a gel structure in absolute ethanol, acetonitrile, toluene and all vegetable oils at -18 ^{0}C. At room temperature, olive oil, xylene and acetonitrile gels could be obtained for this derivative. The **S-O-Oct** derivative formed gelation in absolute ethanol, toluene, n-butyl palmitate and canola oil at -18 ^{0}C. At room temperature, gels could only be obtained in ethyl acetate. The **S-O-Des** derivative formed a gel structure in toluene, DMSO and canola oil at -18 ^{0}C, while at room temperature it formed gels in ethyl laurate, p-xylene, toluene and DMSO.

The obtained organogels will be examined for the purpose of chiral recognition in a future work.

REFERENCES

Adhikari, B., Nanda, J., Banerje, A. (2011). *"Pyrene-containing peptide-based fluorescent organogels: Inclusion of graphene into organogel*", Chemistry–A European Journal, (17, 11488 11496).

Alkorta I, Rozas I and Elguero J (1998), "*Non-conventional hydrogen bonds*", Chemical Society Reviews, (27:163-170).

Allix, F., Curcio, P., Pham, Q. N., Pickaert, G., Jamart-Gregorie, B. (2010). "*Evidence of intercolumnar $\pi-\pi$ stacking interactions in aminoacid based low molecular weight organogelators*", Langmuir, (26, 16818-16827).

Aneesh, P. S., Saleesh Kumar, N. S., Prabhu, D. D., Shinto V., Krishna Prasad, S., Shankar Rao, D. S., Suresh D. (2014) " *Supergelation via purely aromatic π-π driven self-assembly of pseudodiscotic oxadiazole mesogens*", Journal of American Chemical Society, (136, 5416−5423).

Bastiat, G., Plourde, F., Motulsky, A., Furtos, A., Dumont, Y., Quirion, R., Fuhrmann, G., Leroux, J.-C. (2010). "*Tyrosine-based rivastigmine-loaded organogels in the treatment of Alzheimer's disease*", Biomaterials, (31, 6031-8).

Bastiat, G., Plourde, F., Motulsky, A., Furtos, A., Dumont, Y., Quirion, R., Fuhrmann, G., Leroux, J.-C. (2010). "*Tyrosine-based rivastigmine-loaded organogels in the treatment of Alzheimer's disease*", Biomaterials, (31, 6031-8).

Cui, J., Zheng, Y., Shen, Z., Wan, X. (2010). "*Alkoxy tail lenght dependence of gelation ability and supramolecular chirality of sugar-appended organogalators*", Langmuir, (26, 15508-15515).

D'Aleo, A., Pozzo, J-L, Heuze, K., Vögtle, F., Fages, F. (2007). "*Benzyl and ter-butyl carbamate derivatives of 1,ω-amino acids as simple yet efficient gelators*", Tetrahedron, (63, 7482-8).

Debnath, S., Shome, A., Dutta, S., Das, P. K. (2008). "*Dipeptide-based low-molecular weight efficient organogelators and their application in water purification*" Chemistry – A European Journal, (14, 6870-6881).

Demir-Ordu, O., Simsir, H., Alper, K. (2015). "*Synthesis of bis[N-(p-aryl)- carbamoyloxy]alkanes as new low-molecular weight organogelators*", Tetrahedron, (71, 1529 1539).

Dr. Koichi Kodama, Masato Obata, Sho Sugimura, Hiroki Yuhara, Prof Takuii Hirose (2022). '' *Development of Low-Molecular-Weight Organogelators from Cyclic β-Amino Acid: Effect of Stereochemistry and their Application on Visual Chiral Recognition of Amines''*, Chemistry – A European Journal: (Volume 29, Issue 11).

Dutta, A., Chattopadhyay, D., Pramanik, A. (2010). *"Self-assembling tripeptide as organogelator: the role of aromatic π-stacking interactions in gel formation"* Supramolecular Chemistry, (22, 95-102).

Edwards, W., Smith, D. K. 2014. "*Enantioselective Component Selection in Multicomponent Supramolecular Gels*", Journal of the American Chemical Society, (136, 1116-1124).

Esch, J., Schoonbeek, F., Loos, M., Kooijman, H., Spek, A. L., Kellogg, R. M., Feringa, B. L. (1999). "*Cyclic Bis-Urrea Compounds as Gelators for Organic Solvents*", Chemistry – A European Journal, (5, 937-950).

Hanabusa, K., Maesaka, Y., Kimura, M. and Shirai, H. (1999). "*New gelators based on 2-amino 2-phenylethanol: close gelator-chiral structure relationship*", Tetrahedron Letters, (40, 2385-8).

Hardy, J. G., Hirst, A. R., Ashworth, I., Brennan, C. and Smith, D.K. (2007). "*Exploring molecular recognition pathways within a family of gelators with different hydrogen bonding motifs*", Tetrahedron, (6, 7397-7406).

He, Y., Bian, Z., Kang, C., Cheng, Y. and Gao, L. (2010). "*Novel C3-symmetrical triphenylbenzene-based organogelators with different linkers between phenly ring and alkly chain*", Tetrahedron, (66, 3553-3563).

Hirst, A. R., Smith, D. K. (2004). "*Solvent effects on supramolecular gel-phase materials: two component dendritic ge*l", Langmuir, (20, 10851-7).

Hoare T-R, Kohane D-S (2008) "*Hydrogels in drug delivery: Progress and challenges*", Polymer, (49:1993-2007).

Hou X, Butz A, Chen C, Wang Z-D, Zhao J-X, Shiu T, Chu Q-R (2016) "*Low molecular weight organogelators derived from threefold symmetric tricarbamates*", Tetrahedron Letters, (58:1:101-105).

Khan, M. K., Sundararajan, P. (2011). "*Encapsulation of dye molecules and nanoparticles in hollow organogel fibers of a nonchiral polyurethane model compound*" Chemistry – A European Journal, (17, 1184-1192).

Khan, M. K., Sundararajan, P. (2011). "*Encapsulation of dye molecules and nanoparticles in hollow organogel fibers of a nonchiral polyurethane model compound*" Chemistry – A European Journal, (7, 1184-1192).

Khan, M. K., Sundararajan, P. (2013). *"Effects of Spacer Length and Terminal Group on the Crystallization and Morphology of Biscarbamates: A Longer Spacer Does Not Reduce the Melting Temperature*'' Journal of Physical Chemistry B, (117, 5705-5717).

Kollman P-A and Allen L-C (1971) "*The theory of the hydrogen bond*", Department of Chemistry, Princeton University, Princeton, New Jersey, (283-301).

Komba (2024) ''Synthesis of D-glucono-1,4-lactones modified with linear saturated fatty acids and evaluation of their physical properties'' http://doi.org/10.26434/chemrxiv-2024-5wpgn

Laan, S., Feringa, B. L., Kellogg, R. M., Esch, J. (2002). "*Remarkable polymorphism in gels of new azobenzene bis-urea gelators*", Langmuir, (18, 7136-7140).

Laan, S., Feringa, B. L., Kellogg, R. M., Esch, J. (2002). "*Remarkable polymorphism in gels of new azobenzene bis-urea gelators*", Langmuir, (18, 7136-7140).

Lebel, O., Perron, M.-E., Maris, T., Zalzal, S. F., Nanci, A., Wuest, J. D. (2006). "*A new class of selective low-molecular-weight gelators based on salts of diaminotriazinecarboxylic acids*" Chemistry of Materials, (18, 3616-3626).

Li, Y., Wang, T., Liu, M. (2007). "*Ultrasound induced formation of organogel from a glutamic dendron*" Tetrahedron, (63, 7468-7473).

Li, Z., Luo, X., Xiao, W., Wang, Q. and Zhong, J. (2009). *"Self-assembled organogels formed by monochain derivatives of ethylenediamine*", Journal of Colloid and Interface Science, (336: 803-7)

Lim, P. F. C., Liu, X. Y., Kang, L., Ho, P. C. L., Chan, S. Y. (2008). "*Physicochemical effects of terpenes on organogel for transdermal drug delivery"*, International Journal of Pharmaceutics, (358, 102-7)

Lin C-Y, Weiss R-G (1987*)" Liquid-crystalline solvents as mechanistic probes. A novel gelator of organic liquids and the properties of its gels*", Macromolecules, (20:414-417).

Lloyd J-D, Alexander J-E. (1926) Colloid Chemistry, The Chemical Catalog Co. New York, (1:767).

Loos, M., Esch, J. H., Kellogg, R. M., Feringa, B. L. (2007). "*C3-Symmetric, amino acid based organogelators and thickeners: a systematic study of structure-property relations*", Tetrahedron, (63, 7285-7301).

Lucas L-N (2001) "*Dithienylcyclopentene Optical Switches Towards Photoresponsive Supramolecular Materials*", Rijksuniversiteıt Groningen, ISBN, (90:367-1528).

Luo, X., Xiao, W., Li, Z., Wang, Q. and Zhong, J. (2009). "*Supramolecular organogels formed by monochain derivatives of succinic acid*", Journal of Colloid and Interface Science, (329: 372-5).

Maitra, U., Potluri, V. K., Sangeetha, N. M., Babu, P. and Raju, A. R. (2001). "*Helical aggregates from a chiral organogelator*", Tetrahedron-Asymmetry, (12, 477-480).

Mohenmeyer, N., Schmidt, H. -W. (2007). "*Synthesis and structure-property relationships of amphiphilic organogelators*", Chemistry–A European Journal, (13, 4499-4509).

Mohenmeyer, N., Schmidt, H-W. (2005). "*A new class of low-molecular-weight amphiphilic gelators*", Chemistry–A European Journal, (11, 863-872).

Murdan S, Gregoriadis G, Florence A-T (1998) "*Sorbitan monostearate / polysorbate 20 organogels containing niosomes delivery vehicle for antigens*", European Journal of Pharmaceutical Sciences, (99, 8:177-185).

Nigawara, T., Suzuki, M., Yumoto, M., Kimura, M., Shirai, H., Hanabusa, K. (2003). "*L-Lysine based gemini organogelators: their organogelation properties and thermally stable organogels*", Organic and Biomolecular Chemistry, (1, 4124-4131).

Nigawara, T., Suzuki, M., Yumoto, M., Kimura, M., Shirai, H., Hanabusa, K. (2003). "*L-Lysine based gemini organogelators: their organogelation properties and thermally stable organogels*", Organic and Biomolecular Chemistry, (1, 4124-4131).

Ongaratto, R., Conte, N., Montes D'Oca, C. R., Brinkerhoff, R. C., Ruas, C. P., Gelesky, M. A., Montes D'Oca, M. G. (2019). '' *In situ formation of AuNPs using fatty N-acylamino hydrazide organogelators as templates''*, New Journal of Chemistry,(43, 295-303).

Pal A., Dey J. (2011). "*Water-induced physical galation of organic solvents by N-(n alkylcarbamoyl)-L-alanine amphiphiles*", Langmuir, (27, 3401-8).

Pal, A., Ghosh, Y. K. and Bhattacharya, S. (2007). "*Molecular mechanism of physical gelation of hydrocarbons by fatty acid amides of natural amino acids*", Tetrahedron, (63, 7334-7348).

Pang, X., Yu, X., Lan, H., Ge, X., Li, Y., Zhen, X., Yi, T. (2015). "*Visual Recognition of Aliphatic and Aromatic Amines Using a Fluorescent Gel: Application of a Sonication-Triggered Organogel*", American Chemical Society, (7,13569-13577).

Podder, D., Chowdhury, S. R., Nandi S. K., Haldar, D. (2019). '' *Tripeptide based super organogelators: structure and function*'', New Journal of Chemistry, (43, 3743-9).

Qing, G., Shan, X., Chen, W., Lv, Z., Xiong, P., Sun, T. (2014). "*Solvent-Driven Chiral Interaction Reversion for Organogel Formation*", Angewandte Chemistry International Edition, (53, 2124–9).

Rajaganesh, R., Gopal, A., Das, T. M., Ajayaghosh, A. (2012). "*Synthesis and Properties of Amphiphilic Photoresponsive Gelators for Aromatic Solvents*", Organic Letters, (14, 748-751).

Rajaganesh, R., Gopal, A., Das, T. M., Ajayaghosh, A. (2012). "*Synthesis and Properties of Amphiphilic Photoresponsive Gelators for Aromatic Solvents*", Organic Letters, (14, 748-751).

Sahoo S, Kumar N, Bhattacharya C, Sagiri S-S, Jain K, Pal K, Ray S-S and Nayak B (2011) "*Organogels: Properties and Applications in drug delivery*", Designed Monomers and Polymers, (14:95-108).

Smith D-K (2007) "*Molecular gels-underpinning nanoscale materials with organic chemistry*", Tetrahedron, (63:7283-7284).

Sri B-M, Ashok V and Arkendu C (2012) *"As A Review on Hydrogels as Drug Delivery in the Pharmaceutical Field*", International journal of pharmaceutical and chemical sciences", (1, 2:2277-5005).

Suzuki, M., Nigawara, T., Yumoto, M., Kimura, M., Shirai, H., Hanabusa, K. (2003). "*New gemini organogelators linked by oxalyl amide: organogel formation and their thermal stabilities*", Tetrahedron Letters, (44, 6841-3).

Suzuki, M., Nigawara, T., Yumoto, M., Kimura, M., Shirai, H., Hanabusa, K. (2003). "New gemini organogelators linked by oxalyl amide: organogel formation and their thermal stabilities", Tetrahedron Letters, (44, 6841-3).

Suzuki, M., Yumoto, M., Shirai, H., Hanabusa, K. (2008). "*A family of low-molecular-weight organogelators based on Nα, Nε- diacyl-L-lysine: effect of alkyl chains on their organogelation behaviour*", Tetrahedron, (64, 10395-10400).

Tan, C., Su, L., Lu, R., Xue, P., Bao, C., Liu, X. and Zhao, Y. (2006). "*A family of low-molecular weight organogelators based on long chain substituted benzoic acid hydrazides*", Journal of Molecular Liquids, (124, 32-6).

Terech, P., Weiss, R. G. (1997). *" Low molecular mass gelators of organic liquids and the properties of their gels*", Chemical Reviews, (97, 3133-3159).

Tomioka, K., Sumiyoshi, T., Narui, S., Nagaoka, Y., Iida, A., Miwa, Y., Taga, T., Nakano, M. and Handa, T. (2001). "*Molecular assembly and gelating behavior of didodecanoylamides of α, ω- alkylidenediamines*", Journal of the American Chemical Society, (123, 11817-8).

Tripathi, A., Kumar, A., Pandey, P. S. (2012). "*Visual Chiral Recognition Of Mandelic Acid And A-Amino Acid Derivatives By Enantioselective Gel Formation And Precipitation*", Tetrahedron Letters, (53, 5745–8).

Tsai C-C, Cheng Y-T, Shen L-C, Chang K-C, Ho I-T, Chu J-H, and Chung W-S (2013) "*Biscalix[4]arene Derivative As a Very Efficient Phase Selective Gelator for Oil Spill Recovery*", American Chemical Society, (15, 22:5830-5833).

van Esch, J., De Feyter, S., Kellogg, R. M., De Schryver, F., Feringa, B. L. (1997). "*Self Assembly of Bisurea Compounds in Organic Solvents and on Solid Substrates*", Chemistry a European Journal, (3, 1238-1243).

Vintiloiu, A., Leroux, J. C. (2008). "*Organogels and their use in drug delivery-a review*", Journal of Controllled Release, (125, 179-192).

Vintiloiu, A., Leroux, J. C. (2008). "*Organogels and their use in drug delivery-a review*", Journal of Controllled Release, (125, 179-192).

Wang, C., Zhang, D., Xiang, J., Zhu, D. (2007). "*New organogels based on an anthracene derivative with one urea group and its photodimer: Fluoresence after gelation*", Langmuir, (23, 9195-9200).

Wang, Y., Wu, S., Yan, X., Ma, T., Shao, L., Liu, Y., Guo, Z. (2017). "*Alkyl bicarbamates supramolecular organogelators with effective selective gelation and high oil recovery from oil/water mixtures*", Chemosphere, (167,178-187).

Xu L, Hu Y, Liu M, Chen J, Huang X, Gao W, Wu H (2015) “Gelation properties and glucose-sensitive behavior of phenylboronic acid based low-molecular-weight organogels”, Tetrahedron, (71:2079-2088).

Xu L, Hu Y, Liu M, Chen J, Huang X, Gao W, Wu H (2015) “*Gelation properties and glucose-sensitive behavior of phenylboronic acid based low-molecular-weight organogels*”, Tetrahedron, (71:2079-2088).

Zhu, G., Dordick, J. S. (2006). “*Solvent effect on organogel formation by low molecular weight molecules*”, Chemistry of Materials, (18, 5988-5995).

Zweep, N., Hopkinson, A., Meetsma, A., Browne, W. R., Feringa, B. L., Esch, J. H. (2009). “*Balancing hydrogen bonding and van der Waals interactions in cyclohexane based bisamide and bisurea organogelators*”, Langmuir, (25, 8802).